HIGHWAY RESEARCH RECORD

Number 308

Traffic Flow Characteristics

7 Reports

Subject Areas

52 Road User Characteristics
53 Traffic Control and Operations
55 Traffic Measurements

HIGHWAY RESEARCH BOARD
DIVISION OF ENGINEERING NATIONAL RESEARCH COUNCIL
NATIONAL ACADEMY OF SCIENCES—NATIONAL ACADEMY OF ENGINEERING

WASHINGTON, D.C. 1970

Standard Book Number 309-01806-4

Price: $3.00

Available from

Highway Research Board
National Academy of Sciences
2101 Constitution Avenue
Washington, D.C. 20418

Department of Traffic and Operations

Harold L. Michael, Chairman
Purdue University, Lafayette, Indiana

E. A. Mueller
Highway Research Board Staff

COMMITTEE ON CHARACTERISTICS OF TRAFFIC FLOW

(As of December 31, 1969)

Joseph C. Oppenlander, Chairman
The University of Vermont, Burlington

Patrick J. Athol
Jack B. Blackburn
Martin J. Bouman
Kenneth A. Brewer
Kenneth W. Crowley
Olin K. Dart, Jr.
Robert F. Dawson
H. M. Edwards
John J. Haynes
Clinton L. Heimbach
James H. Kell
Russell M. Lewis
Peter A. Mayer
Stuart R. Perkins
F. William Petring
O. J. Reichelderfer
August J. Saccoccio
Charles C. Schimpeler
Joseph Seifert
William P. Sheldon
William C. Taylor
Kenneth J. Tharp
Robert J. Wheeler

Foreword

Interest in the improvement of the safety and efficiency of traffic flow continues to focus the attention of researchers on efforts to foster understanding of traffic flow characteristics. This RECORD contains seven papers that deal with flow properties of automobiles, trucks, and pedestrians, and should prove of interest to flow theorists, planners, practitioners, and others concerned with solving flow problems.

The paper by Worrall, Bullen, and Gur describes an elementary stochastic model of lane-changing behavior that was calibrated by these Northwestern University researchers using data collected on a six-lane Chicago freeway. The structure of the Markovian model and some of its empirical implications are also illustrated by numerical examples.

Torres describes the instrumentation of a standard passenger vehicle to measure acceleration and velocity, and of a digital data recording and processing system for rapid reduction of the measured data. The vehicle has been used to collect extensive freeway flow data under actual driving conditions, including average velocity and acceleration, acceleration noise, power spectral densities, travel times and distances, and other data. Some conclusions are drawn about the relationship among acceleration noise, volume, density, and travel time.

The investigation reported by Sinha and Dawson is concerned with the development of a digital traffic simulator for use as a tool in the analysis of freeway traffic phenomena. Comparisons described as being consistent and reasonable were made between simulated phenomena and data collected on sections of the Eisenhower Expressway and a Long Island parkway.

Brewer, an Iowa State University researcher, has used a basic queuing approach to develop a model attempting to describe the operation of a signal-controlled ramp. Predicted waiting at the signal for fixed-rate metering and for gap-acceptance control is compared to observed study data, and average queues at the signal are also predicted.

Humphreys' attempt to determine the effect of trucks or grades or both on an urban freeway, using acceleration noise as the primary parameter, led to the conclusion that acceleration noise was not adequate to measure the effect of trucks on level of service. This author concluded that trucks tend to stabilize flow and suppress shock waves because of the driving characteristics of truck operators, and human factors research was needed to develop means of assessing the effect of trucks on urban freeway flow.

Interesting behaviorial patterns were observed with time-lapse photography by DiPietro and King. The objective of the study was to measure pedestrian gap acceptance at an unmarked midblock crossing. Findings showed that male pedestrians were willing to accept shorter gaps than females, that the minimum acceptable gap was 3 sec or 75 ft, and that groups of pedestrians accepted shorter gaps and walked more slowly than did individual pedestrians.

The final paper by Schneeberger and Hayman presents results of an experiment to test the applicability of a pulsed Doppler radar device to the measurement of traffic-flow parameters, especially under conditions of high densities and high flow rates. Following the experimentation, the author noted some limitations, but concluded that pulsed Doppler radar may provide a unique instrumentation technique allowing the acquisition of new forms of traffic-flow data.

Contents

AN ELEMENTARY STOCHASTIC MODEL
OF LANE-CHANGING ON A MULTILANE HIGHWAY

R. D. Worrall, A. G. R. Bullen, and Y. Gur 1

ACCELERATION NOISE, POWER SPECTRA,
AND OTHER STATISTICS DERIVED FROM INSTRUMENTED
VEHICLE MEASUREMENTS UNDER FREEWAY DRIVING CONDITIONS

J. F. Torres 13

THE DEVELOPMENT AND
VALIDATION OF A FREEWAY TRAFFIC SIMULATOR

Kumares C. Sinha and Robert F. Dawson 34

ANALYSIS OF A SIGNAL-CONTROLLED RAMP'S CHARACTERISTICS

Kenneth A. Brewer 48

EFFECT OF TRUCKS ON THE URBAN FREEWAY

Jack B. Humphreys 62
Discussion: John J. Haynes 75
Patrick J. Athol 77

PEDESTRIAN GAP-ACCEPTANCE

Charles M. DiPietro and L. Ellis King 80

A PULSED DOPPLER RADAR
EXPERIMENT FOR HIGHWAY TRAFFIC RESEARCH

Richard F. Schneeberger and Robert A. Hayman 92

An Elementary Stochastic Model of Lane-Changing on a Multilane Highway

R.D. WORRALL, Peat, Marwick, Mitchell and Company;
A.G.R. BULLEN, University of Illinois; and
Y. GUR, Northwestern University

Lane-changing on a multilane highway may be treated conveniently as a stochastic phenomenon. This paper describes an elementary stochastic model of lane-changing behavior, based on its interpretation as a homogeneous Markov chain. The model is calibrated using data collected on a section of 6-lane freeway in Chicago.

•CONSIDER A SECTION OF HIGHWAY, m lanes wide in one direction, with the lanes numbered 1 . . . m from the right (Fig. 1). The section is divided into subsections, each of L length such that the probability of a vehicle making more than 1 lane change in each L length is negligible. Assume that

1. Lane-changing is an isolated event in the traffic stream, with an equal probability of occurrence for all vehicles;
2. Lane changes are independent; and
3. $X_{ij}^{Kt} \geq 0$ if $|i - j| = 1$; $X_{ij}^{Kt} = 0$ if $|i - j| \neq 1$.

Let

X_{ij}^{Kt} = number of lane changes observed between lanes i and j within subsection K during time t, and

λ_{ij}^{K} = average number of lane changes between lanes i and j within subsection K during unit time.

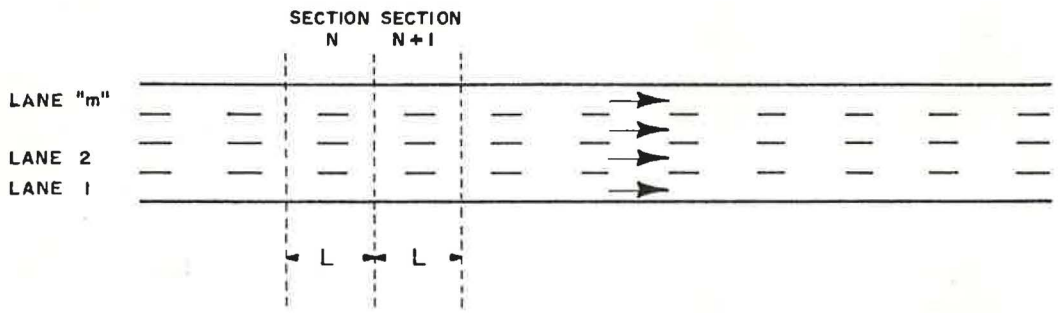

Figure 1. Highway section.

Paper sponsored by Committee on Freeway Operations and presented at the 49th Annual Meeting.

Then, the frequency of lane-changing from lane i to lane j in section K during successive intervals t may be modeled simplistically as a Poisson process $\left\{X_{ij}^{Kt};\ t > 0\right\}$, where

$$\text{Prob}\left\{X_{ij}^{Kt} = N\right\} = \frac{\exp\left(-\lambda_{ij}^{K} \cdot t\right) \cdot \left(\lambda_{ij}^{K} \cdot t\right)^{N}}{N!}$$

The aggregate frequency of maneuver across all lanes in section K may likewise be treated as a Poisson process $\left\{X^{Kt};\ t > 0\right\}$, where

$$\text{Prob}\left\{X^{Kt} = N\right\} = \frac{\exp\left(-\lambda^{K} \cdot t\right) \cdot \left(\lambda^{K} \cdot t\right)^{N}}{N!}$$

and

$$\lambda^{K} = \sum_{i}\sum_{j}\left(\lambda_{ij}^{K}\right)$$

No mention is made here of the reason for changing lanes. Lane-changing within section K is treated simply as a sequence of independent "rare events," with no regard for their internal structure or causation. Given this simple framework, systematic effects of highway design or traffic conditions on lane-changing may be reflected within the model structure in 1 of 2 ways. They may appear as changes in the value of λ_{ij}^{K} (e.g., λ_{ij}^{K} may take on different values under light and heavy traffic conditions, or according to the proximity of ramp terminals to section K), or they may be reflected as deviations from the assumed pattern of randomness.

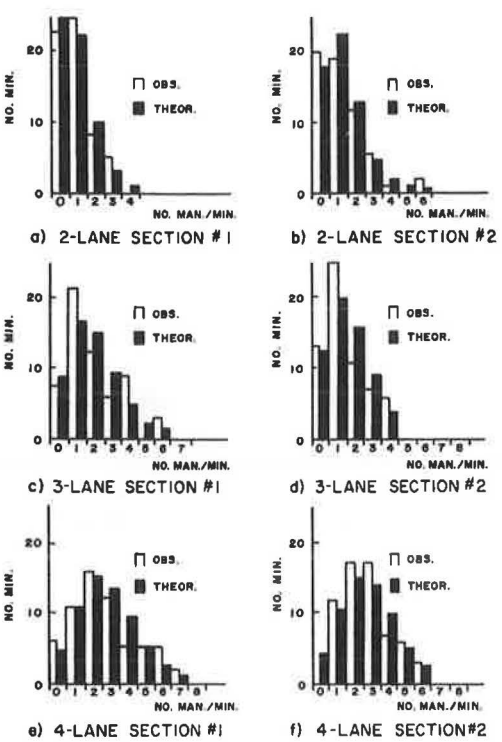

Figure 2. Typical lane-changing frequency distributions.

Figures 2 and 3 show a selection of typical numerical results for 2-, 3-, and 4-lane unidirectional roadways. In each case, the frequency of lane-changing maneuvers may be effectively described by the simple stochastic structure outlined here. A more detailed discussion of related empirical analyses is given elsewhere (1).

AN ELEMENTARY MARKOVIAN MODEL OF LANE-CHANGING

Consider again the 1-way highway shown in Figure 1, m lanes wide, divided into equal n sections of L length. Again, let the value of L be such that the probability of a vehicle changing lanes more than once in L distance is negligible. Let X(r) be a random variable denoting the lane in which a typical vehicle v is traveling as it leaves the r th section of highway (Fig. 1).

If it is assumed that the probability of vehicle v changing lanes in section r is a function only of its position in section (r - 1) and of the lane into which the change is to be made, then the position of the vehicle may be described as the outcome of a finite Markov process $\{X(r);\ L > 0\}$; i.e., if

$$P\{X(r) = j | X(o), \ldots, X(r-1); L\} = P\{X(r) = j | X(4-1); L\} \quad (1)$$

Then $\{X(r); L > 0\}$ is a finite Markov process whose structure is defined by an $m \times m$ transition matrix $P(r)$, and an initial state vector $a(o)$, where

$$P(r) = \begin{bmatrix} p(r)_{11}, & \ldots, & p(r)_{1j}, & \ldots, & p(r)_{1m} \\ p(r)_{i1}, & \ldots, & p(r)_{ij}, & \ldots, & p(r)_{im} \\ p(r)_{m1}, & \ldots, & p(r)_{mj}, & \ldots, & p(r)_{mm} \end{bmatrix}$$

$p(r)_{ij}$ = probability that a vehicle in lane i in section $(r-1)$ will be in lane j in section r

$p(r)_{ij} \geq 0$; all i, j

$$\sum_{j=1}^{m} p(r)_{ij} = 1, \text{ all i}$$

and

$a(o) = [a(o)_1, \ldots, a(o)_i, \ldots, a(o)_m]$

$a(o)_i$ = probability of vehicle V occupying lane i as it enters first section of highway

$a(o)_i \geq 0$; all i

$$\sum_{i=1}^{m} a(o)_i = 1$$

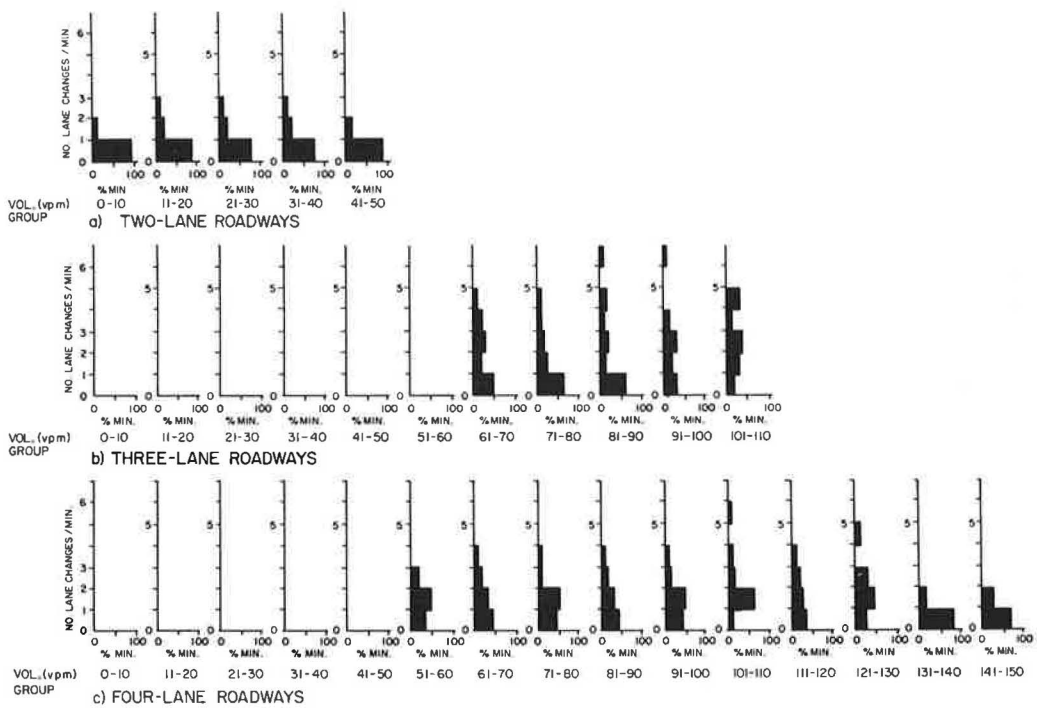

Figure 3. Variation in lane-changing frequency.

If multiple lane changes are banned (as they are by the definition of L), then

$$p(r)_{ij} = \begin{cases} 0 \le p \le 1 & \text{if } |i - j| = 1 \\ 0 & \text{if } |i - j| > 1 \\ 1 - p_i,\ i - 1 - p_i,\ i + 1 & \text{if } i = j \end{cases}$$

In general, a(r) will be taken as the state vector $\{a(r)_1, \ldots, a(r)_i, \ldots, a(r)_m\}$ defining the probability that vehicle V occupies lane i $(i = 1, \ldots, m)$ as it leaves any section r.

If it is assumed that P(r) is constant for all vehicles and for all flow conditions, the aggregate distribution of vehicles by lane at the end of section r may be estimated as

$$a(r) = a(r - 1) \cdot P(r) = a(o) \cdot P(1) \cdot P(2) \ldots P(r) \tag{2}$$

Hence, the expected number of lane changes $N(r)_{ij}$ in section r from lanes i to j during T time may be estimated as

$$N(r)_{ij} = q \cdot T \cdot a(r - 1)_i \cdot p(r)_{ij} \tag{3}$$

where q is the total rate of flow in section r. The total expected number of lane changes in section r between all lanes is then

$$N(r) = \sum_{i=1}^{m} \sum_{j=1}^{m} N(r)_{ij} \tag{4}$$

Similarly, if it is assumed that the matrix P(r) is constant for all r, i.e., $\{X(r);\ L > 0\}$ is a finite Markov chain, the aggregate distribution of vehicles at any point distance $(u \cdot L)$ from the initial section may be estimated as

$$a(u) = a(o) \cdot p^u \tag{5}$$

Ultimately, as u becomes large, this distribution will tend toward a steady state, representing the equilibrium distribution of vehicles across the highway. This condition may be represented symbolically as

$$a(s) = a(s) \cdot P \tag{6}$$

where a(s) denotes the steady-state vector. This framework provides a convenient mechanism for describing the trajectory of a particular set of vehicles (e.g., those located in lane j at section u) as they traverse the highway.

The diffusion of vehicles located in lane 1 at section o, for example, downstream of section o may be modeled by setting $a(o)_1 = 1$; $a(o)_i = 0$, all $i \neq 1$, and applying the expression $a(u) = a(o) \cdot p^u$.

Alternatively, the upstream trajectories of vehicles known to be located in lane 1 at section u may be modeled by specifying lane 1 in the matrix p to be an absorbing state and examining the resultant times-to-absorption at varying distances upstream of section u.

The former treatment is clearly applicable to the diffusion of entering vehicles downstream from an entrance ramp, whereas the latter provides a means for analyzing the movement of exiting vehicles upstream from an exit ramp. In combination, they provide a mechanism for the analysis of complex weaving sections.

The structure of this simple Markovian model and some of its empirical implications are illustrated by a series of simple numerical examples in the next section of this paper. Under conditions of uninterrupted flow (i.e., in the absence of extraneous systematic factors such as ramps influencing the pattern of lane-changing), the transition

matrix P(r) may be validly considered to remain constant across all sections r. The state vector a(r) will also be constant for all r under these conditions; i.e., flow will be in an equilibrium condition equivalent to the steady state of the process $\{X(r);\ L \geq 0\}$:

$$P(r) = P(r + 1) = P$$
$$a(r) = a(r + 1) = a$$

By definition, in the steady state $a(s) = a(s) \cdot P$. Thus

$$a_i = (a_{i-1} \cdot P_{i-1, i}) + a_i(1 - P_{i, i-1} - P_{i, i+1}) + (a_{i+1} \cdot P_{i+1, i})$$

or

$$a_i \cdot P_{i, i-1} + a_i \cdot P_{i, i+1} = a_{i-1} P_{i-1, i} + a_{i+1} P_{i+1, i} \tag{7}$$

but for i = 1

$$a_1 p_{12} = a_2 p_{21} \tag{8}$$

and Eqs. 7 and 8 give for i = 2

$$a_2 p_{23} = a_3 p_{31}$$

and in general

$$a_i p_{i, i+1} = a_{i+1} P_{i+1, i}$$

or

$$N_{i, i+1} = N_{i+1, i}$$

Hence, in the steady-state or "uninterrupted flow" condition, the number of lane changes from lane i to lane j (N_{ij}) will exactly balance those made from lane j to lane i (N_{ij}).

This simple result provides a useful mechanism for detecting the influence on lane-change maneuvers of a particular geometric feature such as a ramp, based simply on a count of lane-to-lane movements. For example, in Figure 9, a count of lane-to-lane movements may indicate that the mainstream flow is "undisturbed" in sections B-D and G-H (i.e., all lane-to-lane movements balance) but is subject to a systematic lane-changing bias in sections of E-F because of the presence of the entrance ramp.

NUMERICAL EXAMPLES

Example 1—Lane-Changing in Uninterrupted Traffic

Consider the section of 4-lane freeway shown in Figure 4. Let

$L = 250$ ft;

$a(o) = \{0.4,\ 0.6\}$;

$P = P(r)$, all $r = \begin{bmatrix} 0.975 & 0.025 \\ 0.017, & 0.983 \end{bmatrix}$; and

$q = 1{,}000$ vehicles per hour.

Then the expected number of lane changes in section 1, N(1), is given by

$$\begin{aligned} N(1) &= N(1)_{12} + N(1)_{21} \\ &= 1{,}000\ \{(0.4)\ (0.025)\} + 1{,}000\ \{(0.6)\ (0.017)\} \\ &= 20 \text{ lane changes per hour} \end{aligned}$$

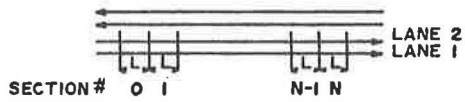

Figure 4. Highway section for example 1.

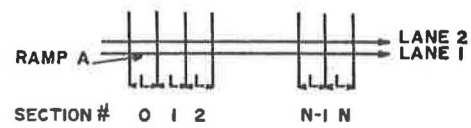

Figure 5. Highway section for example 2.

Example 2—Lane-Changing Downstream of an Entrance Ramp

Consider a flow of 100 vehicles per hour entering the 4-lane freeway, shown in Figure 5, via ramp A. Ignore, for the moment, all through traffic. Assume that all merges are completed within the 250-ft section labeled section o in the figure. Let $L = 250$ ft; and set $a(0) = \{1, 0\}$; and assume that $P = P(r)$, all $r = \begin{Bmatrix} 0.5, & 0.5 \\ 0.4, & 0.6 \end{Bmatrix}$.

Then, for section 1 downstream of the ramp,

$$a(1) = [1, 0] \cdot \begin{bmatrix} 0.5, & 0.5 \\ 0.4, & 0.6 \end{bmatrix} = [0.5, 0.5]$$

Thus, at a point 250 ft downstream of the end of the ramp merge area, 50 percent of the merging vehicles will be located in lane 1 and 50 percent in lane 2.

Similarly, for section 3,

$$a(2) = [1, 0] \cdot \begin{bmatrix} 0.5, & 0.5 \\ 0.4, & 0.6 \end{bmatrix}^2 = [0.45, 0.55]$$

That is, at the end of section 2, 300 ft downstream of the ramp, 45 percent of the entering vehicles will be in lane 1 and 55 percent in lane 2.

The steady-state distribution achieved at section s downstream of the ramp is given by

$$a(s) = [0.444, 0.556]$$

In the present case, this condition is reached after approximately 6 state transitions, implying that a stable distribution of entering vehicles across the mainstream lanes (44.4 percent in lane 1, 55.6 percent in lane 2) is achieved approximately 1,500 ft downstream of the ramp.

Example 3—Lane-Changing Upstream of an Exit Ramp

Consider a flow of 10 vehicles exiting at ramp B (Fig. 6) during a 5-min period. Again, ignore all through vehicles, but assume that their volume remains approximately constant over the 5-min period. Assume that all exits are made from lane 1 and section b. Designate lane 1 as an absorbing state (i.e., set $p_{11} = 1$, $p_{12} = 0$ in the matrix P).

Let

$$P = P(r), \text{ all } r = \begin{bmatrix} 1, & 0 \\ 0.3, & 0.7 \end{bmatrix}$$

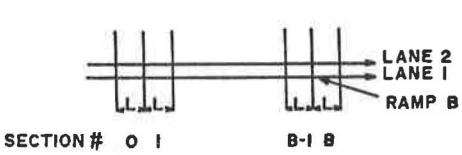

Figure 6. Highway section for example 3.

Assume that an initial equilibrium lane distribution of exiting vehicles at section o upstream of the ramp is

$$a(o) = [0.55, 0.45]$$

All exiting vehicles must clearly be absorbed into lane 1 by the time section b is reached.

The distance of roadway required to do this may be estimated if the time, i.e., number of iterations of the expression $a(r) = [a(o) \cdot P^r]$, required to achieve this condition is estimated. For simplicity, assume that the time to total absorption may be approximated by the number of transitions required to absorb 96 percent of the vehicles wishing to exit at ramp B; i.e., assume that $a(b)_1 \geq 0.96$. Setting $a(b) = [a(o) \cdot P^b]$ then yields

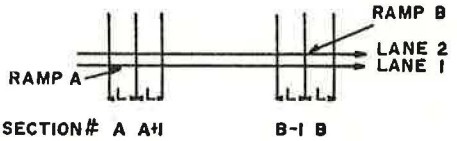

Figure 7. Highway section for example 4.

$$[0.96,\ 0.04] = [0.55,\ 0.45] \cdot \begin{bmatrix} 1, & 0 \\ 0.3, & 0.7 \end{bmatrix}^7$$

That is, a distance of $7 \cdot L = 1{,}750$ ft is required to ensure absorption of 96 percent of exiting vehicles in lane 1 by the time section b is reached.

If the volume of through traffic increases, the probability that a lane change will be successfully completed in a length of 250 ft will tend to drop; i.e., the structure of the matrix P may be expected to change to a value such as

$$P_2 = \begin{bmatrix} 1, & 0 \\ 0.1, & 0.9 \end{bmatrix}$$

In this case, the distance to absorption is given by $(0.964,\ 0.036) = (0.55,\ 0.45) \cdot (P_2)^{25}$; i.e., a distance of 6,250 ft (equivalent to 25 successive sections L = 250 ft) is now required to absorb 96 percent of all existing vehicles in lane 1.

Furthermore, if the 2 matrices P_1 and P_2 in this example may be taken, illustratively, to represent the extremes of free-flowing and congested traffic, one may argue that a maneuver distance of between 1,750 and 6,250 ft should be allowed upstream of an exit ramp, suggesting the location of exit-ramp signs at distances of roughly 1½ miles and ½ mile upstream of the ramp nose.

a) 2-LANE SECTION #1

FROM \ TO	LANE 1	LANE 2
LANE 1	0.9897 (0.0002)	0.0103 (0)
LANE 2	0.0468 (0)	0.9532 (0.0448)

b) 2-LANE SECTION #2

FROM \ TO	LANE 1	LANE 2
LANE 1	0.9824 (0)	0.0176 (0)
LANE 2	0.0371 (0)	0.9629 (0.0003)

c) 3-LANE SECTION #1

FROM \ TO	LANE 1	LANE 2	LANE 3
LANE 1	0.9710 (0.0001)	0.0290 (0)	
LANE 2	0.0085 (0)	0.9851 (0.0001)	0.0074 (0)
LANE 3		0.0134 (0.0004)	0.9866 (0.0199)

d) 3-LANE SECTION #2

FROM \ TO	LANE 1	LANE 2	LANE 3
LANE 1	0.9894 (0.0004)	0.0106 (0)	
LANE 2	0.0220 (0.0001)	0.9570 (0.0412)	0.0210 (0.0001)
LANE 3		0.0078 (0)	0.9925 (0.0001)

e) 4-LANE SECTION #1

FROM \ TO	LANE 1	LANE 2	LANE 3	LANE 4
LANE 1	0.9910 (0.0001)	0.0090 (0)		
LANE 2	0.0340 (0)	0.9485 (0.0488)	0.0175 (0.0001)	
LANE 3		0.0218 (0.0001)	0.9568 (0.0414)	0.0216 (0.0001)
LANE 4			0.0148 (0.0001)	0.9852 (0.0146)

f) 4-LANE SECTION #2

FROM \ TO	LANE 1	LANE 2	LANE 3	LANE 4
LANE 1	0.9932 (0)	0.0068 (0)		
LANE 2	0.0089 (0)	0.9849 (0.0001)	0.0063 (0.0001)	
LANE 3		0.0144 (0)	0.9769 (0.0002)	0.0087 (0)
LANE 4			0.0057 (0.0001)	0.9943 (0)

0.9568 = Mean Transition Probability

(0.0414) = Variance of Sample Transition Probabilities

Figure 8. Typical lane-changing transition matrices.

Example 4—Weaving Section

The values of a(r) in example 3 between r = 0 (equilibrium lane distribution upstream of the ramp in the mainstream lanes before any absorption of lane 2 vehicles occurs) and r = a (where a denotes the number of iterations required to achieve 96 percent absorption) yield estimates of the proportion of exiting vehicles in lane 1 at varying distances upstream of the ramp. These estimates, when coupled with the estimates of a(r) derived from the entrance ramp example, suggest a possible alternative approach to the calculation of ramp terminal and weaving section capacities to that outlined in the Highway Capacity Manual (2).

Consider the weaving section shown in Figure 7. Assume that a volume Y of vehicles entering the freeway via ramp A wish to exit at ramp B. Assume that the probability of an exiting vehicle making a successful lane change from lane 1 to lane 2 within each successive section of 250 ft is 0.153 and that this value remains constant over the entire section A-B. Designate lane 2 upstream of exit B as an absorbing state, and set $a(o) = [1, 0]$ to define the lane distribution of ramp vehicles as they enter the freeway from ramp A. If the same 96 percent absorption criterion as before is used, and the concern is solely with the volume Y, the calculation of the necessary weaving section length may be treated in a manner analogous to example 3.

In this case, successive applications of $a(r) = a(o) \cdot P^r$ yield the expression $(0.04, 0.96) = a(o) \cdot P^{19}$. Hence, the distance to 96 percent absorption for the volume Y is 19 x 250 ft = 4,750 ft, suggesting a desirable minimum weaving section of slightly less than 1 mile between ramp terminals.

Figure 8 illustrates 6 typical, empirical transition matrices, developed for sections of 2-, 3-, and 4-lane roadway in Chicago. In each case, the data are based on a sequence of 15-min observations at the location in question. Note the dominance of the values along main diagonals and the extremely low transition probability variances, indicating a stable transition pattern. A more detailed discussion of the empirical characteristics of lane-changing is given in another report (1).

EXTENSIONS OF THE SIMPLE MODEL

Clearly, in all 4 of the preceding examples, a critical assumption was that the matrix P was both constant and measurable for all highway sections, all vehicles, and all flow conditions.

Conceptually, these assumptions may be readily relaxed. Consider, for example, the case of K vehicle types and Z different traffic flow conditions. By superposition, the aggregate process $\{X(r); L > 0\}$ may be generated from a set of $(K \cdot Z)$ separate processes $\{X(r)_{k,z}; L > 0\}$, yielding an aggregate vector $\bar{a}(r)$ and an aggregate transition $\bar{P}(r)$ defined as

$$\bar{a}(r) = \frac{1}{\sum_{i=1}^{m} \sum_{k=1}^{K} \sum_{z=1}^{Z} n(r)_{i,k,z}} \cdot \sum_{k=1}^{K} \sum_{z=1}^{Z} n(r)_{k,z} \cdot a(r)_{k,z}$$

and

$$\bar{P}(r) = \bar{p}(r)_{ij}$$

where

$$\bar{P}(r)_{ij} = \begin{cases} \dfrac{\sum_{k=1}^{K} \sum_{z=1}^{Z} a(r)_{i,k,z} \cdot n(r)_{k,z} \cdot p(r)_{i,j,k,z}}{\sum_{k=1}^{K} \sum_{z=1}^{Z} a(r)_{i,k,z} \cdot n(r)_{k,z}} & \text{if } \bar{a}(r)_i > 0 \\ \delta_{ij} & \text{if } \bar{a}(r)_i = 0 \end{cases}$$

where $n(r)_{k,z}$ is the total flow of vehicles of type k in periods of flow condition z, and $n(r)_{i,k,z}$ is the equivalent volume of vehicles k in condition z in lane i. The condition

δ_{ij} is defined to ensure that $\bar{p}(r)$ is a stochastic matrix. The definition does not affect the result. It can be shown that the expression $\bar{p}(r)_{ij}$ such that

$$\bar{p}(r)_{ij} = \frac{\sum_{k=1}^{K} \sum_{z=1}^{Z} a(r)_{i,k,z} \cdot n(r)_{k,z} \cdot p(r)_{i,j,k,z}}{\sum_{k=1}^{K} \sum_{z=1}^{Z} a(r)_{i,k,z} \cdot n(r)_{k,z}}$$

is the only solution for $\bar{P}(r)$ that ensures that

$$\bar{a}(r+1) = \bar{a}(r) \cdot \bar{P}(r)$$

and

$$\bar{N}(r)_{ij} = \sum_{k=1}^{K} \sum_{z=1}^{Z} N(r)_{i,j,k,z}$$

A METHOD FOR APPROXIMATING A VARIABLE TRANSITION MATRIX

When the assumption of homogeneity for the transition matrix P is clearly invalid—e.g., over the section A-B in Figure 7, where the values of a(A) and a(B), P(A), and P(B) are not equal—the simple Markov chain of the preceding example becomes a non-homogeneous Markov process. Conceptually, this presents no particular problems, provided that the values of P(K) are known for all subsections K within A-B. Empirically, however, it presents a serious difficulty, as it is clearly infeasible to develop estimates of P(K) for each subsection.

The final section of this paper outlines a simple method for approximating the matrix P(I) by a "characteristic matrix," P(AB), representing the average transition probability for lane-changing with any single subsection K of the section A-B, such that n successive premultiplications of P(AB) by a(A) yield the vector a(B), where the number of subsections in A-B = n.

Assume that the values of a(A), a(B), P(A), P(B), n, q, and t are given. Assume that the aggregate lane-changing behavior over the N subsections of L length in A-B may be approximated by a single matrix P. Then the problem is to find a value of P such that

$$a(B) = a(A) \cdot P^n \tag{9}$$

where n is the number of subsections in A-B.

As there is usually no unique solution for P, some conditions must be imposed to obtain a suitable $P = \{p_{ij}\}$ that satisfies Eq. 9.

Assume that the intensity of lane-changing varies linearly between A and B, and that the vector a(K), K = 1, . . . , n is also approximately linear. Then, the first assumption implies that the average number of lane changes between lanes i and j in the section A-B is given by

$$nq\left[\sum_{k=1}^{n} a(K)_i \, p_{ij}\right] = nq\left[\frac{a(A)_i \, p(A)_{ij} + a(B)_i \, p(B)_{ij}}{2}\right] \tag{10}$$

Let

$$\bar{a}_i = \frac{1}{n} \sum_{k=1}^{n} a(K)_i$$

Then the second assumption implies that

$$\bar{a} = \tfrac{1}{2}\,[a(A) + a(B)] \tag{11}$$

From Eqs. 10 and 11

$$P_{ij} = \frac{1}{a(A)_i + a(B)_i}\left[\frac{a(A)_i p(A)_{ij} + a(B)_i p(B)_{ij}}{2}\right] \tag{12}$$

Using this approximation for P_{ij} in Eq. 9 gives

$$a(A)\,\hat{P}^n = \hat{a}(B) \tag{13}$$

where $\hat{P}$ is the first approximation for P from Eq. 12.

Usually $\hat{a}(B) \neq a(B)$, and the problem is now to find a better value for P such that $a(B) - \hat{a}(B) \to 0$. Let

$$a(B) - \hat{a}(B) = E \tag{14}$$

and

$$p_{ij} - \hat{p}_{ij} = \Delta p_{ij} \tag{15}$$

Define

$$E_{ij} = \bar{a}_j \cdot \Delta p_{ij} - \bar{a}_i \Delta p_{ij} = \text{the error in lane i caused by lane changes between lanes i and j.} \tag{16}$$

Then

$$E_{ij} = -E_{ji} \tag{17}$$

Because of the linearity assumption for a(K), Eqs. 14 and 16 give

$$\begin{aligned} E_i &= n[E_{i,\,i+1} + E_{i,\,i-1}] \text{ for } 2 \le i \le m - 1 \\ E_1 &= n\,E_{12} \\ E_m &= n\,E_{m,\,m-1} \end{aligned} \tag{18}$$

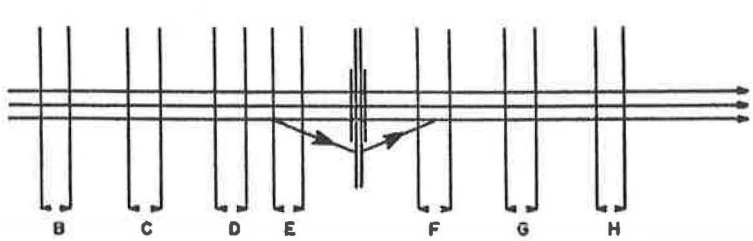

Figure 9. Highway section for calculation of characteristic transition matrix.

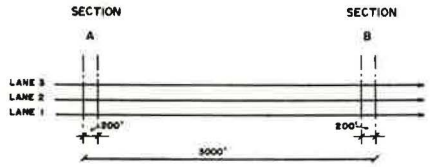

GIVEN:

$a(A) = (0.27050, 0.35880, 0.37070)$

$a(B) = (0.32170, 0.33530, 0.34300)$

$$P(A) = \begin{bmatrix} 0.98152, & 0.01848, & 0.00000 \\ 0.01324, & 0.97186, & 0.01490 \\ 0.00000, & 0.01026, & 0.98974 \end{bmatrix}$$

$$P(B) = \begin{bmatrix} 0.99043, & 0.00957, & 0.00000 \\ 0.02478, & 0.96463, & 0.01059 \\ 0.00000, & 0.01277, & 0.98723 \end{bmatrix}$$

$L = 200'$; $\mu = 15$

CALCULATE:

CHARACTERISTIC TRANSITION MATRIX FOR SECTION A-B, L=200':

$$\|P(A\text{-}B)\| = \begin{Vmatrix} 0.98713, & 0.01287, & 0.00000 \\ 0.02058, & 0.96949, & 0.00993 \\ 0.00000, & 0.01405, & 0.98595 \end{Vmatrix}$$

ERROR IN ESTIMATE OF a(B) USING $\|P(A\text{-}B)\|$:

$$\zeta = (-0.00126, +0.00314, -0.00188)$$

Figure 10. Calculation of characteristic lane-changing matrix.

If Eqs. 17 and 18 are used, the E_{ij} can be obtained from the E_i, which are known. Assume that the errors in P are proportional, i.e.,

$$\frac{\Delta p_{ij}}{\hat{p}_{ij}} = \frac{\Delta p_{ji}}{\hat{p}_{ji}} \qquad (19)$$

Then Eqs. 16 and 19 give

$$\Delta p_{ij} = \frac{-E_{ij}\hat{p}_{ij}}{\bar{a}_i\hat{p}_{ij} - \bar{a}_i\hat{p}_{ji}}$$

and

$$\Delta p_{ji} = \frac{E_{ji}\hat{p}_{ji}}{\bar{a}_i\hat{p}_{ij} - \bar{a}_j\hat{p}_{ji}}$$

A new estimate of $P = \hat{P} + \Delta P$ can then be computed and the process repeated until the system converges to an accurate estimate of P.

NUMERICAL RESULTS

Figure 9 shows a section of 3-lane, unidirectional freeway in Chicago for which a characteristic matrix $\|P\|$ was developed from data on lane-changing behavior derived from a series of time-lapse movie studies. Figure 10 shows the procedure used in the calculation of the matrix $\|P\|$. Closure in this case was achieved after 5 iterations, yielding a characteristic matrix $\|P\|$ that may be taken to represent the aggregate pattern of lane-changing per 200 ft over section A-B, a length of roughly 3,000 ft. $\|P\|$ represents the matrix of transition probabilities p_{ij}, defining the probability of changing lanes from lane i to lane j within a distance of 200 ft, such that successive multiplication of the known, initial lane distribution vector a(A) by $\|P\|$ yields an estimate of the known lane distribution a(B) at a point 3,000 ft downstream that is correct within a margin of ±5 percent.

Similar application of the model would yield a characteristic lane-change transition matrix for any section, or series of subsections, of road, given an initial and final lane distribution for the section and estimates of the lane-to-lane transition probabilities over short lengths of road at the section termini. The model thus provides a convenient descriptor of the pattern of lane-changing both at a point and along a section of road, which in turn provides a mechanism for comparing quantitatively the lane-changing characteristics associated with different roadway locations or different traffic conditions.

No attempt was made here to study the spatial autocorrelation of the matrices P_{ij} for contiguous road sections or to develop transition matrices for specific groups of vehicles, e.g., ramp vehicles. Equally, no attempt was made to calibrate and test the simple entrance and exit ramp models outlined previously.

CONCLUDING REMARKS

This paper has outlined a simple, macroscopic model of lane-changing on a multilane highway. The model is based on the interpretation of lane-changing as a stochastic process. It generates as output statements of both the frequency and the pattern of

lane-changing under varying road and traffic conditions. A series of illustrative examples have been provided, together with a limited empirical analysis, indicating the potential applicability of the model to highway design and capacity analysis.

Emphasis has been placed throughout on the description of lane-changing as a systematic characteristic of multilane flow. No attempt has been made to describe the reasons why drivers change lanes or to model the determinants of individual maneuvers.

The model suggests a number of intriguing possibilities for the practicing highway designer and traffic engineer. In its simplest form, for example, the notion of a Markovian, lane-to-lane, transition matrix provides the engineer with a convenient metric for describing lane-changing behavior and for drawing comparisons among lane-changing patterns.

ACKNOWLEDGMENT

The paper is based on research conducted in the Civil Engineering Department at Northwestern University in cooperation with the U.S. Department of Transportation, Federal Highway Administration, Bureau of Public Roads.

REFERENCES

1. Worrall, R. D., and Bullen, A. G. R. Lane-Changing on Multi-Lane Highways. Northwestern University, Evanston, Ill., final report for the U.S. Dept. of Transportation, 1969.
2. Highway Capacity Manual. HRB Spec. Rept. 87, 1965.

Acceleration Noise, Power Spectra, and Other Statistics Derived From Instrumented Vehicle Measurements Under Freeway Driving Conditions

J. F. TORRES, Transportation Systems Department,
System Development Corporation, Santa Monica, California

A standard passenger vehicle has been instrumented to measure fore-and-aft acceleration and velocity, and most significantly, a digital data recording and processing system has been developed and implemented that provides for convenient and rapid reduction of the measured data. This system, consisting of both hardware and software, has been checked out and debugged, and has been applied to the collection of a fairly extensive set of field data over a heavily traveled urban freeway. The most extensive subset of data was collected using six drivers, each on a different day, making eight runs for each direction of flow (during the morning peak traffic period). Statistics computed from the data included average acceleration, average velocity, standard deviation of acceleration (or acceleration noise), standard deviation of velocity, autocorrelation functions, power spectral densities, travel time, and distance traveled. Acceleration noise has been related to volume and density, and has been shown to have a correlation coefficient of 0.75 with travel time. Indications are that individual driver differences are more evident with acceleration noise than with travel time. Speed-volume-density relationships are also examined.

•ACCELERATION AND SPEED, as functions of time for individual vehicles, are important characteristics of traffic flow. Few data are available concerning these characteristics, let alone in-depth data. In order to obtain comprehensive measurements of acceleration and speed, there was a need for the instrumentation of a passenger vehicle with appropriate equipment to conveniently obtain such data. Special attention would have to be given to the generation of data in a form that would be more amenable to convenient analysis. Data reduction and data processing have been a particular bottleneck in the collection of such data in the past. It appeared that the techniques of digital recording and processing could be well applied to the problem.

Certain statistics of vehicular acceleration and velocity are of particular interest in studies of traffic operations. Among these are the means, variances, autocorrelation functions, and power spectral densities of acceleration and velocity. Acceleration noise, a traffic performance measure of increasing interest, is defined as the standard deviation of the acceleration process (1). With the availability of measured time series of acceleration and velocity, attention could also be profitably directed to the development of computer software that would compute selected statistics. Software would also have to be developed to ensure the reliable use of digitally recorded data; for example, through a program that would edit the recorded data, which might have erroneously recorded data sequences, into a computer-compatible format.

Paper sponsored by Committee on Characteristics of Traffic Flow and presented at the 49th Annual Meeting.

OBJECTIVES OF THE STUDY

The overall objective of the study was to address the stated need for individual vehicle's motion characteristics data. A research program was conducted to investigate the fore-and-aft vehicle motion characteristics in the traffic environment of selected sections of some heavily traveled urban freeways.

The program was oriented, primarily, to satisfy the needs of a broader program of study, "Analytical Models of Unidirectional Multi-Lane Traffic Flow," conducted for the U.S. Bureau of Public Roads. Among the applications for this data collection system would be

1. Validation of various car-following models;
2. Setting up the parameters of a program for estimating positions and velocities from aerial photographs; and
3. Estimation of the errors in the aerial data collection system by providing a method for measuring the velocity-time curve that is independent of the aerial photography method.

It is expected that the availability of this system will stimulate other applications.

The conduct of this research program first required the development of an appropriate set of research tools. In particular, the detailed objectives of the study were the following:

1. Instrument a standard passenger vehicle to measure and record, in a convenient form, (a) fore-and-aft acceleration and (b) fore-and-aft velocity, independently, as functions of time.
2. Develop and check out computer software to reduce and process the measured data in order to produce, in printout or plot form or both, the following statistics: (a) mean and variance of the measured acceleration data; (b) mean and variance of the measured velocity; (c) autocovariance and autocorrelation of acceleration; (d) autocovariance and autocorrelation of velocity; (e) power spectral density of acceleration; (f) power spectral density of velocity; (g) travel time of each measured run; and (h) distance traveled for each run.
3. Collect a fairly extensive set of field data that would be representative of conditions on heavily traveled urban freeways, through the use of the vehicle-software system.
4. Examine the distributions of acceleration and velocity, and their relationship to traffic, for a sample of the collected field data. Test the hypothesis of normality for acceleration.
5. Examine the effect of traffic on the autocorrelation function.
6. Examine the effect of traffic and vehicle operation on the power spectral density.
7. Relate acceleration noise to traffic density and traffic volume.
8. Relate travel time and average speed to traffic volume. Also examine the speed-flow-density relationships.

The spectral analysis was expected to give a more informative and convenient way of comparing the various time series obtained from the experimental program. It can be shown by a well-known theorem that the integral of the power spectral density is equal to the acceleration noise. Thus, the power spectral density is generally expected to provide more information. The power spectral density presents, in a compact form, the characteristics of a time series in the frequency domain. Formally, it is the Fourier transform of the autocorrelation function. The distribution of power, particularly for the acceleration time series, was expected to vary over the frequency axis, depending on the prevailing traffic conditions and on the driver and road environment.

EQUIPMENT AND INSTRUMENTATION DESCRIPTION

The test bed vehicle selected for instrumentation is a standard 1967 Plymouth sedan. The total instrumentation system installed in the vehicle includes the following major components:

1. A Systron-Donner servo-accelerometer (with a range of ± 1 g);
2. A Labeco fifth-wheel device;
3. Optysin shaft angle encoder;
4. A digital data processor, ITC Model 8110;
5. A Deltacorder Model II incremental magnetic tape recorder;
6. Argo-Kienzle tachograph;
7. Control boxes on the vehicle dashboard;
8. Supporting power supplies and cables; and
9. A radio transmitter-receiver.

The servo-accelerometer is located on the floorboard right behind the front seat, along the vehicle's fore-and-aft axis. The digital processor is located right behind it, with the tape recorder sitting on top of the processor. The tachograph is installed in the trunk area. The fifth-wheel device is hinged, so that it can be retracted back over the trunk when not in use. The instrument controls are conveniently located below the dashboard.

The digital data processor is a special-purpose piece of equipment that was developed to record acceleration and velocity data in a form that can be readily processed by a general-purpose digital computer.

An analog-to-digital converter is used to convert the accelerometer analog voltage outputs into digital form. A series of pulses is generated, which is proportional to the distance traveled (over a given increment of time), through an Optisyn shaft angle encoder that is mechanically connected to the fifth wheel. This provides the speed measurements. The output data from the digital processor are recorded incrementally, every prescribed time increment on a 7-track magnetic tape on a 6-in. minireel. The tape recoder (a Deltacorder digital incremental recorder) records at 200 bpi (bytes per inch). The Argo-Kienzle tachograph is employed as back-up equipment for velocity measurement; the device is attached to the speedometer cable connector.

Two modes of operation are available through a switch on a control box on the dashboard: the recording of both acceleration and velocity, and the recording of only acceleration. For the first mode, the recording time increment is $^2/_{10}$ sec. For the second mode, the recording time increment is $^1/_{10}$ sec.

Figure 1 shows the functions performed by the digital processor on the acceleration and velocity data. The figure also suggests data link communication with a helicopter.

The tape record is formatted in terms of 6-byte words with one decimal digit per byte. The first recorded word is the manual data word, where the first 4 bytes denote header data and the fifth byte describes the fifth-wheel in or out. The sixth byte is a dummy. Acceleration and velocity are then alternately recorded, as 6-byte words, whenever the fifth-wheel is indicated to be on. The first byte for acceleration describes the sign, the next 3 describe the magnitude, and the last 2 are dummy characters.

Three decimal digits of precision appear to be adequate for the vehicle performance studies that are considered to be of interest. This precision implies that velocity can be recorded to within 0.2 ft/sec and acceleration can be recorded to within 0.001 g (or 0.32 ft/sec^2). This velocity precision figure follows from the fact that the shaft angle encoder generates 50 pulses per foot of wheel travel, and we can resolve no better than one pulse for each 0.1 sec (incremental recording period).

SOFTWARE DESCRIPTION

Computer programs were developed to reduce and process the data collected with the instrumented vehicle. The programs were developed for operation on the IBM 7094. Two kinds of programs were required: assembly language programs and FORTRAN programs. These programs are as follows:

1. A program to print out the contents of the raw data (tape dump), formatted into 6-character words. This is necessary in order to check the integrity of the data recorded on the tapes.
2. A program to process the raw data tapes from the instrumented vehicle and prepare it into FORTRAN-compatible binary tapes. A distinctive feature of this program

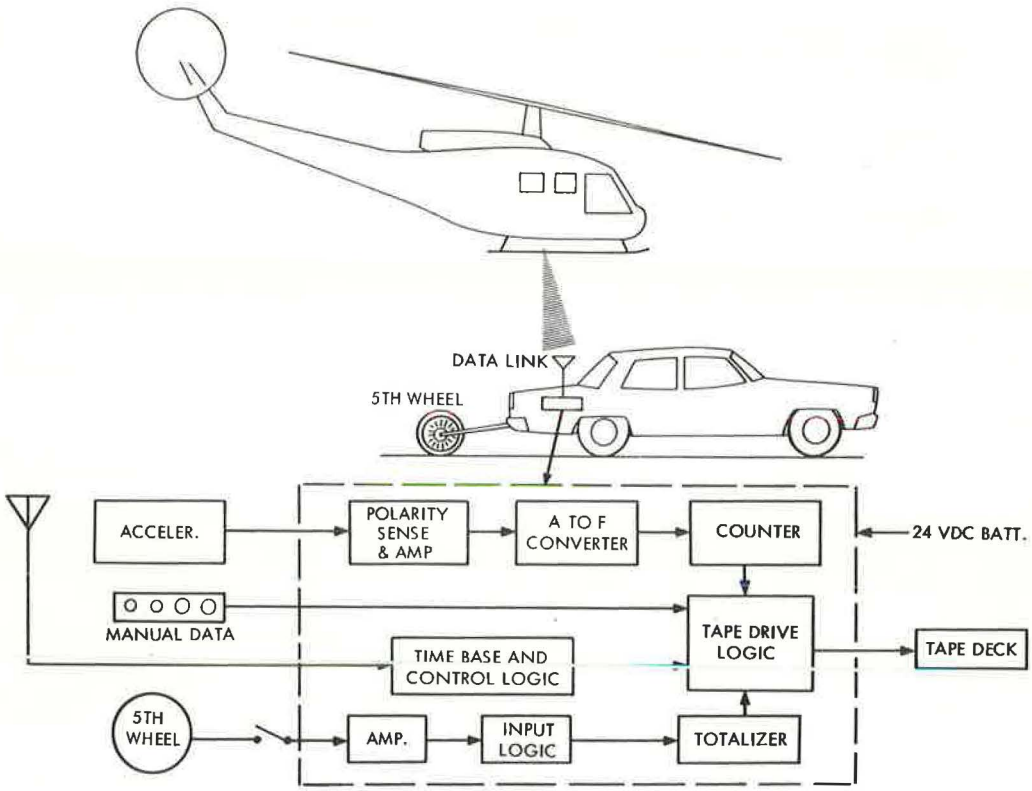

Figure 1. Block diagram of processing function.

is that it can detect data coding errors that may occasionally arise from the vehicle instrumentation, and then perform remedial action by editing out those errors, at the same time retaining the integrity of the remainder of the data. This program has been coded in IBM 7094 macro-assembly language. Free use is made of information relevant to the IBM 7094-specific hardware configurations, including data channels and tapes.

3. A program, coded in FORTRAN IV, to process the tapes obtained with the program, to print out and plot acceleration, velocity, and the autocorrelation functions and autocovariances of each. The program also computes and prints out the power spectral density of acceleration data that have been first processed to eliminate slow trends that are not pertinent to the driver-traffic interactions. Other outputs of the program include travel time and distance traveled.

4. A program, coded in FORTRAN IV, to generate an artificial random series with a known autocorrelation function (and, consequently, a known power spectral density). This program was used to check out the foregoing program.

5. A program, coded in FORTRAN IV, to produce histograms for the acceleration and velocity data.

Some of the details on key processing aspects of these programs will be discussed in subsequent sections. It is pointed out that printouts or computer plots, or both, of the processed data are obtainable with the system available.

FIELD DATA COLLECTION

Essentially, three sets of detailed field data have been collected with the instrumented vehicle, the last set being the most extensive set. The three sets consist of:

1. A set of 14 runs, 7 for each of two drivers, made on a section of the Ventura Freeway approximately 1 mile in length during the morning peak traffic period. Traffic counts were taken corresponding to the passage of the vehicle past the counting site.
2. A set of 7 runs made with one driver on a section of the San Diego Freeway approximately 2 miles in length. These data were used as a basis for conclusions by Breiman (2).
3. Six sets of 16 runs, each set corresponding to a different day, on a section of the Ventura Freeway approximately 2 miles in length (four lanes in each direction). The runs were made during the morning peak traffic period from 7:00 a.m. to 9:30 a.m. A different driver was used for each set. Eight runs of each set were made in one direction; the remaining 8 were made in the other direction. Traffic counts were made over a 5-minute period that was synchronized with the passage of the test vehicle by the counting site.

The procedure that was followed in each run was to enter the freeway and start the data-recording after the vehicle was well beyond the on-ramp acceleration lane. This was designed to minimize any on-ramp artifacts. Similarly, the recording of data was stopped well before the vehicle was ready to exit on the off-ramp. After exiting on the off-ramp, the drivers were typically allowed to rest for about 3 to 4 minutes at a convenient spot on or off the arterial, before proceeding to enter the freeway again for the next run. The drivers were instructed to drive over the test site as they normally do. As a consequence of this, an appreciable amount of lane-changing and passing was observed.

An observer-experimenter accompanied the driver; his functions included the operation of the data-collection equipment and the proper scheduling of the runs. On the extensive last set of runs, he also coordinated, by radio communication, the traffic counts taken by a ground observer, so that the traffic counting period could coincide with the time of passage of the test vehicle past the counting site.

The basic measurements available for the most extensive set of field tests are (a) fore-and-aft acceleration, (b) fore-and-aft velocity, (c) travel time, (d) distance traveled, and (e) 5-minute traffic counts. All statistics and inferences were derived from these five basic measurements, supplemented by the experimenter-observer's observations for each run.

On the first two sets of runs, it was observed that grade variations were significantly reflected into the measurements of acceleration (because the servo-accelerometer also measures the g-force component). Because this acceleration component is not the consequence of driver actions, such as throttle or brake applications, it was felt to be desirable to remove this "trend" from the set of measurements. The removal of this "trend" also satisfies the requirements for performing a spectral analysis of the acceleration series corresponding to each run. The full spectral analysis was performed on only the last set of data, which is also the most extensive data set.

DATA PROCESSING PROCEDURES

Preliminary Processing of Acceleration Series

The detrending of the acceleration series was achieved through the application of a triangular weighted moving average to the original series. A new series was then given by the differences between the original series and the moving average. The average should be taken over a time interval large enough not to obscure local effects, such as those due to dynamic interactions with the road traffic, but small enough to account for the varying grades. A triangular weighted moving average seems to be the most appropriate, which would give the greatest weight to the point being estimated and zero weight to the two end points. An average over a 30- to 60-second time period seems adequate for this type of weighting function. Before applying the moving average, the original series would first have to have a "correction" applied to each end.

The procedure first requires obtaining the average over the initial T seconds of the series. The original acceleration time series, a(t), is shown in Figure 2 and extends

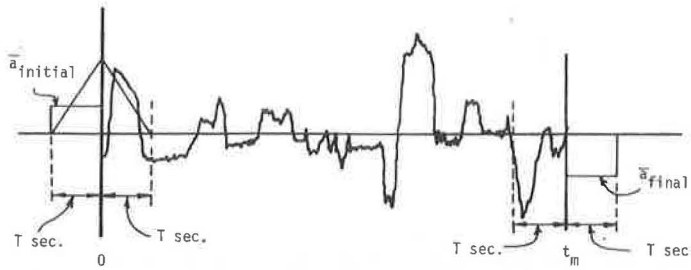

Figure 2. Preparation of record for filtering.

from 0 to t_m. The average over the first T seconds is added as a constant value to the left end of the series, over a T-second interval and is denoted as $\bar{a}_{initial}$, where

$$\bar{a}_{initial} = \frac{1}{T}\int_0^T a(t)\,dt$$

Similarly, the average over the last T seconds of the series

$$\bar{a}_{final} = \frac{1}{T}\int_{t_m-T}^{t_m} a(t)\,dt$$

would be added as a constant value to the right end of the original series. The new series is now $t_m + 2T$ seconds in length.

The moving average, with triangular weighting, is now computed over this modified series. The initial computation gives the average value for t = 0. The triangular weighting function is shown in Figure 3, corresponding to $\hat{a}_i$. The triangular weighted average $\hat{a}_i$, corresponding to the value $t_i = i\Delta t$, where $\Delta t = 0.2$ second, is given by

$$\hat{a}_i = \frac{1}{150}\left(\frac{1}{150}a_{i-149} + \cdots \frac{149}{150}a_{i-1} + a_i + \frac{149}{150}a_{i+1} + \cdots \frac{1}{150}a_{i+149}\right)$$

where $a_i = a(t_i)$. Thus, in the estimation of $\hat{a}_i$, the ith value of a is given the maximum weight, and values to the left and right of the ith value are given proportionately smaller values depending on the distance from a_i. This filtered acceleration time series is expressible in the following compact general form:

$$\hat{a}_i = \sum_{j=-150}^{j=150} a_{i-j}h_j$$

where

$$h_j = \frac{1}{T}\left(1 - \frac{|j\Delta t|}{T}\right), \text{ and}$$

$$j = -150, -149, \ldots, -1, 0, 1, \ldots, 149, 150.$$

In the particular case that we have considered, T = 30 seconds and $\Delta t = 0.2$ second.

If a_i represents the original series, the detrended series is then given by $a_i' = a_i - \hat{a}_i$. The detrending process acts as a high-pass filtering operation on the original series.

The low-frequency variations are attenuated. It thus has an effect on the power spectrum of the measured acceleration series and on its variance. It is of interest to determine the filtering effect on the original series.

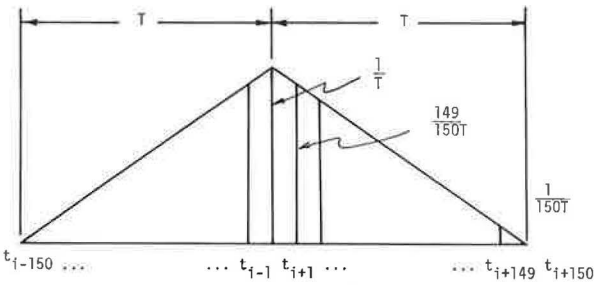

Figure 3. Weighting function.

The High-Pass Filtering Effect

The effect of detrending (or, equivalently, high-pass filtering) is examined by making use of the continuous case representation for the filtering operation. Thus, the analog to the discrete series is given by

$$\hat{a}(t) = \int_{-\infty}^{\infty} a(t - \tau)h(\tau)d\tau$$

where $h(t) = \frac{1}{T}\left(1 - \frac{|t|}{T}\right)$.

With $\omega = 2\pi f$, let

$$H(f) = \int_{-\infty}^{\infty} h(t)e^{-i\omega t}dt$$

$$= \left(\frac{\sin \pi fT}{\pi fT}\right)^2$$

It then follows from standard spectral analysis theory that the power spectrum of the filtered acceleration process $a(t) - \hat{a}(t)$ is given by

$$P(f) = |1 - H(f)|^2 P_r(f)$$

where $P_r(f)$ represents the power spectrum of the raw (unfiltered) data and is described by

$$P_r(f) = \int_{-\infty}^{\infty} R_r(\tau)e^{-i\omega\tau}d\tau$$

where $R_r(\tau)$ is the autocovariance function, $R_r(\tau) = E\{a(t)a(t + \tau)\}$.

Denote the power transfer function by $G^2(f) = |1 - H(f)|^2$. The graph of this transfer function is shown in Figure 4. From this graph it can be seen that, for practical purposes, the frequency contributions occurring at $fT < 1$ are rejected by the filtering process. More precisely, because $T = 30$ seconds for the application employed, then only those frequency contributions such that $f > 1/30$ cps are the elements in the original series retained by the filtering process.

These frequency contributions that are retained are principally comprised of those that are associated with the driver actions in the traffic environment. However, it is also expected to include those frequency contributions that result from the vehicle-

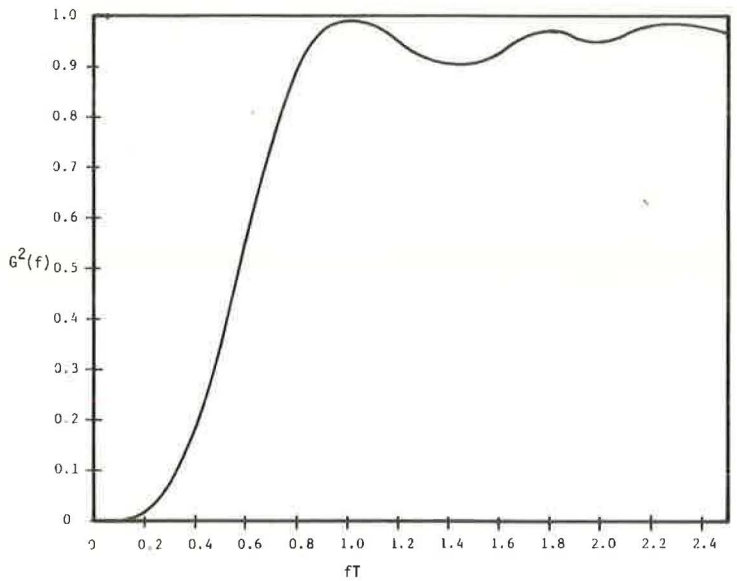

Figure 4. Transfer function characteristics for high-pass filter.

highway interactions. For example, it may include vehicle pitching contributions caused by the roughness of the road or by wind buffeting. These will occur, however, at a frequency range significantly higher than the frequency range corresponding to that for driver actions.

An estimate can be made of the decrease in the variance caused by the high-pass filtering process. Recalling that $a'(t) = a(t) - \hat{a}(t)$, then

$$E\left\{a'(t)^2\right\} = \int_{-\infty}^{\infty} |1 - H(f)|^2 P_r(f)\, df$$

If we denote the change in variance by $\Delta\sigma^2 = E\left\{a^2\right\} - E\left\{a'^2\right\}$, then

$$\Delta\sigma^2 = \int_{-\infty}^{\infty} H(f)\left[2 - H(f)\right] P_r(f)\, df$$

And if we assume that $R(t) = \sigma^2 e^{-\gamma|t|}$, which is the approximate shape that the auto-correlation function is observed to have, then it can be shown that

$$\frac{\Delta\sigma^2}{\sigma^2} = \frac{8}{3\gamma T}$$

Then, for a typical $\gamma = 0.5$ and $T = 30$ seconds,

$$\frac{\Delta\sigma^2}{\sigma^2} = \frac{8}{145} = 0.178$$

or about 18 percent.

The Autocorrelation Function and Spectral Analysis

The approach taken to perform the spectral analysis follows Blackman and Tukey (3). The autocovariance of the acceleration series is first computed:

$$R(\tau) = \frac{1}{n-p} \sum_{i=1}^{n-p} \alpha_i \alpha_{i+p}$$

where $p = 0, 1, 2, \ldots, m$, $\tau = p\Delta t$, and $m\Delta t$ is the maximum lag considered, which was chosen to be 40 sec (conservatively to resolve narrow spikes), and where

$$\alpha_i = a_i - \bar{a}'$$

$$\bar{a}' = \frac{1}{n} \sum_{i=1}^{n} a_i'$$

and $n\Delta t$ is the total length of the original series. The incremental lag is represented by Δt and in this program takes on either one of two values: 0.1 or 0.2 second, depending on the mode of operation chosen for the equipment in the vehicle. The autocorrelation function is given by

$$r(\tau) = \frac{R(\tau)}{R(0)}$$

The smoothed ("hamming") estimates of the power spectral density are given by

$$P(0) = 0.54Q(0) + 0.46Q(1)$$
$$P(h) = 0.23Q(h - 1) + 0.54Q(h) + 0.23Q(h + 1)$$

for $0 < h < m$, and

$$P(m) = 0.54Q(m) + 0.46Q(m - 1)$$

where

$$Q(h) = \frac{2\Delta t}{\pi} \sum_{p=0}^{m} \epsilon_p r(p\Delta t) \cos \frac{hp\pi}{m}$$

for $h = 0, 1, \ldots, m$ and where

$$\epsilon_p = \begin{cases} 1, & 0 < p < m \\ 1/2, & p = 0, m \end{cases}$$

We note that the frequency, f, in cycles per second depends on h and is given by

$$f = \frac{h}{2m\Delta t} \text{ cps}$$

In particular, in our case, $f = \frac{h}{80}$ cps, where $h = 1, 2, \ldots$. In terms of radians per

second, frequency is given by $\omega = 2\pi f$. We have used a well-known theorem to provide a gross check on the computations. This theorem (3) states that the autocovariance for lag zero is equal to twice the integral of the power spectrum, over its positive domain of definition. Thus, the sum

$$\frac{\pi}{m\Delta t}\left\{\frac{1}{2}\left[P(0) + P(m)\right] + \sum_{h=1}^{m-1} P(h)\right\}$$

should equal one (because we have chosen to work with the autocorrelation function, rather than with the autocovariance).

Acceleration Noise

Acceleration noise is defined as σ_a, where

$$\sigma_a^2 = \frac{1}{t_m}\int_0^{t_m} a^2(t)dt - \left[\frac{1}{t_m}\int_0^{t_m} a(t)dt\right]^2$$

We note that σ_a^2 is related to the value of the autocovariance for $\tau = 0$, $\sigma_a^2 = R(0)$. This measure will be used in subsequent discussions as an indication of traffic operations performance.

RESULTS FROM ANALYSIS OF THE FIELD MEASUREMENTS

The results to be presented in the following discussion will concentrate primarily on the last experimental program, which provided the most extensive set of data by far. This experimental set was also able to take advantage of the increased precision that was introduced into the equipment in the latter stages of the study. The discussion will not necessarily follow the order in which the data were collected.

Attention will first be focused on general properties of the data that were collected. Relationships and inferences obtained from these basic data will be subsequently discussed.

TABLE 1

SUMMARY DATA SET FOR DRIVER 2

Trip No.	Mean Raw Acceleration (ft/sec²)	σ Smoothed Acceleration (ft/sec²)	Mean Velocity (ft/sec)	σ Velocity (ft/sec)	5 Minute Traffic Count	T-Time/ Mile (sec)	Estimated Density (vehicle/mile)	τ (sec)
			Eastbound					
201	0.14	1.46	27.38	15.25	547	192.5	350	2.5
203	0.09	0.36	44.77	6.56	629	118.0	147	2.3
205	0.25	0.83	46.03	7.17	617	114.5	236	2.0
207	0.24	1.32	43.07	10.96	640	122.5	262	2.2
209	0.22	1.55	37.77	15.21	607	139.5	282	2.6
211	0.21	1.09	41.73	11.48	599	127.0	254	2.1
213	0.23	1.42	29.13	15.21	522	181.5	316	2.2
215	0.20	1.64	45.14	18.54	418	117.5	164	2.4
			Westbound					
202	0.21	0.47	87.74	4.90	329	60.3	66.2	0.2
204	0.23	0.52	84.19	3.67	460	62.7	96.2	1.7
206	0.37	0.58	81.49	6.40	574	65.0	124.2	2.0
208	0.48	0.91	89.96	7.15	384	59.0	150.8	2.2
210	0.21	0.87	88.27	4.47	414	60.0	163.6	1.8
212	0.40	0.77	93.58	7.45	438	57.0	83.2	1.6
214	0.29	0.60	92.77	7.26	365	56.0	68.2	0.7
216	0.41	0.76	94.53	6.92	319	55.0	58.6	1.6

General Properties of the Data Collected

A summary data set corresponding to one of the six drivers that was used in the last experimental program is given in Table 1. The data were subdivided into eastbound runs and westbound runs, because the morning peak-hour traffic was in the eastbound direction and differences were expected between the two groups. Each column on the table presents, in respective order,

1. Trip number identification (in chronological order);
2. Mean raw acceleration, before filtering, in ft/sec^2;
3. Standard deviation (or acceleration noise) of the filtered acceleration series, in ft/sec^2;
4. Mean velocity, in ft/sec;
5. Standard deviation of velocity, in ft/sec;
6. Five-minute unidirectional traffic count at the test site;
7. Travel time per mile, in sec;
8. Estimated traffic density, in vehicles/mile; and
9. Correlation time, in sec.

Traffic density was estimated by multiplying the measured traffic volume by the travel time of the vehicle corresponding to that time period. This estimate is expected to be slightly biased, depending on the driver. It was observed that, under similar traffic conditions, some drivers tend to drive slightly faster than others. Correlation time is defined to be that time lag at which the autocorrelation function attains the value 1/e.

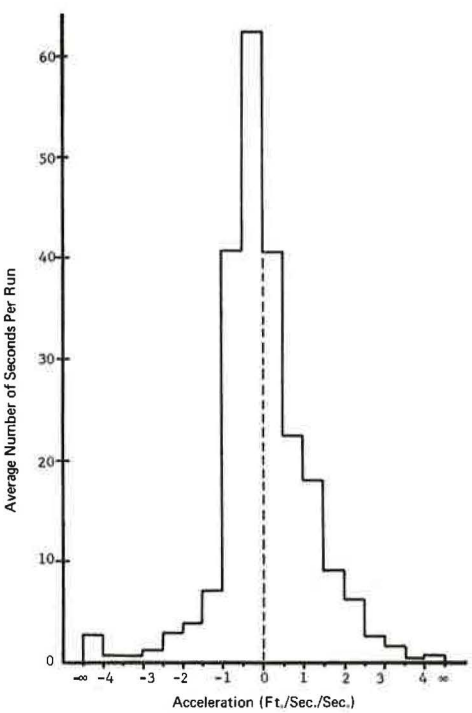

Figure 5. Acceleration histogram for the average over three runs at high density: average concentration = 252 vehicles/mile; average 5-minute volume = 625 vehicles; and average acceleration noise = 1.203 ft/sec2.

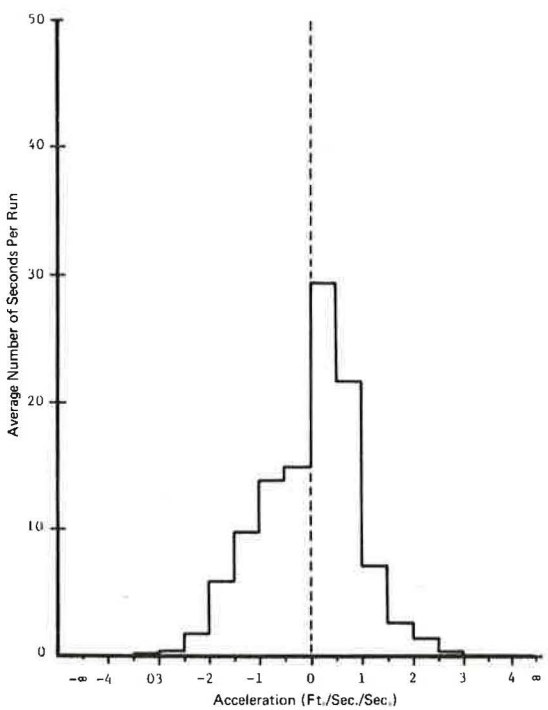

Figure 6. Acceleration histogram for the average over three runs at low density: average concentration = 71.1 vehicles/mile; average 5-minute volume = 400 vehicles; and average acceleration noise = 0.91 ft/sec2.

The means of the raw acceleration curves were observed to be positive in every case. This implies that the accelerometer was not properly calibrated after the final equipment modifications on the instrumented vehicle. This bias, however, is not expected to affect the inferences on the data since the acceleration series is filtered through a high-pass filter.

The manner in which the data were digitally processed made it relatively convenient to obtain histograms on the frequency of occurrence of acceleration and velocity values. Histogram data were developed for a sample of runs corresponding to half of the driver set. A specially developed computer program was used to process the data into the required form. Some expected variation was found between the histograms corresponding to each run. However, the tendency was for the shape and location of the histograms to follow a similar pattern for similar traffic conditions.

Tests for normality, using the modified χ^2 test (4), were applied to several of the acceleration histograms. Typically, the hypothesis of normality had to be rejected for these tests, at a significance level of 1 percent.

A sample of some of the acceleration and velocity histograms is shown in Figures 5, 6, and 7. Figures 5 and 6 show acceleration histograms for one driver, each for different traffic conditions. The average over three homogeneous runs has been taken for each case in order to give a more representative result. Figure 5 shows the distribution corresponding to a fairly heavy vehicle concentration; it is positively skewed, with the mode between - ½ and 0 ft/sec^2. Figure 6 shows the distribution corresponding to a low vehicle concentration; it is negatively skewed, with the mode between 0 and ½ ft/sec^2. We also note that the acceleration noise is higher for the high concentration case.

In one run, when a driver was instructed to try to maintain a constant speed of 65 mph (by his speedometer) throughout the extent of the test section, under low concentration traffic conditions, this resulted in considerably lower dispersion in acceleration, generally within ± 0.5 ft/sec^2.

A sample of velocity histograms is presented in Figure 7. Two concentration levels are represented on the graphs (a high and a low level). The average over three homogeneous runs is used for each case. The average velocity is also indicated for each case.

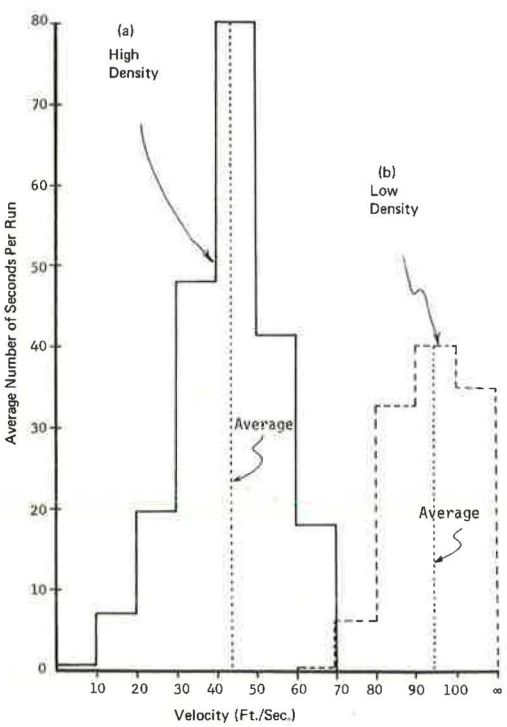

Figure 7. Velocity histograms for two traffic conditions at (a) high density with an average for three runs, average density = 252 vehicles/mile; and (b) low density with an average for three runs, average density = 74.4 vehicles/mile.

Results of the Spectral Analysis

A small sample of power spectral densities and autocorrelation functions, for some data sets corresponding to some representative situations, is shown in Figures 8, 9, and 10 to exemplify the kind of results that we obtained for this extensive set of runs. We first point out that an objective of performing this spectral analysis was to observe the driver-vehicle contributions due to driving under varying traffic conditions. It was assumed that no significant driver-vehicle spectral contributions would occur at frequencies above 1 cycle per second. Hence, with a sampling interval of 0.2 sec, no aliasing would be expected from these contributions because the "cutoff" frequency is

$$f_0 = \frac{1}{2\Delta t} = \frac{1}{0.4} = 2.5 \text{ cps}$$

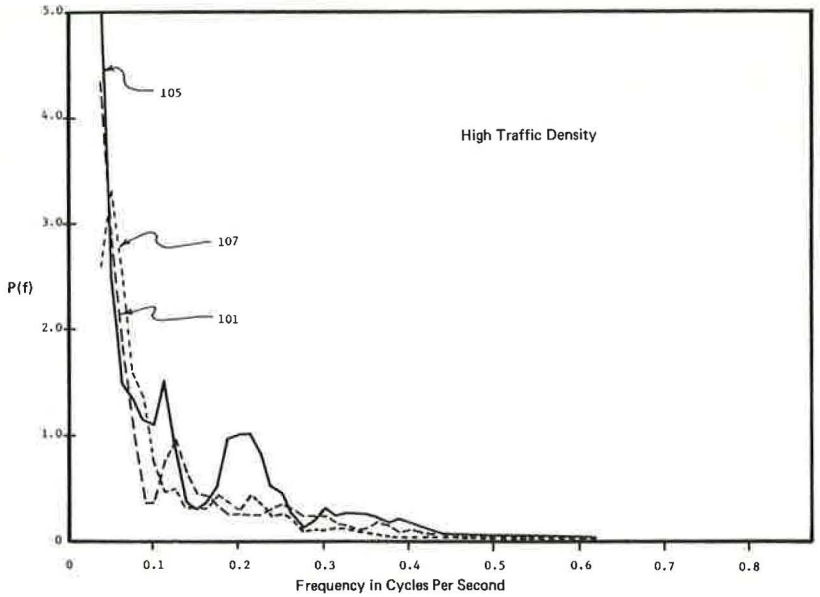

Figure 8. Power spectral densities for three runs at high density.

Also, because we have passed the autocorrelation series through a high-pass filter (to attenuate the changing grade effects), then only those frequencies f > 0.033 cps are pertinent for representation. Hence, all graphs are plotted from this left end-point. Frequency resolution is about 0.025 cps.

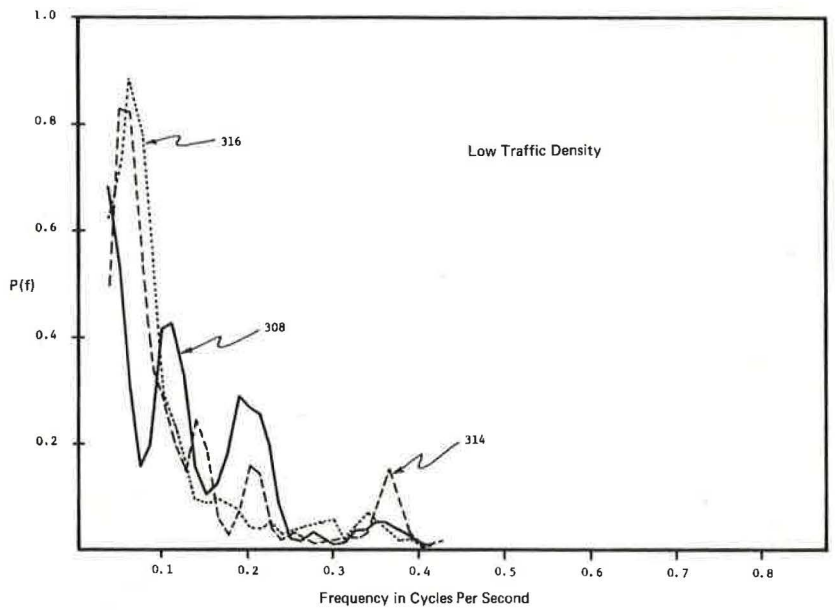

Figure 9. Power spectral densities for three runs at low density.

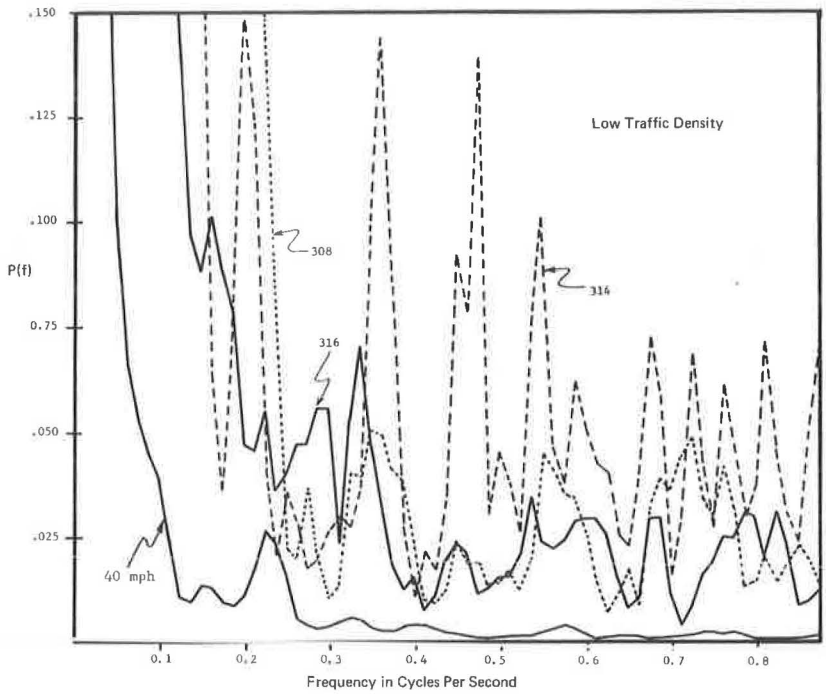

Figure 10. Power spectral densities for three runs and controlled 40-mph run.

Figure 8 shows a typical array of power spectral densities for a specific driver, driving in a high traffic concentration environment. We observe that most of the power is concentrated in the frequency range below 0.4 cps. The spectral density then tapers off to a negligible value for the higher frequencies.

Figure 9 shows a set of three power spectral densities for a specific driver driving under relatively low traffic density conditions. A large proportion of the power is once again concentrated in the frequency range below 0.4 cps. However, the proportion of power in this range seems to be significantly less than for the set of spectra at high traffic densities. Nevertheless, this supports the hypothesis that the power associated with driver actions in any driving situation is concentrated in the frequency range below 0.4 cps. An amplified look of the frequency contributions in the higher frequency range is shown in Figure 10 (which we note has a new ordinate scale). The large power contributions at the higher frequencies are evident.

It is hypothesized that the higher frequency contributions may depend on the vehicle speed in combination with one or more of several other factors, such as (a) road roughness, (b) vehicle suspension and structural system, and (c) wind buffeting. The effect of speed is definitely demonstrated by observing the power spectral density obtained for a run where the driver was instructed to try to maintain a constant speed of 40 mph, at low traffic density conditions. The difference in the power spectral densities at the higher frequencies is quite significant between the controlled run and the other runs. The other three runs were made at an average velocity of 65 to 70 mph. We point out that run 314 has unusually higher peaks than any of the other runs. This may be due to the particular lane that the driver chose for that particular run, or to some of the other factors noted or not yet identified. We note that aliasing may be playing a role here, also.

A sample set of autocorrelation functions is presented in Figure 11. Curves 105 and 107 correspond to high traffic density situations. Curve 116 corresponds to a low traffic density situation.

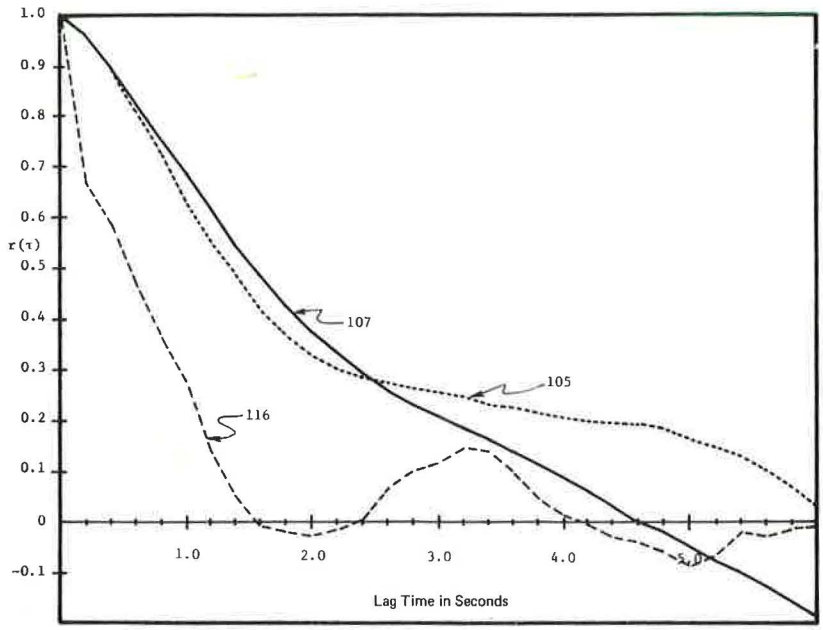

Figure 11. Autocorrelation functions for three runs.

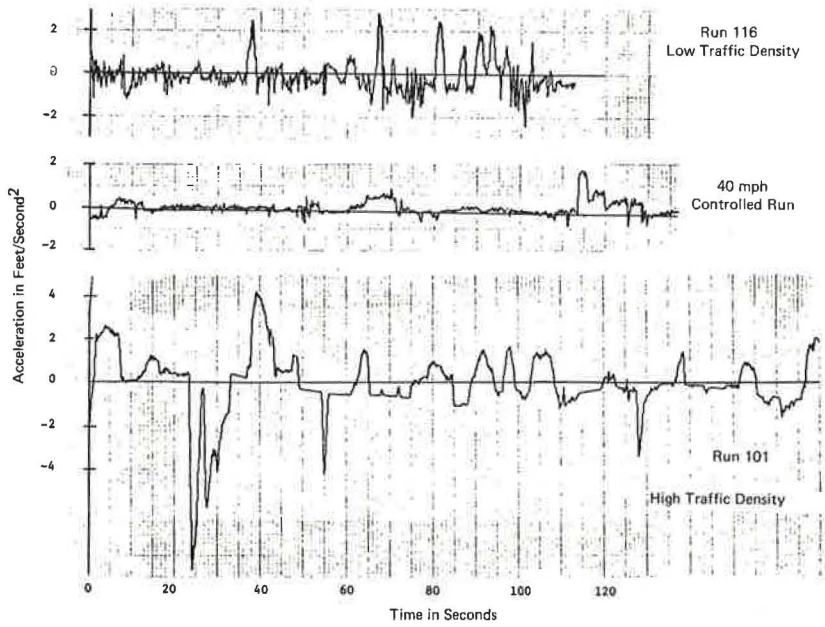

Figure 12. Acceleration versus time computer plots.

Some Sample Computer Plots

A sample of the computer plots obtainable with our system is presented in Figure 12. Three acceleration records are shown for varying traffic conditions, for a given driver. Note the increased high-frequency noise for low-density traffic (high-speed). Similar computer plots can be generated for velocity.

RELATIONSHIPS BETWEEN VARIABLES

The relationships between speed, volume, and density have been under study for some time by traffic researchers. Also, speed, or equivalently travel time, is often used as a measure of traffic performance. In such cases, it is not unusual to try to infer these performance measures from volume or density or both. Acceleration noise is also believed to be a good measure of traffic performance. It is of interest to examine the relationship between this measure and some of the more common traffic variables that we have also measured with our instrumented vehicle. Some of the relationships that we have investigated for the data collected and processed under this experimental program are discussed in the following.

We first note that, in assessing the performance of a given facility, for example in terms of travel time, an estimate must be derived that is representative of the population that is being sampled. Hence, the more reliable estimates are those based on large samples. That is to say, measurements should be made on samples comprised of a large number of vehicles. However, in some cases, reasonable estimates of performance can be derived by using a few, or possibly even one, sampling vehicle (when we talk of vehicle, we are actually referring to the driver-vehicle combination; in fact, the driver usually plays the key role in the performance of the vehicle under typical traffic conditions). These few vehicles would perform several run replications over the test site, and thus obtain a sample that will provide a representative sample of the

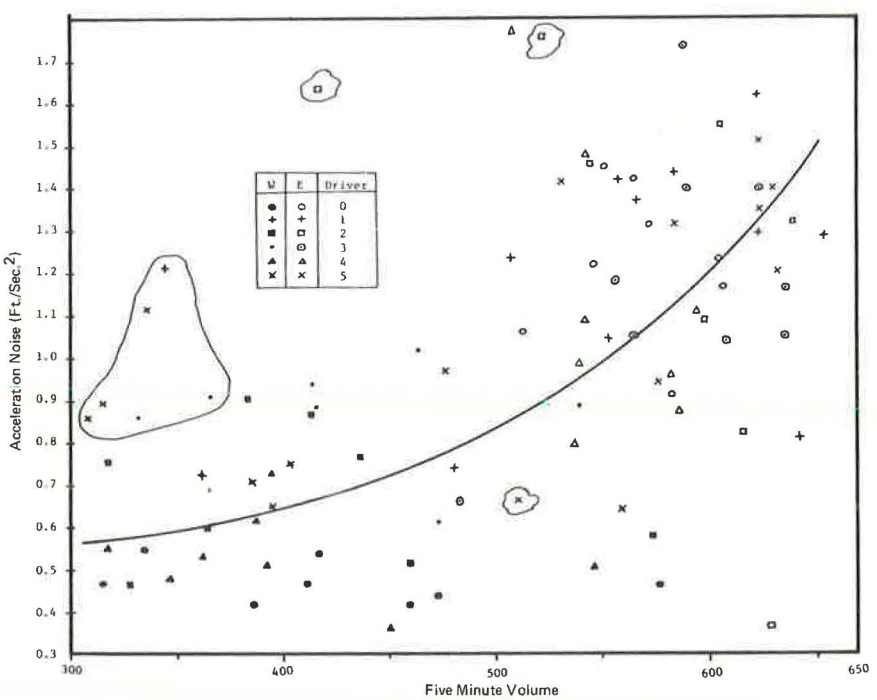

Figure 13. Acceleration noise versus volume.

traffic conditions. Our approach, of course, uses our instrumented vehicle, operated by several drivers, each making several runs.

The first relationship that is noted to be of interest is that between acceleration noise and traffic volume (Fig. 13). The individual points corresponding to each observation (average over a run) are plotted and each driver is distinguished by a different symbol. The direction of motion is also distinguished. Certain individual observations were made while there was a traffic incident (such as an accident) at some point along the test site; these are singled out by an irregular contour around them and are censored out in the development of the trend line.

Acceleration noise as well as other factors (5) can be considered to be a measure of driver effort or driver stress. Thus, as the geometrics of the highway change, or as the prevailing traffic conditions change, the driver is forced to take action in order to adapt himself to his dynamically changing immediate environment. The measurement equipment, however, also measures road-vehicle interactions, which are essentially extraneous to the driving task. The amount of this contribution, as noted, depends on the road, speed, and other factors. If the objective is to infer driver effort from the acceleration measurements, then those values that are biased heavily by road-vehicle interactions should be censored from the observation set. Some of the values that have been observed to have these heavy biases have been identified and censored out and are shown enclosed by an irregular contour; these naturally occur at the low-volume end where the high speeds typically occur. A trend line has been fitted using a least squares criterion to the set of points exclusive of the censored points, to indicate the relationship to volume (however, the dispersion is so large that the line is somewhat arbitrary).

A comparison of this relationship with that of travel time versus volume can be made by referring to Figure 14. We point out that each measurement of travel time and acceleration noise was made simultaneously during the trip of the instrumented vehicle;

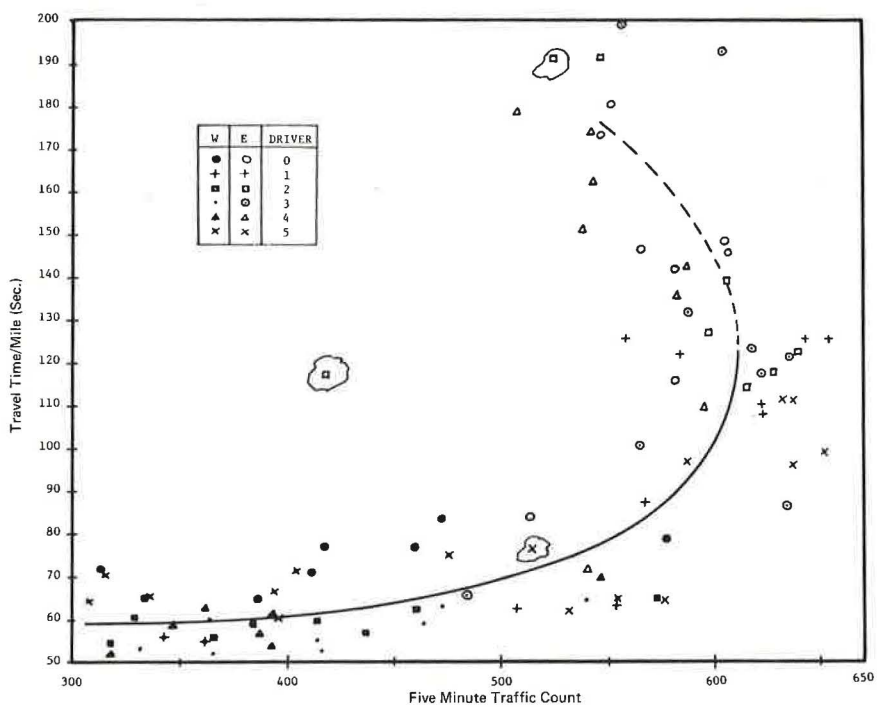

Figure 14. Travel time versus volume.

thus, they correspond to exactly the same array of prevailing traffic conditions. Travel time is observed to remain essentially constant, until it reaches near-capacity, when traffic then "breaks down." Some indication is given that the curve may loop back again, analogous to the idealized speed-volume curves. However, the dispersion is quite high at the high-volume levels. The corresponding speed-volume curve is shown in Figure 15. Here the looping characteristic appears to be more evident, although there seems to be higher dispersion at the low-volume levels.

A tentative conclusion that can be reached when comparing these last three figures is that acceleration noise appears to give a more graduated variation from low to high volume than travel time or speed. However, it seems to have more dispersion. An earlier correlation analysis performed on the first data set collected to compare the relationships between acceleration noise, standard deviation of velocity, and travel time with volume produced the following results:

Variable	Correlation Coefficient
Acceleration noise	0.748
Travel time	0.587
Standard deviation of velocity	0.659

Acceleration noise thus appears to provide a good performance measure which is relatable to an easily measured field variable and which is also a direct measure of driver stress.

Figure 16 presents the plot of acceleration noise versus travel time. This paired set was found to have a correlation coefficient of 0.75, which was indicated to be highly

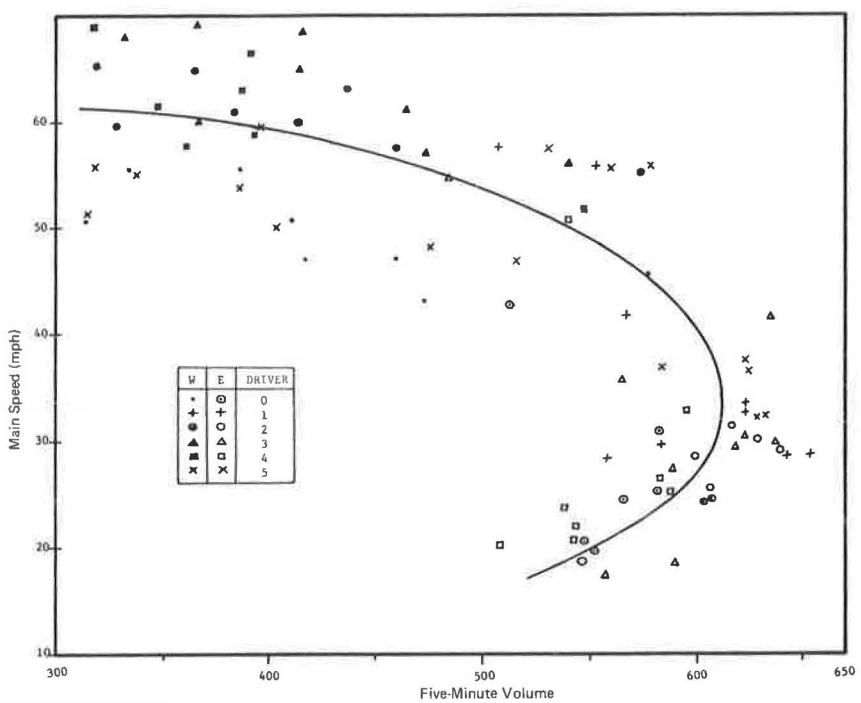

Figure 15. Mean speed versus volume.

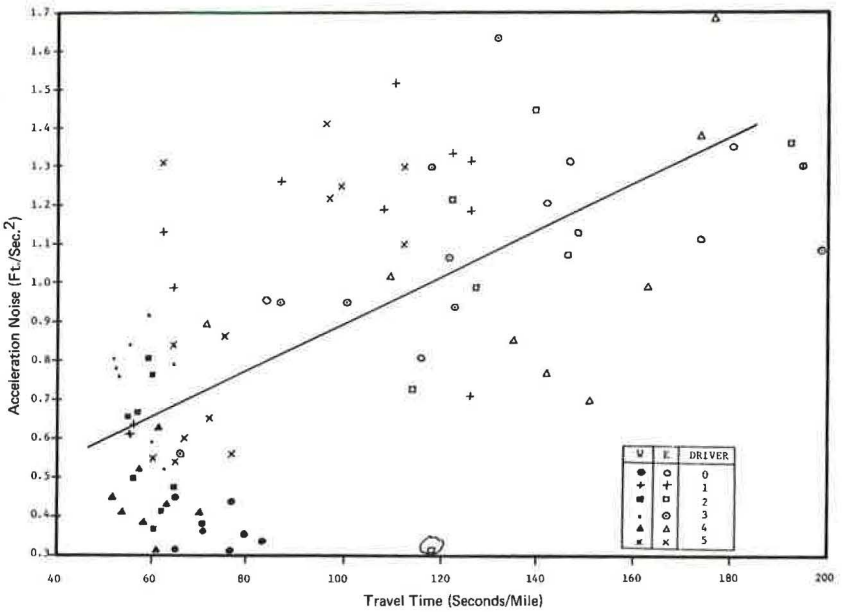

Figure 16. Acceleration noise versus travel time.

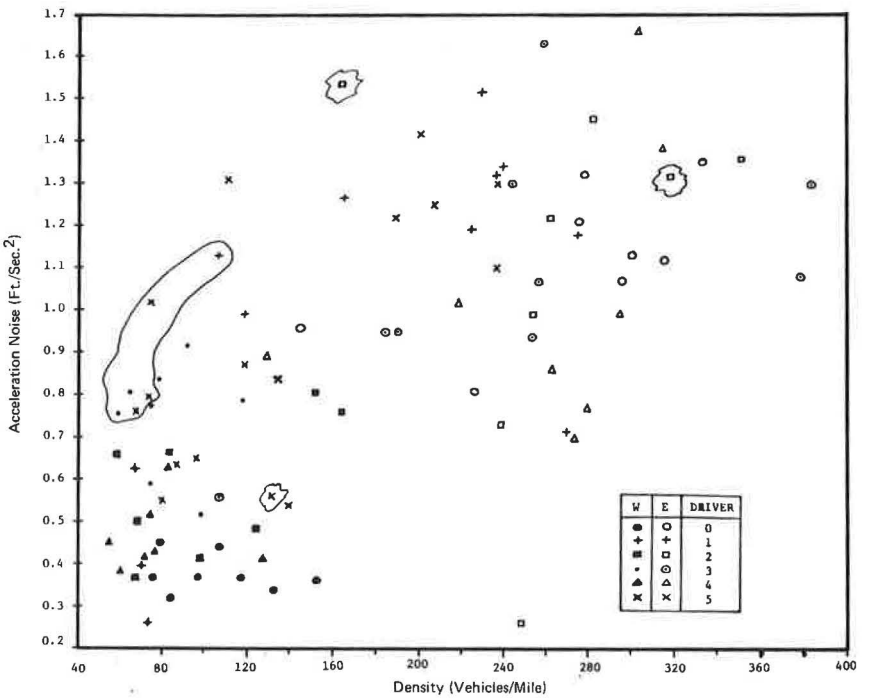

Figure 17. Acceleration noise versus density.

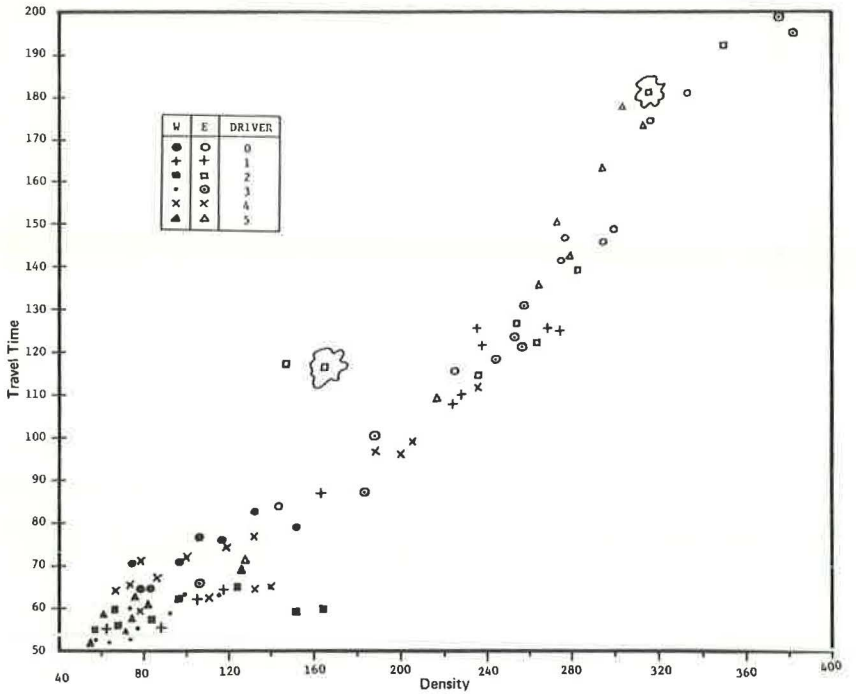

Figure 18. Travel time versus density.

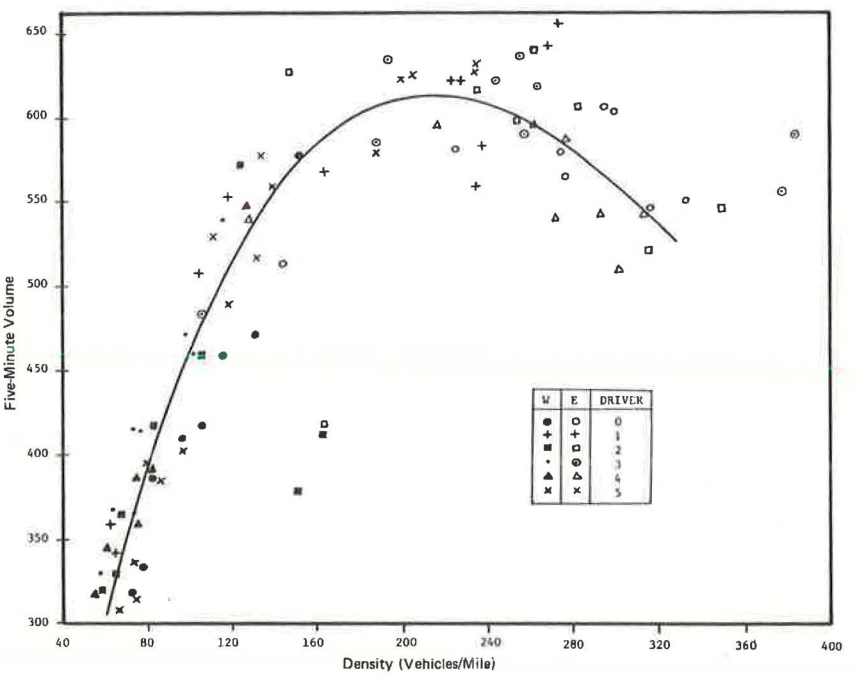

Figure 19. Volume versus density.

significant by the Fisher test (6). The least squares regression line of acceleration noise versus travel time is also shown in Figure 16.

Acceleration noise was also plotted against traffic density, as shown in Figure 17. A drastic difference is observed between this plot and the corresponding plot between travel time and density, shown in Figure 18. The latter has surprisingly low dispersion. The higher dispersion shown in Figure 17 is attributed to individual differences in driving techniques. Although most drivers may have the same goal of minimizing travel time, the driving tactics employed to achieve that goal may vary.

Figure 19 shows the volume-density relationship obtained for the set of data collected. It shows a significant number of observations on the right side of the peak of the curve.

CONCLUSIONS

A unique integrated hardware-software system has been demonstrated to expeditiously produce reduced and processed acceleration and velocity data from direct measurements taken in a vehicle. In particular, this system has been applied to the collection of a set of field data with different objectives in mind. The data were collected while driving the test vehicle on a heavily traveled urban freeway using different drivers. The application of results from this program to an aerial data collection program is discussed in another report. The effects of traffic and different drivers on several variables have been examined in this paper. These variables have included travel time, acceleration noise, autocorrelation function, and power spectral density. The travel time and speed studies confirmed the hypothesized relationships with volume and density. An interesting result is that acceleration noise is positively correlated with traffic volume. The principal source of variation seems to be the drivers. The large dispersion obtained for acceleration noise versus density when compared to travel time versus density suggests that acceleration noise may be a more sensitive measure for use in examining driver effects. A possible subsequent study that could be conducted to shed further light onto the subject is one in which the drivers are constrained to drive on either one of two prescribed lanes. A significant source of acceleration noise observed at the higher speeds appears to be due to the vehicle road-interactions or wind buffeting or both; this noise contribution is located at a higher frequency range than that caused by driver actions. The availability of this system and methodology is expected to stimulate other applications, particularly in vehicle-driver performance evaluation and human factors studies.

ACKNOWLEDGMENT

Leo Breiman made major contributions in the initial planning of the study, the development of data processing procedures, and in the analysis of the data. The program further profited by the stimulating guidance of A. V. Gafarian, who also contributed significantly in helping to resolve several technical problems.

REFERENCES

1. Herman, Robert, Montroll, E. W., Potts, R. S., and Rothery, R. W. Traffic Dynamics: Analysis of Stability in Car Following. Operations Research, Vol. 7, No. 1, 1959, pp. 86-106.
2. Breiman, Leo. On Estimating Position and Velocity of Cars From Discrete Time Aerial Photographic Data. SDC TM-3858/009/01, March 1, 1969.
3. Blackman, R. E., and Tukey, J. W. The Measurement of Power Spectra. Dover Publications, New York, 1958.
4. Bartlett, M. S. Stochastic Processes, pp. 238-240.
5. Torres, J. F. Development of Criteria for Evaluating Traffic Operations, Final Report, NCHRP Project 3-1, Volume I and II. Cornell Aeronautical Laboratory, Inc., Buffalo, New York, Rept. No. VJ-1978-G-1, Jan. 1966.
6. Brownlee, K. A. Statistical Theory and Methodology in Science and Engineering. John Wiley and Sons, 1960, pp. 365.

The Development and Validation of a Freeway Traffic Simulator

KUMARES C. SINHA, Marquette University; and
ROBERT F. DAWSON, University of Vermont

This paper presents the development and validation of a digital traffic simulator for use as a tool in the analysis of freeway phenomena. The simulator was constructed as a general model. Different freeway traffic situations can be simulated by merely inputing the descriptive geometric characteristics and pertinent traffic data including the total traffic volume on the freeway, speed distributions, and the percentage of commercial vehicles in the stream. The model has a capacity for the simultaneous, dynamic analysis of traffic flow on 5 freeway lanes, 4 on-ramps, and 6 off-ramps. The ramps may be located either on the right-hand or left-hand side of the freeway. When the simulator is processed on a 256K IBM 360/65 system, freeway sections up to 3½ miles in length can be simulated. However, with proper consideration for computer storage capacity, any of these limits can be modified via input information.

The freeway simulation model was validated at both microscopic and macroscopic levels. Several different macroscopic comparisons were made between simulated phenomena and data collected on sections of the Eisenhower Expressway in Chicago and a Long Island parkway, and data reported in the 1965 Highway Capacity Manual. The comparisons were consistent and reasonable.

•THE CONSTRUCTION of the proposed digital simulation model was realized in essentially two steps. First, models representing the component functions of the system were constructed in a mathematical format and programmed for dynamic processing on a digital computer to synthesize changes in the state of the system. Then various freeway situations were simulated for comparison and validation of the simulated phenomena with real-world traffic flow.

COMPONENTS OF THE PROPOSED MODEL

Mode of Representation

Apart from the usual vehicle characteristics, such as desired speed and vehicle position, several indexes representing various modes of vehicle-driver decision processes are identified for each vehicle. This results in a total of 14 characteristics that are updated and stored in the computer for each vehicle at each scan interval. These 14 characteristics are packed into only 4 computer words that can be unpacked at any point in time to give the stored characteristics for a particular vehicle. Figure 1 shows the storage of characteristics in computer words.

The entire system is represented by a two-dimensional array—the first dimension is an index for identification of a particular vehicle and the second dimension is an

Paper sponsored by Committee on Characteristics of Traffic Flow and presented at the 49th Annual Meeting.

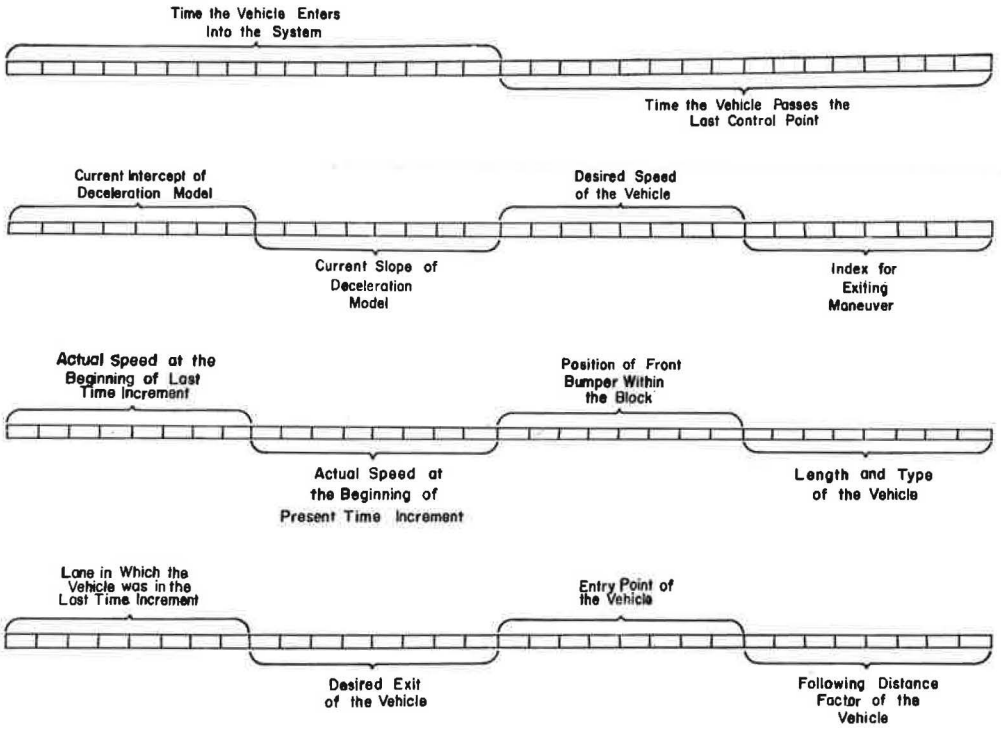

Figure 1. Image of computer words in which vehicle-driver characteristics are stored.

index of the corresponding four packed words. A second two-dimensional array is used to generate the image of the physical layout of the roadway system in the core of the computer. The entire freeway section under study, including warm-up sections, is divided into a number of unit blocks that are each 17 ft long and one lane wide. The first dimension of the freeway image array represents the number of the block in which the vehicle is located; the second dimension of the array represents the corresponding traffic lane. Three different locations are created for the vehicle-index array to separate the locations of through lanes, on-ramps including acceleration lanes, and off-ramps including deceleration lanes. The array itself contains the storage addresses of the characteristics describing the vehicles occupying the two-dimensional roadway.

As vehicles are introduced into the system, they are numbered sequentially and stored in the system in one of the three vehicle-index arrays, depending on their location. During the simulation process, the movement of any particular vehicle is represented by shifting its index number within the same matrix or from one matrix to another, and the general register is updated accordingly.

Roadway Characteristics

The logic to simulate ramp situations was designed without consideration for the angle of convergence or divergence of the ramp with the freeway. The effect of these variables is introduced in the gap-acceptance models for the on-ramp vehicles and in the desired speed models for the off-ramp vehicles respectively. There is no provision for traffic control in the merging and diverging areas. The overall freeway section is assumed to be straight and level, but, with modification to the program logic, variations in vertical and horizontal geometry can be introduced.

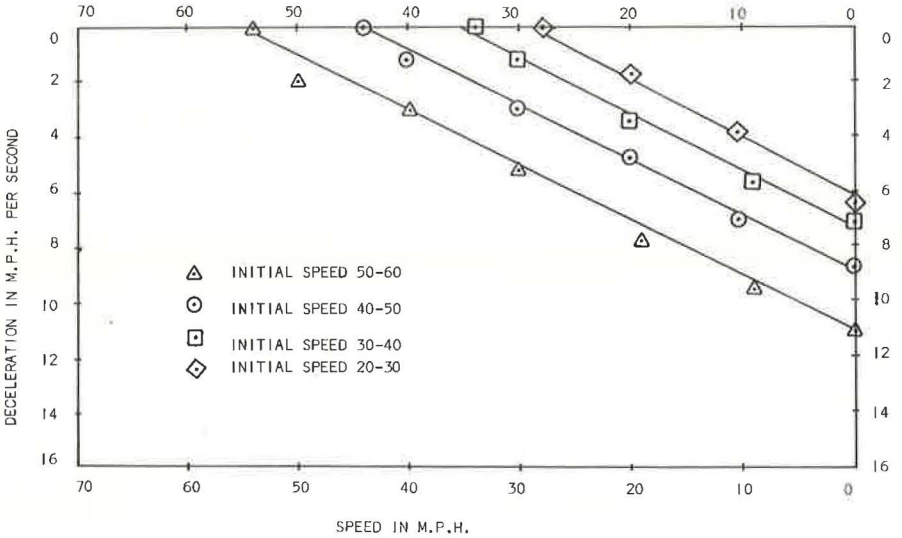

Figure 2. Observed speed and free-flowing deceleration of vehicles.

Vehicle-Driver Characteristics

Minimum Desired Spacing—A mathematical model was developed to describe minimum desired vehicle spacing as a linear function of actual vehicle speed. The model generates minimum desired spacings that follow a statistical distribution based on a normally distributed parameter that was introduced into the desired spacing equation.

Acceleration Model—In most of the previous simulation studies, both acceleration and deceleration rates were assumed to have constant values for all the drivers. These values were provided as input information and were held constant throughout the simulation process. Such a generalization is unrealistic. In this study the acceleration was expressed as an inverse linear function of speed. The parameters of the model were obtained by regression analyses of the data presented in the 1965 Traffic Engineering Handbook (1).

Deceleration Model—Vehicle deceleration was also expressed in a linear form. A set of deceleration curves, obtained from information provided in the 1965 Traffic Engineering Handbook (1), is shown in Figure 2. In this family of curves, the rate of change of deceleration remains essentially the same for all the deceleration curves. Pending further research, the normal value of the slope, B_d, was set at -0.2. This value approximately represents all the deceleration curves. The intercept, A_d, is computed at every increment of time on the basis of the action of the driver during the preceding time interval. A_d is zero at the start of the deceleration process. If a vehicle decelerates at a normal rate over several time increments, the deceleration can be expressed in the form of the following differential equation:

$$\frac{dV}{dT} = A_d + B_d\,(V)$$

or

$$\frac{dV}{A_d + B_d\,(V)} = dT \qquad (1)$$

The velocity vector, V, can be obtained by integrating Eq. 1 over time boundaries representing one increment of time, t and t + Δt, as follows:

$$V_1' = \frac{\left(A_d + B_d * V_1\right)}{B_d} e^{B_d * \Delta t} - \frac{A_d}{B_d} \quad (2)$$

Equation 2 is a general model that describes the speed of a decelerating vehicle at the end of one time increment. If it is assumed that the vehicle begins to decelerate at time, t, the intercept, A_d, is equal to zero at this point, and the resulting speed, V_1', is given by

$$V_1' = V_1 e^{B_d * \Delta t} \quad (3)$$

If the vehicle continues to decelerate normally for another time increment, Δt, the resulting speed, V_1'', at the time, $t_1 + 2\Delta t$, can be obtained from the following equation:

$$V_1'' = \frac{1}{B_d}\left(A_{d_1} + B_d * V_1'\right) e^{B_d * \Delta t} - \frac{A_{d_1}}{B_d} \quad (4)$$

The value of the parameter, A_{d_1}, is obtained as follows:

$$A_{d_1} = A_{d_0} + (V_1 - V_1')B_d \quad (5)$$

V_1'' can then be computed by substituting the values of A_{d_1}, V_1', B_d, and Δt in Eq. 4. If the deceleration continues over successive time increments, the resulting speeds can be obtained in the same manner, until the mode of vehicle behavior changes.

Car-Following Model—A car-following model was developed on the basis of the acceleration and deceleration models discussed above. The most critical case in a car-following condition is the situation in which the following vehicle is traveling faster than the leading vehicle. In Figure 3 a time-space diagram shows such a situation. The following vehicle is traveling at a speed, V_1, and the leading vehicle is traveling at a speed, V_2, at time, t. After a time increment, Δt, the leading vehicle is traveling at a speed, V_2', and V_1 is faster than V_2'. If V_2' remains constant, the following vehicle traveling at a constant speed, V_1, will eventually collide with the leading vehicle. In order to avoid collision, the following vehicle must adjust its trajectory so that after some time lag, t_{eq}, it will achieve the same speed as that of the leading vehicle and a safe spacing, d_m, will exist between the leading and following vehicles. The decision to slow down is obviously dependent on the available spacing between the two vehicles at any instant of time. The critical spacing, d_{cr}, at which the following vehicle must start to adjust its trajectory is developed below.

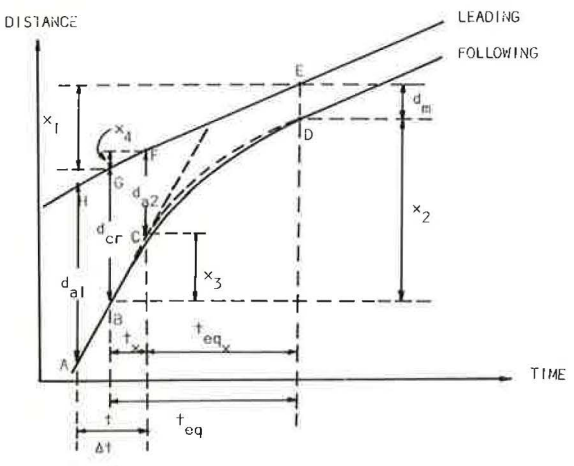

Figure 3. Time-space diagram of a situation when the following vehicle is traveling faster than the leading vehicle.

If the following vehicle decelerates at a normal rate, Eq. 1 can be solved over boundaries, V_1 and V_2', to compute the time of equilibrium, t_{eq}, as follows:

$$t_{eq} = \frac{1}{B_d} \log \left(\frac{A_d + B_d * V_2'}{A_d + B_d * V_1} \right) \tag{6}$$

The final speed of the following vehicle can be written as

$$\frac{dX}{dT} = \frac{\left(A_d + B_d * V_1\right)}{B_d} e^{B_d * T} - \frac{A_d}{B_d} \tag{7}$$

The distance traveled by the following vehicle, x_2, during the time period, t_{eq}, can then be obtained by integration:

$$\int_0^{x_2} dX = \int_0^{t_{eq}} \left[\frac{\left(A_d + B_d * V_1\right)}{B_d} e^{B_d * T} - \frac{A_d}{B_d} \right] dT$$

or

$$x_2 = \frac{A_d}{B_d^2} \left(e^{B_d * t_{eq}} - 1 \right) + \frac{V_1}{B_d} \left(e^{B_d * t_{eq}} - 1 \right) - \frac{A_d}{B_d} t_{eq} \tag{8}$$

The value of x_1 can be obtained approximately as $x_1 = 0.5 (V_2 + V_2') \Delta t + V_2' (t_{eq} - \Delta t)$. The value of the safe spacing, d_m, can be established from the linear minimum spacing model. Then, from Figure 3, the critical spacing can be obtained:

$$d_{cr} = x_2 + d_m - x_1 \tag{9}$$

At any point in time, the available spacing between the leading vehicle and the following vehicle can be computed, and there are three distinct conditions that might exist:

1. The available spacing is equal to the critical spacing;
2. The available spacing is greater than the critical spacing; and
3. The available spacing is less than the critical spacing.

Under the first condition, the vehicle will decelerate at its normal rate, and the resulting speed can be computed from Eq. 2. The distance traveled, Δx, can be obtained as follows:

$$\Delta x = \frac{A_d}{B_d^2} \left(e^{B_d * \Delta t} - 1 \right) + \frac{V_1}{B_d} \left(e^{B_d * \Delta t} - 1 \right) - \frac{A_d}{B_d} \Delta t \tag{10}$$

Under the second condition, the following vehicle must either maintain a constant speed over the current time increment, or acceleration in accordance with the acceleration model. However, the vehicle must maintain the minimum safe spacing to the leading vehicle.

The third condition arises when the initial position of the following vehicle is within the critical region, and the available distance, d_{a2}, is less than the critical distance, as shown in Figure 3. In such a case, the time available for reaching the equilibrium is less than the time, t_{eq}, computed on the basis of either the normal rate or its current rate of deceleration if it is already in the process of deceleration. It is obvious, therefore, that the following vehicle must decelerate more rapidly to reach the point D with minimum safe spacing. In Figure 3, the point C is the position of the following vehicle, t_x is the elapsed time, and t_{eq_x} is the time available to adjust its trajectory

so as to reach the point D. The elapsed time, t_x, can be approximately computed as follows:

$$x_3 = d_{cr} + x_4 - d_{a2}$$

$$V_1 * t_x = d_{cr} + 0.5\ (V_2 + V_2')\ t_x - d_{a2}$$

or

$$t_x = \frac{d_{cr} - d_{a2}}{V_1 - 0.5\ (V_2 + V_2')}$$

and

$$t_{eq_x} = t_{eq} - t_x \tag{11}$$

If t_{eq_x} is known, a new value B_n (Fig. 4) for the slope of the deceleration curve can be obtained as follows:

$$\frac{A_d + B_n * V_2'}{A_d + B_n * V_1} - e^{B_n * t_{eq_x}} = 0 \tag{12}$$

This equation can be solved for B_n by a method of successive approximation (8). By substituting B_n into Eqs. 2 and 10, the resulting speed, V_1', and the distance traveled, Δx, at the end of time increment, Δt, can be computed respectively.

In the next time increment, the critical spacing can be computed on the basis of this updated rate of deceleration, and if it is still necessary for the vehicle to decelerate the necessary computations can be repeated. This process continues until the vehicle ceases to decelerate.

During the actual simulation, vehicles are processed in an order moving from the downstream end to the upstream end of the roadway system. As any particular following vehicle is being processed at an instant in time, the vehicle ahead of it has already been processed and its characteristics have already been updated. In this way, the maneuver of a leading vehicle affects the maneuvers of the following vehicle, which, in turn, acts as a leading vehicle to subsequent vehicles. The car-following procedure provides continuity to this discrete chain process and affords a more realistic simulation model.

Gap-Acceptance—In the proposed simulation system two variable, probit models were used to describe gap-acceptance. These models were developed by Drew et at. (5) for ramp merging situations. Gap-acceptance in the lane-change maneuver was assumed to be analogous to merging from a long, parallel acceleration lane.

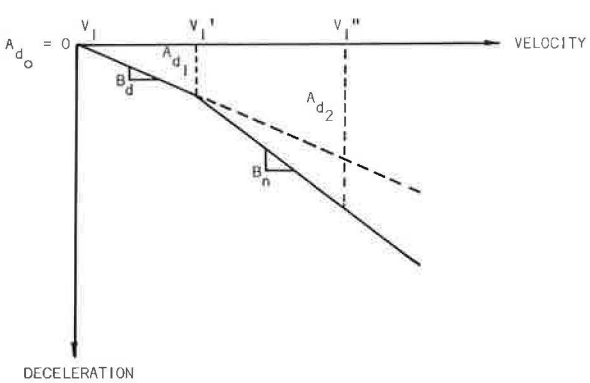

Figure 4. Typical speed-deceleration curve for a car-following situation.

Vehicle Type and Length—All of the vehicles in the system were assumed to have geometric and operating characteristics typical of either passenger cars or commercial vehicles. The overall length of passenger cars was set at 17 ft, and the length of commercial vehicles was established at 34 ft.

Traffic and Environmental Characteristics

Generation of Vehicles—Based on a comparison of the resulting cumulative headway distribution with the data as presented in the 1965 Highway Capacity Manual (2), the shifted exponential model (4) was selected as the descriptor of intervehicular time spacings on the freeway. There were no data available to test the effectiveness of any model for ramp vehicle generation. However, the hyper-Erlang distribution as developed by Dawson and Chimini (3) was found to be an efficient descriptor of headways in one-lane streams on two-lane, two-way highways. Although the characteristics of on-ramp traffic are probably governed by the geometric configuration of the ramp, on-ramp traffic can be expected to be similar to traffic on one lane of a two-lane, two-way highway with restricted passing. Thus, the hyper-Erlang function was selected for the generation of on-ramp traffic.

Speed Models—Desired speeds were generated as normally distributed random variables subject to the following conditions: mean, $\overline{V}_d = C_d$ (maximum freeway speed), and standard deviation, $S_d = 0.05\ (\overline{V}_d)$, where C_d = desired speed coefficient dependent on the lane and its location. The mean desired speed for trucks was established at 90 percent of that for passenger cars, whereas the standard deviation was assumed to be the same.

Operating speeds for vehicles on entrance ramps were also generated according to normal distribution of random numbers with a mean of 28.0 mph and a standard deviation of 1.0 mph. Because there is little variation between the speeds for passenger cars and for trucks on ramps, the mean and the standard deviation for both types were considered to be the same. This assumption is justified because the ramp geometry is generally more restrictive than prevailing traffic conditions on the ramp.

PROGRAMMING OF THE PROPOSED MODEL

Following the development of the mathematical models for the component parts of the simulator, these models were integrated into an operational system. This integrated system was then coded in the FORTRAN IV and IBM 360 Assembler Language codes for dynamic processing on an IBM 360/65 computer.

Discussion of the Simulation Logic

The overall logic of the proposed simulator is shown schematically in the flow diagram of Figure 5. A subroutine contained the necessary logic to preload the simulated roadways with vehicles and to assign distinctive characteristics to each of the vehicles. A routine was structured to simulate a real-time clock to be advanced at the start of each scan interval, which was set at 1 second.

Vehicles on Off-Ramps—The logic for detecting off-ramp vehicles that would be processed out of the system during the scan currently under execution is considered first. Upon detecting exiting off-ramp vehicles, this subroutine removes them from the system. Subsequent off-ramp vehicles are then processed (moved down the ramp) in accordance with logic that is dependent on whether the vehicle is a free-flowing vehicle or a vehicle under the influence of a leading vehicle.

Then the freeway is scanned from the lane adjacent to the shoulder toward the median lane to locate the vehicle nearest to the downstream end of the simulated section. If the vehicle encountered is located on either a deceleration lane or an acceleration lane, the program control is passed to a subroutine that contains the deceleration-lane logic or the acceleration-lane logic respectively.

Vehicles on Deceleration Lanes—Vehicles on a deceleration lane are processed separately from the vehicles on the following off-ramps. Although these vehicles are allowed to move only forward and the logic governing their movement is essentially the same as that for off-ramp vehicles, they are scanned along with the through-lane vehicles and updated accordingly at every time increment. As soon as the scanning index reaches the nose of an off-ramp, the order of lane searching is modified to begin with the deceleration lane instead of the shoulder lane. In this way the diverging maneuvers from shoulder lane to deceleration lane can be simulated in a more realistic manner.

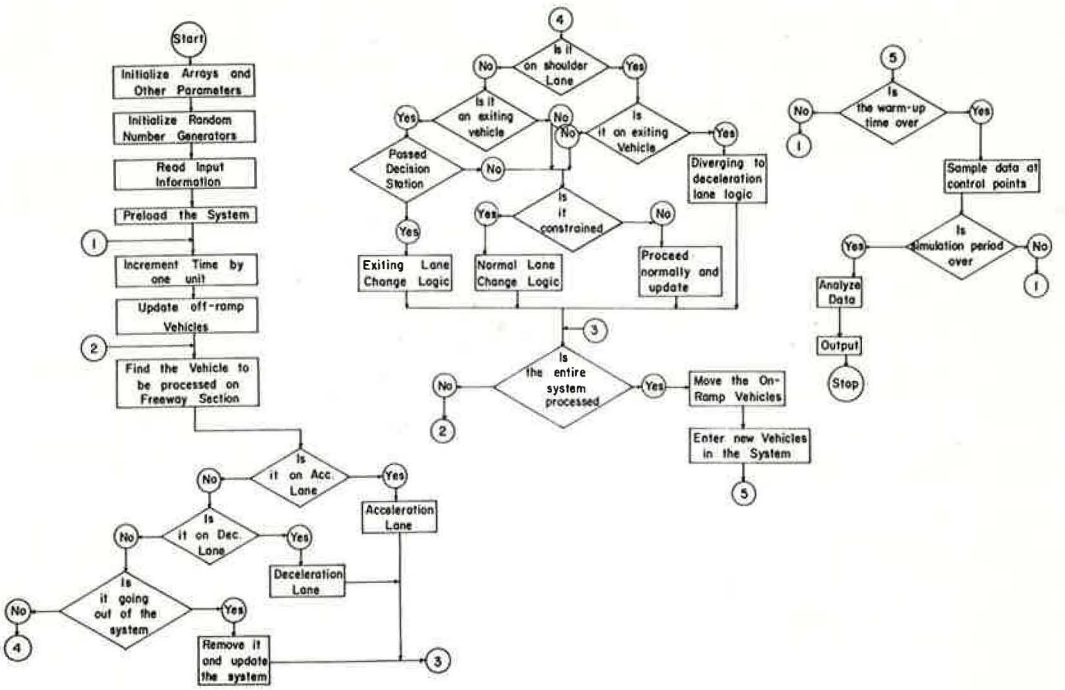

Figure 5. Flow diagram of general simulation logic.

Vehicles on Acceleration Lanes—A vehicle on an acceleration lane is processed into the adjacent through lane as soon as it reaches the nose of the on-ramp. The relative positions of the merging vehicle with respect to the prospective leading and following vehicles on the adjacent through lane are evaluated in a manner similar to the lane-changing maneuver. In order to select a merging speed, five different speeds are considered in sequential order until a satisfactory speed is found. These five possible speeds include a speed based on its maximum rate of acceleration, a speed based on its normal rate of acceleration, its current speed, a speed based on its normal rate of deceleration, and a speed based on its maximum rate of deceleration.

The desired safe spacing in front of a merging vehicle is assumed to be half of the normal value if the leading vehicle merges during the same time increment. When the physical constraints for merging are satisfied, a test is made to determine if the merging vehicle will accept the available time gap in the adjacent lane. The test involves a random decision process based on the gap-acceptance models.

If the merging attempt is unsuccessful, the vehicle is maintained in the acceleration lane until it can merge into the through-lane stream. The processing of unsuccessful merging vehicles is divided into two parts. In the first part, vehicles that are already at a stop at the end of the acceleration lane are processed. In the second part, moving vehicles that are slowed down as they approach the end of the acceleration lane, or the tail end of a queue waiting to merge, are processed.

If the vehicle encountered is on one of the through lanes, the vehicle characteristics are processed to determine if the vehicle will leave the system during the current span period. Those vehicles that will pass beyond the bounds of the simulation section are processed out of the system. Other vehicles are processed in accordance with logic compatible with lane position and desired system exit.

Nonexiting Vehicles on the Freeway—As a nonexiting, through-lane vehicle is processed within the critical region, it is decelerated if its current speed, V_1, exceeds the updated speed of the leading vehicle, V_2'. Otherwise, a tentative speed, V_{tn}, is computed on the basis of a free-flowing acceleration model. Computations are made to

determine if a safe spacing will be maintained throughout the scan interval. If the following distance is at least equal to the required distance, the updated speed of the vehicle is set at V_{tn}. Otherwise, the possibility of lane-changing to improve status is evaluated. In the event that it is not possible to make a lane change, a test is made to determine if it is possible to accelerate and still maintain a safe spacing. If it is not possible, the vehicle is updated at its current speed.

On the other hand, if V_1 is less than, or equal to, V_2', it is checked to determine if a safe spacing can be maintained at this speed. If it cannot be, a lane change is attempted. If this attempt is unsuccessful, the vehicle is decelerated at an appropriate rate and updated. If the vehicle can maintain its speed during the current time increment, it does so unless it can accelerate to achieve a speed nearer to its desired speed.

Normal Lane-Changing Between Adjacent Through Lanes—The available physical distance between the leader in the adjacent lane and the merging vehicle, f_{df}, is compared with the distance required for merging, r_{df}. This latter distance is computed using a tentative lane-change speed based on maximum acceleration for the merging vehicle. If f_{df} is less than r_{df}, the test is repeated using another tentative lane-change speed based on normal acceleration of the vehicle. If this speed is also unsatisfactory and the vehicle cannot maintain its current speed in its current lane, a check made to determine the feasibility of a lane-change attempt is abandoned.

When the distance requirement between the merging vehicle and the new leader is found to be satisfactory, the relative position between the merging vehicle and the following vehicle in the adjacent lane is evaluated. After all physical constraints have been checked, a test is made to determine if the lane-changing vehicle will accept the available time gap. This decision is effected by a random sampling process. If the outcome is positive, the vehicle is moved to the adjacent lane and updated. Otherwise, it is maintained in the same lane and its movement is governed by the appropriate logic.

The distance from the vehicle of concern to its desired exit is computed for vehicles in the shoulder lane that are exiting from the system via an off-ramp, and if the vehicle is in the proximity of the particular deceleration lane, control is passed to a subroutine containing the logic to diverge the vehicle into the deceleration lane.

Exiting Vehicles on the Shoulder Lane—An exiting vehicle located on the shoulder lane attempts to diverge into the appropriate deceleration lane. This logic is separated into two parts: (a) for vehicles adjacent to the deceleration lane, and (b) for those vehicles just approaching the deceleration lane within the current time increment. In the first situation, if the current speed is greater than the maximum allowable off-ramp speed the diverging maneuver is attempted first at the current speed, then at a normally decelerated speed, and finally at a speed based on maximum deceleration. Otherwise, the exiting vehicle is accelerated to the maximum ramp speed for diverging. The spacings are evaluated in the same manner as described in the normal lane-changing maneuver. In the second situation, it was assumed that an exiting vehicle, approaching the deceleration lane, is only concerned with its relative position to the nearest vehicle located on the deceleration lane. If after necessary maneuvers the vehicle can maintain a safe spacing to the leading vehicle on the deceleration lane, and on doing so can reach the deceleration lane, diverging is possible and the vehicle is updated accordingly. If an exiting vehicle, located on an inner lane, has already passed an exit decision station (point at which signing is observed), control is passed to the logic to effect the lane-change process.

Exiting Vehicles on Inner Lanes—Vehicles marked to exit and located on inner lanes attempt to weave to the right until they reach the shoulder lane. The logic for this sequential lane-changing maneuver is essentially similar to that for a normal lane-change process with the following exceptions:

1. An exiting vehicle might not increase its speed while changing lanes; and
2. In order to satisfy the physical constraints on lane-changing, an exiting vehicle will decelerate normally or even at its maximum rate, if required.

If the lane-changing attempt is unsuccessful, an exiting vehicle is moved ahead at its current speed, provided that it is safe to do so. Otherwise, it is decelerated at a normal rate.

Vehicles on the On-Ramps—After the vehicles on the freeway portion of the system have been processed for the current scan interval, the on-ramp vehicles are then considered. Vehicles on the on-ramps are processed sequentially from the ramp nose upstream to the local ramp terminal. The logic governing the movement of on-ramp vehicles is essentially the same as that for off-ramp vehicles. Subsequently, new vehicles are introduced into the system according to the vehicle-generation logic.

VALIDATION OF THE PROPOSED MODEL

As the model was being developed, simulation runs were made for short periods of time and the operating characteristics for each vehicle in the system were output at the end of each simulation time increment. The movements of each vehicle and the decisions involved in these movements were analyzed and compared to data available in the literature. These microscopic examinations were useful in the process of modifying the logic associated with different parts of the model. After the microscopic evaluations were completed, the program was ready for macroscopic verification.

A detailed presentation of the simulation results is not within the scope of this paper. Therefore, only a brief description of some of the simulation runs devised for the macroevaluation of the model is discussed in the following paragraphs.

Surveillance of Operating Characteristics

As each vehicle is processed during a simulation interval, a check is made to determine whether it will pass any of several pre-established control points. If each vehicle will pass, several descriptive operating characteristics are computed and stored on disks outside the core area of the computer. When the total time for simulation is over, the stored characteristics are statistically analyzed and output to provide a description of traffic operations along the simulated section of freeway.

Distribution of Headways Upstream of the On-Ramps

Field data on time headways in lanes adjacent to right-hand and left-hand on-ramps were available for a portion of the westbound half of the Eisenhower Expressway in Chicago (7). Several simulation runs were devised to obtain headway data for comparison with the field data. The input geometry for these simulation runs is shown in Figure 6, and other input data required for the runs are given in the Appendix. The experimental headways and the headways obtained from simulation runs for two cases are shown in Figures 7 and 8. The results for the simulation runs are in reasonable overall agreement with the experimental observations, especially in the range above 3 seconds. It is interesting to note that Kobett and Levy (6) also obtained the best agreement in this region.

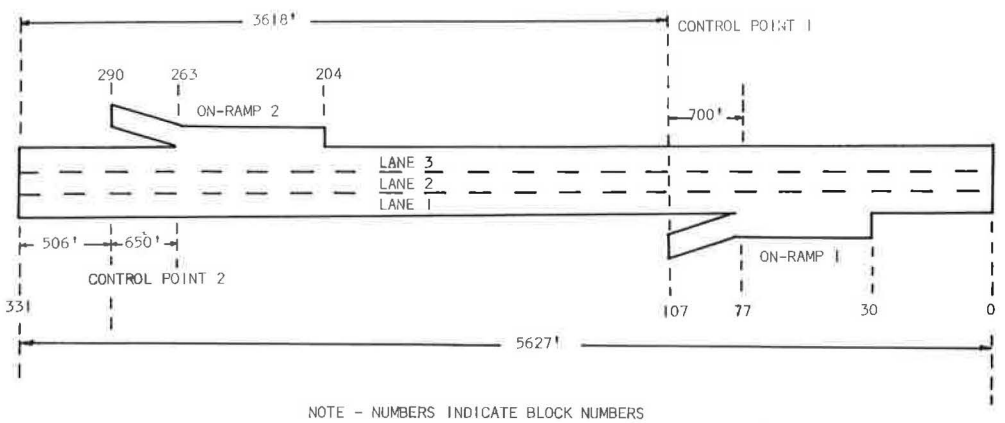

Figure 6. Input geometry for simulation runs to obtain distributions of headways upstream of on-ramps.

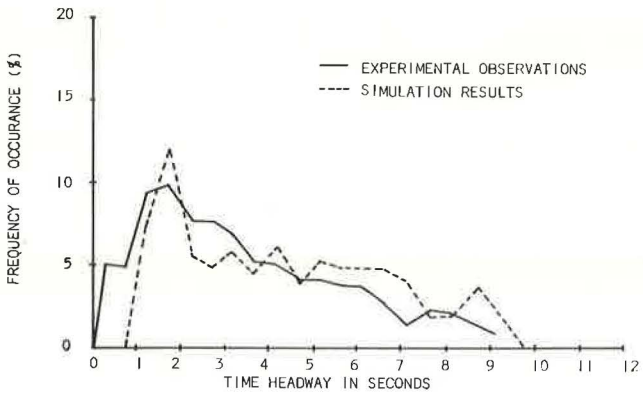

Figure 7. Frequency distribution of headways in adjacent lane upstream of right-hand on-ramp at low volume.

Because the minimum time headway in the vehicle-generation models was established at 0.75 second, headways smaller than 0.75 second did not appear in the simulation results. In addition, the simulated distributions present higher peaks than the observed distributions between 1.5 and 2.5 seconds. These discrepancies can be attributed to the empirical models used to regulate the minimum desired distance spacing. The empirical models forced long minimum-distance spacings that in turn generated long time spacings between vehicles in platoons.

Weaving Behavior on a Freeway Section

The output from several simulation runs was compared with experimental data collected on a section of a Long Island parkway with relatively heavy weaving movements (6). The results obtained from simulation runs are in general agreement with the experimental observations. The input geometry for these simulation runs is shown

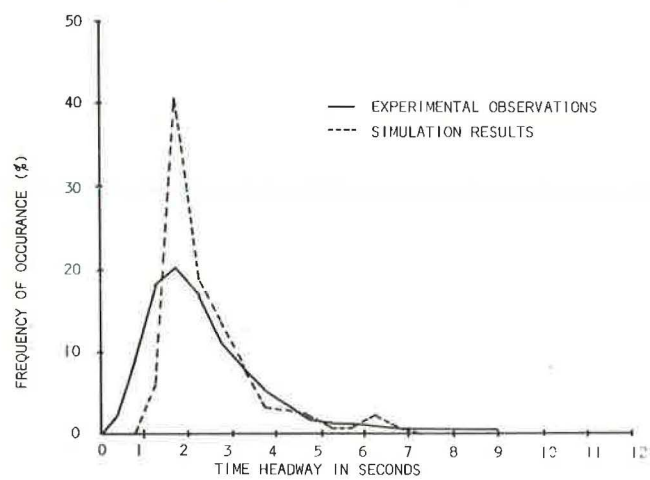

Figure 8. Frequency distribution of headways in adjacent lane upstream of left-hand on-ramp at high volume.

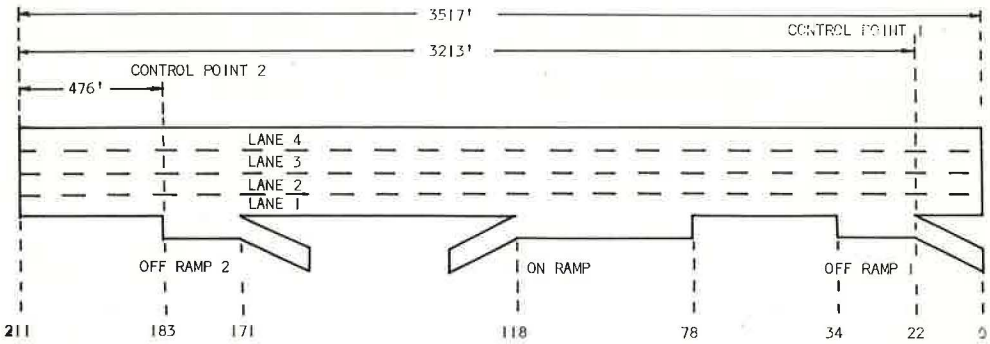

Figure 9. Input geometry for weaving simulation runs (numbers indicate the block numbers).

in Figure 9, and other input data required for one of these simulation runs are tabulated in the Appendix. Input volumes were specified on the basis of the information reported by Kobett and Levy (6). The results obtained from this simulation run are compared with the experimental observation in Figure 10.

The through volumes upstream of off-ramp 2 compare very closely. However, the through volumes downstream of off-ramp 1 deviate from the observed volumes. This discrepency is due, in part, to the fact that the simulated on-ramp volume was 150 vph (vehicles per hour) whereas the observed on-ramp volume was 50 vph. Simulator input parameters are not currently available for on-ramp volumes below 150 vph. Consequently a greater number of ramp vehicles merged into the shoulder lane and forced an excessive volume into lane 1.

Traffic Characteristics on an Open Section of Freeway

Several simulation runs were made to investigate traffic characteristics on an open section of a freeway that was essentially free of any influence from on- and off-ramps.

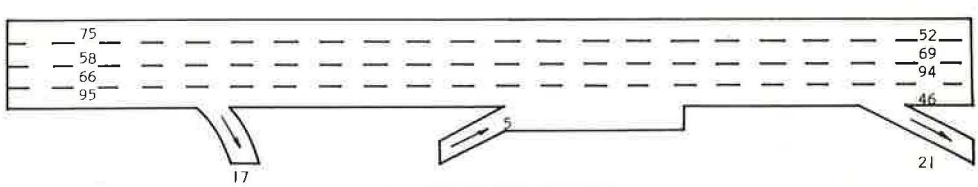

(a) EXPERIMENTAL OBSERVATIONS

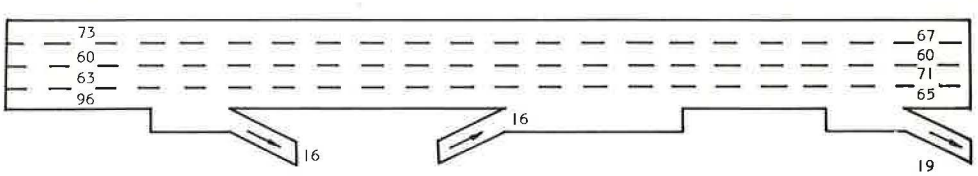

(b) SIMULATION RESULTS

Figure 10. Results of the low-volume weaving simulation (numbers shown represent 6-minute volumes).

A freeway section with five through lanes, two on-ramps, and two off-ramps was selected and runs were made at different levels of traffic flow. The distribution of volumes, headways, and speeds at each lane were obtained by sampling for a period of 10 minutes during each simulation run.

The results obtained from these simulation runs were consistent and reasonable. But, because there were no available field data for five-lane freeways, these results could not be verified with observed phenomena. However, some general observations can be made on the basis of the simulation findings. The percentage of vehicles in the shoulder lane is lowest and it increases in successive lanes. The average highway speed is also lowest in the shoulder lane and increases successively in inner lanes. Thus, lanes 4 and 5 were observed to be the most heavily traveled as well as the fastest lanes on the open section of a five-lane freeway. These observations are generally consistent with flow phenomena that have been observed on freeways with less than five lanes.

Effects of an Auxiliary Lane

The proposed general traffic simulation model does not contain any special design features for simulating flow on freeway sections with unusual geometric configurations such as exist on highways with auxiliary or operational lanes. However, with minor modifications to the program logic this feature was readily simulated. As an example problem, a study area consisting of two through lanes and a 629-ft long operational lane between an on-ramp and an off-ramp was considered. Several simulation runs were devised with different combinations of freeway and ramp volumes.

The simulation results indicated that most of the entering on-ramp vehicles merged onto the shoulder lane within the first half of the operational lane. It was also observed that the most heavily traveled portion of the shoulder lane was at about the middle of the operational lane. These observations are consistent with the experimental observations presented in the 1965 Highway Capacity Manual (2). Furthermore, the distribution of traffic between lanes at different sections of the weaving area was in close agreement with the result reported in the same source.

SUMMARY AND CONCLUSIONS

1. The program logic for the processing of vehicles in the system was divided into five parts. Separate routines were prepared for processing vehicles on through lanes, on-ramps, acceleration lanes, deceleration lanes, and off-ramps. A basic premise for all vehicular movements was that vehicles must maintain a safe intervehicular spacing.
2. The proposed model can be utilized to analyze traffic flow on any freeway system with appropriate modifications to the program logic.
3. The performance of the model is dependent on the adequacy of the submodels describing the component functions of the system, and on the accuracy of the input information specified for the simulation runs. The micromodels were formulated on the basis of the present understanding of traffic flow theory. In some cases, assumptions were made due to the lack of experimental information.
4. The common index for the efficiency of a simulator, namely the computer time to real time ratio, is misleading and perhaps even unimportant with third-generation computers. The amount of computer time required for a simulation run depends directly on the size and complexity of the specific situation to be simulated. The required computer time varied widely from problem to problem, and, even for particular runs, the ratio of computer time to real time decreased considerably as the period of simulation was increased. The actual ratios of computer time to real time, observed in the study, ranged from $\frac{1}{2}$ to $\frac{1}{10}$ for several different problems.

ACKNOWLEDGMENTS

This study was sponsored jointly by the University of Connecticut and the Connecticut Highway Department via the Highway Research Project at the University of Connecticut. Validation data were graciously provided by the Bureau of Public Roads, U.S. Department of Transportation. The IBM 360/65 computer system that was utilized during the

course of the study was partially supported by National Science Foundation Grant GP-1819 to the University of Connecticut.

REFERENCES

1. Baerwald, J. W., ed. Traffic Engineering Handbook. Institute of Traffic Engineers, Washington, D.C., 1965.
2. Highway Capacity Manual, 1965. HRB Spec. Rept. 87, 1965, 397 pp.
3. Dawson, R. F., and Chimini, L. A. The Hyperlang Probability Distribution—A Generalized Traffic Headway Mode. Highway Research Record 230, 1968, pp. 1-14.
4. Dawson, R. F., and Michael, H. L. Analysis of On-Ramp Capacities by Monte Carlo Simulation. Highway Research Record 118, 1966, pp. 1-20.
5. Drew, D. R., LaMotte, L. R., Wattleworth, J. A., and Buhr, J. H. Gap Acceptance in the Freeway Merging Process. Highway Research Record 208, 1967, pp. 1-36.
6. Kobett, D. R., and Levy, S. L. Study of Expressway Traffic Flow Through Digital Simulation. Final Report. Midwest Research Institute, Missouri, 1965.
7. May, A. D., Jr. Gap Availability Studies. Highway Research Record 72, 1965, pp. 101-136.
8. Sinha, K. C. The Development of a Digital Simulator for the Analysis of Freeway Traffic Phenomena. Univ. of Connecticut, unpublished PhD dissertation, 1968.

Appendix

INPUT DATA FOR SIMULATION RUNS

Headway Distribution Runs	Weaving Simulation Runs
Volumes in vph	Volumes in vph
On-ramp 1 - 200 (400)	On-ramp - 150
On-ramp 2 - 200 (400)	Lane 1 - 1,000
Lane 1 - 600 (1,200)	Lane 2 - 600
Lane 2 - 1,080 (1,720)	Lane 3 - 450
Lane 3 - 720 (1,380)	Lane 4 - 850
Proportion of Commercial Vehicles	Proportion of Exiting Vehicles
On-ramp 1 - 0.03 (0.03)	for Off-Ramp 1 / for Off-Ramp 2
On-ramp 2 - 0.03 (0.03)	Lane 1 - 0.06 / Lane 1 - 0.14
Lane 1 - 0.06 (0.06)	Lane 2 - 0.033 / Lane 2 - 0.05
Lane 2 - 0.03 (0.03)	Lane 3 - 0.25
Lane 3 - 0.01 (0.01)	Lane 4 - 0.04
Factors of Mean Desired Speed	Factors of Mean Desired Speed
On-ramp 1 - 0.75 (0.7)	On-ramp - 0.75
On-ramp 2 - 0.75 (0.7)	Lane 1 - 0.8
Lane 1 - 0.85 (0.7)	Lane 2 - 0.8
Lane 2 - 0.9 (0.7)	Lane 3 - 0.85
Lane 3 - 0.85 (0.7)	Lane 4 - 0.9
Maximum Freeway Speed - 60 mph	Maximum Freeway Speed - 50 mph
Warm-Up Time - 200 seconds	Warm-Up Time - 200 seconds
Sampling Period - 5 minutes	Sampling Period - 6 minutes

NOTE: Numbers in parentheses represent input data for high-volume runs.

Analysis of a Signal-Controlled Ramp's Characteristics

KENNETH A. BREWER, Department of Civil Engineering and Engineering Research Institute, Iowa State University, Ames

Although it is evident which measurements describe an uncontrolled ramp operation, measurements relevant to describing the operation of a signal-controlled ramp are not readily apparent. A basic queuing approach is utilized to develop a model attempting to describe the operation of a signal-controlled ramp. The assumptions of Poisson arrivals into the ramp, a negligible move-up time in the queue, and an Erlang distribution of freeway gaps inherent in the model are verified by study measurements. A rate of service (wait at the signal) is then predicted for both fixed-rate metering and gap-acceptance control. The average queue at the ramp signal is also predicted for both types of signal control. The predicted values are compared to observed study data. The study was conducted on the Dumble Street inbound entrance ramp on the Gulf Freeway (Interstate 45), Houston, in 1968. Because the computerized data collection system was not fully operational at the time the study was conducted, a field data collection scheme was developed to monitor in-place loop detectors.

•THE MEASUREMENT of the characteristics of a particular freeway entrance ramp is a relatively straightforward problem, even though it may be somewhat laborious. It is not necessarily obvious, in the case of a metered (or signal-controlled) ramp, which measurements are relevant to establish the ramp characteristics. Drew, Buhr, and Whitson (1) developed a relationship to estimate the theoretical merging capacity of a signal-controlled ramp. Brewer et al. (2) established a capacity and service volume relationship for a controlled ramp, whereas Buhr et al. (3) documented traffic characteristics of merging control systems. Weiss and Maradudin (4) have studied the theoretical delay characteristics of a stop-sign-controlled ramp. However, none of these approaches sufficiently describe a controlled ramp to readily indicate what characteristics should be measured for operational analysis. It was therefore necessary to develop a model describing a signal-controlled ramp, verify its assumptions as completely as possible, check values for the predicted ramp characteristics, and estimate the unaccounted influence of other characteristics.

PREDICTIVE MODEL

Because the vehicles wanting to enter the freeway by the signal-controlled entrance ramp must wait in line for a green signal and then enter the freeway one vehicle at a time, some form of queuing theory should be applicable to this process. The use of queuing theory requires some knowledge about the stochastic nature of the vehicular arrivals to the ramp and the length of time a vehicle has to wait on red at the ramp signal.

In 1936 Adams (5) indicated that the arrival of vehicles at a point on a roadway was often very well described mathematically by the Poisson distribution. Since then the

Paper sponsored by Committee on Characteristics of Traffic Flow and presented at the 49th Annual Meeting.

Poisson distribution has been used as an appropriate vehicular counting distribution, and it would seem to be applicable to the ramp arrivals. No historical backlog of data exists on wait at a signal, which is strictly a function of traffic conditions. Therefore, Kendall's (6) development of queuing relations for a Poisson input and an arbitrary service was utilized. As such, the average line of vehicles at the ramp signal might be expected to be described by

$$E(\ell) = q_r \cdot E(s) + \frac{q_r^2 \cdot \sigma_s^2 + \left[q_r \cdot E(s)\right]^2}{2\left[1 - q_r \cdot E(s)\right]} \tag{1}$$

where

ℓ = the number of vehicles waiting at the ramp signal,

s = the length of time a vehicle waits at the ramp signal on red,

q_r = average rate of ramp arrivals,

$E(s)$ = expectation of wait at the signal,

σ_s^2 = variance of wait at the signal, and

$E(\ell)$ = expectation of waiting line.

The length of time a vehicle waits in line before reaching the signal would be

$$E(w) = \frac{E(\ell)}{q_r} - E(s) \tag{2}$$

and the total expected time from arrival until release at the ramp signal would be

$$E(v) = \frac{E(\ell)}{q_r} \tag{3}$$

To obtain values for the expressions in Eqs. 1, 2, and 3 the form of $E(s)$ and σ_s^2 must be known. One of the methods of signal control of ramps strongly advocated by some persons is metering vehicles on a constant rate with a fixed time signal cycle (7). For a fixed-rate metering type of control, $E(s)$ would be a constant and σ_s^2 would be zero (at least in theory) because vehicles would be allowed to enter the freeway on a regular basis. Equations 2 and 3 would remain the same but Eq. 1 would become

$$E(\ell) = q_r \cdot E(s) + \frac{\left[q_r \cdot E(s)\right]^2}{2\left[1 - q_r \cdot E(s)\right]} \tag{4}$$

Another method is to allow vehicles to enter the freeway when a gap in the outside freeway lane (large enough for a ramp vehicle to reasonably accept it) is expected to be in the merge area at the same time the ramp vehicle reaches the merge area (8). In this case, the actual form of $E(s)$ and σ_s^2 may be quite complicated. However, because each vehicle is released at the signal one at a time on a first-come, first-served basis, an expression may be obtained for $E(s)$ and σ_s^2.

When a gap in the freeway stream greater than or equal to T seconds is detected, a vehicle can be released into it. Thus, the probability of selecting a gap can be denoted by

$$g(t) = o, \quad t < T \tag{5a}$$

$$g(t) = 1, \quad t \geq T \tag{5b}$$

where t is the freeway gap in seconds. Furthermore, the gaps in the outside freeway stream as a whole will be taken to be independent random variables with a probability density function, h(t). Because the start of a gap detected does not necessarily coincide with the beginning of the search for a gap large enough to release the ramp vehicle,

the probability density of the detection of the first freeway vehicle on a gap search is denoted by

$$h_o(t) = B \int_t^\infty h(\chi)d\chi = \frac{\int_t^\infty h(\chi)d\chi}{\int_t^\infty \chi \cdot h(\chi)d\chi} \tag{6}$$

A conditional probability, b(t)dt, is defined as the probability that a gap is selected in the time interval (t, t + dt) given that no gap was selected in the interval (0, t). The probability density of the time waited at the signal, a(t), is

$$a(t) = d(t) \int_0^\infty h_o(\chi) \cdot g(\chi) + b(t) \int_0^\infty h(\chi) \cdot g(\chi)d\chi$$

$$= d(t) \cdot D_o + b(t) \cdot D \tag{7}$$

where d(t) is a delta function. Equation 7 indicates a wait of zero time for the ramp vehicle if the first gap (or partial gap) is selected with a probability D_o, or a wait of time t until a gap appears that is greater than T seconds.

In considering the last term of Eq. 7, either the freeway vehicle that arrives at time t is the first vehicle to appear since time t = o and the time t is unsatisfactory, or the last vehicle passed the detector at time t_o and the time $(t - t_o)$ is unsatisfactory. From this,

$$b(t) = h_o(t)\left[1 - g(t)\right] + \int_0^t b(t_o) \cdot h(t - t_o)\left[1 - g(t - t_o)\right]dt_o$$

$$= G_o(t) + \int_0^t b(t_o) \cdot G(t - t_o)dt_o \tag{8}$$

which is an integral equation of convolution form. Application of Laplace transforms to Eq. 8 will yield the following for E(s):

$$E(s) = \frac{1}{D} \int_0^\infty t\left[D \cdot G_o(t) + (1 - D_o) \cdot G(t)\right]dt \tag{9}$$

Similarly, for the second moment of the wait at the signal,

$$E(s^2) = \frac{1}{D^2}\left\{ \int_0^\infty t^2\left[D^2 \cdot G_o(t) + (1 - D_o) \cdot D \cdot G(t)\right]dt \right.$$

$$\left. + 2 \int_0^\infty t \cdot G(t)\,dt \cdot \int_0^\infty t\left[D \cdot G_o(t)dt + (1 - D_o) \cdot G(t)\right]dt \right\} \tag{10}$$

The variance of the wait at the signal, σ_s^2, can be calculated from the relationship of the first and second moments:

$$\sigma_s^2 = E(s^2) - [E(s)]^2 \tag{11}$$

In order to establish a numerical value for E(s) and σ_s^2 a specific distribution must be assigned to h(t). A general distribution yielding a mathematical tractible expression is the Erlang distribution,

$$h(t) = \frac{(aq)^a \, t^{a-1} \, e^{-aqt}}{(a-1)!} \tag{12}$$

where

a = the Erlang parameter,
q = the average vehicular flow rate, and
t = the gap size.

If a = 1 (implying simple Poisson traffic on the outside freeway lane), then

$$E(s) = \frac{e^{qT} - qT - 1}{q^2} \tag{13a}$$

and

$$\sigma_s^2 = \frac{e^{2qt} - 2qTe^{qT} - 1}{q^2} \tag{13b}$$

Numerical evaluations of E(s) and σ_s^2 have been calculated for numerous combinations of parameter variations (9). Figure 1 shows the variation of both expressions for different values of Erlang "a", freeway flow rate, and ramp-controller gap setting.

STUDY METHODOLOGY

The study was conducted on the Dumble Street inbound entrance ramp to the Gulf Freeway in Houston. Normally data would have been collected using the computerized detection system. However, at the time this study was conducted, the computer available at the Freeway Surveillance Center was not fully operational and more data inputs were required than were computerized.

Data were collected by recording events on an Esterline-Angus 20-pen graphic recorder. In order to attain the desired accuracy in measuring vehicle speed based on the actuation of two consecutive, closely spaced induction loop detectors, the recorder was modified for a chart drive speed of 30 in. per minute. This allowed the measurement of speeds up to 50 mph with an accuracy of 2 mph over a 30-ft speed trap.

To collect the desired data, use was made of the permanent loop detector installations as well as temporary loops that were taped on the ramp and the freeway outside lane. The locations of these detection stations are shown in Figure 2. Some data were also collected by observers with microswitches. The detector amplifier units and 20-pen recorder were housed in the back of a station wagon. Permanent detector amplifiers and permanent circuit terminals were located in cabinets beside the frontage road. The station wagon was located near a detector cabinet to connect the recorder to the permanent circuit relays, and to obtain power for the recorder and temporary loop amplifier units.

Two observers were utilized during the study. One observer recorded the arrival of vehicles to the ramp queue and the departure of impatient drivers from the ramp queue. The second observer recorded the time at which the ramp vehicle merged, the ramp vehicle classification, and the delay incurred by a vehicle that became trapped

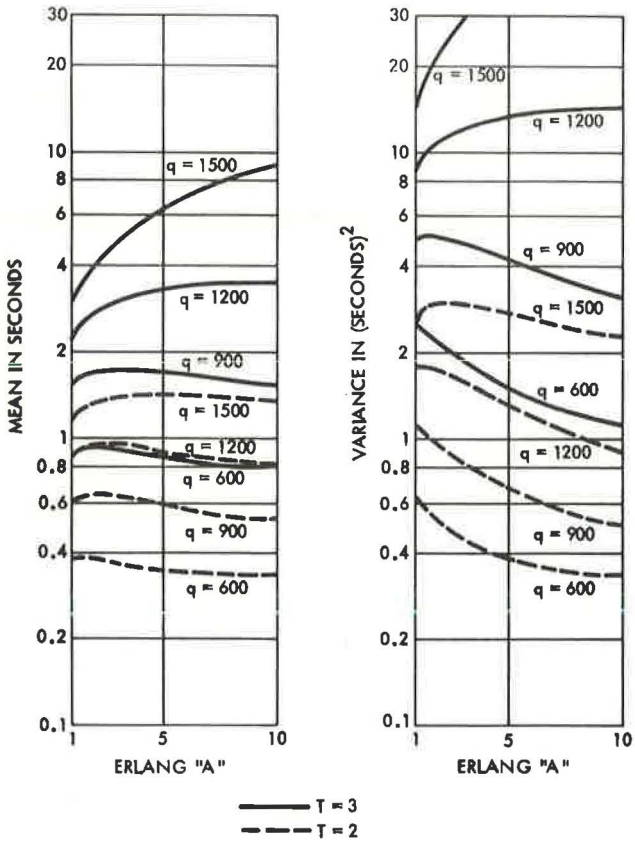

Figure 1. Mean and variance of wait at ramp signal.

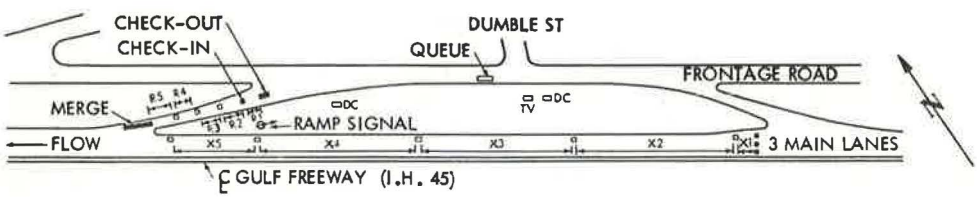

DIMENSIONS

R1 = 15 ft
R2 = 24 ft
R3 = 23 ft
R4 = 25 ft
R5 = 36 ft
X1 = 25 ft

LEGEND

- TEMPORARY 6 ft x 6 ft LOOP
- PERMANENT 6 ft x 6 ft LOOP
- PERMANENT SPECIAL SIZE LOOP
- DC DETECTOR CABINET
- SURVEILLANCE TV CABINENT

SCALE:

Figure 2. Layout of site.

TABLE 1

SUMMARY OF DATA SETS COLLECTED

Data Set	Study Date	Time	Type of Control	Number of Freeway Vehicles	Number of Ramp Vehicles
1	Dec. 21, 1967	a.m.	Fixed rate	611	187
2	Dec. 20, 1967	a.m.	Fixed rate	523	118
3	Dec. 20, 1967	a.m.	Fixed rate	815	283
4	Dec. 21, 1967	a.m.	Fixed rate	693	126
5	Jan. 24, 1968	a.m.	Gap-acceptance	643	103
6	Jan. 24, 1968	a.m.	Gap-acceptance	763	222
7	Jan. 25, 1968	a.m.	Gap-acceptance	679	219
8	Jan. 25, 1968	a.m.	Gap-acceptance	535	86
9	Dec. 21, 1967	p.m.	None	353	168
10	Dec. 20, 1967	p.m.	None	445	195
11	Jan. 26, 1968	a.m.	Capacity-demand	678	99
12	Jan. 26, 1968	a.m.	Capacity-demand	779	259
13	Dec. 22, 1967	a.m.	Fixed rate	769	186
14	Dec. 22, 1967	a.m.	Fixed rate	617	152

TABLE 2

DATA SETS PROCESSED THROUGH ANALYSIS PROGRAMS

Analysis Program	Data Set Number													
	1	2	3	4	5	6	7	8	9	10	11	12	13	14
Ramp speed and acceleration	√	√	√	√	√	√	√	√	√	√	√	√	√	√
Ramp arrival pattern	√	√	√	√	√	√	√	√	√	√	√	√	√	√
Ramp queue	√	√	√	√	0	√	√	√	√	0	√	√	√	√
Ramp system input-output	√	√	√	√	√	√	√	√	√	√	√	√	√	√
Ramp travel times	x	x	√	√	√	√	√	√	x	x	√	√	√	√
Freeway approach speed	√	√	√	√	√	√	√	√	√	x	√	√	√	√
Freeway arrival pattern	√	√	√	√	√	√	√	√	√	√	√	√	√	√
Freeway gap pattern	√	√	√	√	√	√	√	√	√	√	√	√	√	√

NOTES:
√ = Data set has been successfully processed through program.
x = Data set cannot be processed through program because of failure in data collection.
0 = Data set cannot be processed through program because of unidentifiable error.

at the end of the acceleration lane. Weather conditions prohibited conducting all studies on consecutive weekdays. Two separate study periods were required necessitating a second preparation of the site. The total quantity of data collected is given in Table 1.

Each graphic data record was processed through a Gerber analyzer to reduce the graphic data record to a BCD punched card data record. The data analysis was computerized as much as possible. The reduced data presented a semirandomly organized set of data points because of the nature of the process through the Gerber analyzer. Consequently, most computer programs were organized in two sections: (a) a main program that read all the data cards from a data set, reorganized the data, and stored the data in arrays representing the order in which events occurred during the original study; and (b) one or more subroutines that contained the analytic procedures. The one exception to this scheme of organization was a main program section that calculated the speed and acceleration of ramp vehicles.

Table 2 gives the extent to which all data collected and reduced were processed through the analysis programs. Note that some data sets were not compatible with all analysis programs because of either a failure in a hardware component of the data collection system, or an unidentifiable data inconsistency.

VERIFICATION OF ASSUMED TRAFFIC CHARACTERISTICS

Poisson Ramp Arrivals

In order to develop the model, Poisson arrivals into the ramp queue had to be assumed. Although this may not be a particularly crucial assumption, it is worthwhile to investigate its validity. The fact that a control period spans the build-up, peak period, and dissipation of a transient traffic demand is sufficient justification. Table 3 gives the results of testing the hypothesis, using the chi-square test, that arrivals in each data set were Poisson-distributed. If the hypothesis is rejected when the probability of chi-square exceeding the calculated chi-square is less than 0.05, then only 8 out of the 42 tests indicate that the observed arrivals were significantly different from a Poisson distribution. On this basis, the assumption of Poisson arrivals is valid.

TABLE 3

RESULTS OF TESTING RAMP ARRIVALS FOR POISSON BEHAVIOR

Data Set	Interval (minute)	Chi-Square Value	Degrees of Freedom	Probability of Greater Chi-Square
1	0.5	3.46	7	0.80
1	1.0	6.34	6	0.30
1	5.0	1.21	4	0.80
2	0.5	6.14	5	0.20
2	1.0	8.38	6	0.20
2	5.0	7.23	3	0.05
3	0.5	6.60	8	0.50
3	1.0	6.96	8	0.50
3	5.0	4.92	4	0.20
4	0.5	6.23	5	0.20
4	1.0	2.74	6	0.80
4	5.0	4.31	3	0.20
5	0.5	8.03	5	0.10
5	1.0	17.18	4	0.001
5	5.0	7.60	3	0.05
6	0.5	27.96	7	0.0005
6	1.0	2.05	7	0.95
6	5.0	2.38	4	0.60
7	0.5	4.79	8	0.70
7	1.0	2.51	7	0.90
7	5.0	3.03	4	0.50
8	0.5	6.17	4	0.10
8	1.0	3.95	5	0.50
8	5.0	2.26	2	0.70
9	0.5	2.18	8	0.975
9	1.0	8.24	6	0.20
9	5.0	2.31	2	0.30
10	0.5	12.64	7	0.05
10	1.0	16.88	6	0.005
10	5.0	7.81	2	0.01
11	0.5	8.25	5	0.10
11	1.0	3.79	5	0.50
11	5.0	5.05	4	0.20
12	0.5	6.47	8	0.50
12	1.0	7.71	8	0.40
12	5.0	6.85	5	0.20
13	0.5	3.44	6	0.70
13	1.0	5.28	6	0.50
13	5.0	7.83	3	0.025
14	0.5	32.23	5	0.0005
14	1.0	22.82	4	0.0005
14	5.0	11.55	3	0.005

Move-Up Time (Starting Delay)

Because the basic queuing approach inherently assumes that a negligible time is required for each vehicle to move forward one position in the queue, the starting delay at the ramp signal was measured. To investigate the driver-vehicle response to the ramp signal stimulus, the time interval between the instant that the ramp signal turned green and the instant that the check-out detector (located 9.5 ft from the signal) was actuated was measured for each vehicle facing an unobstructed ramp. The resultant histograms are shown in Figure 3. From this figure the response times appear to be normally distributed. Table 4 gives the results of testing for normality with the chi-square test. By rejecting the null hypothesis that the driver-vehicle response is normally distributed when the calculated chi-square exceeds the chi-square with 5 percent confidence, only data sets 3, 6, and 11 are considered normal.

Data sets 3, 6, and 11 were tested for equality of variances, and all F-test statistics are not significant at the 95 percent level of confidence. The results of the tests are given in Table 5. Combinations of the three data sets were tested against the null hypothesis that the means were equal. All combinations were not significant at 95 percent confidence. Because all the data sets indicate a strong central tendency, even though a few deviant values prevent all sets from testing as normally distributed, the

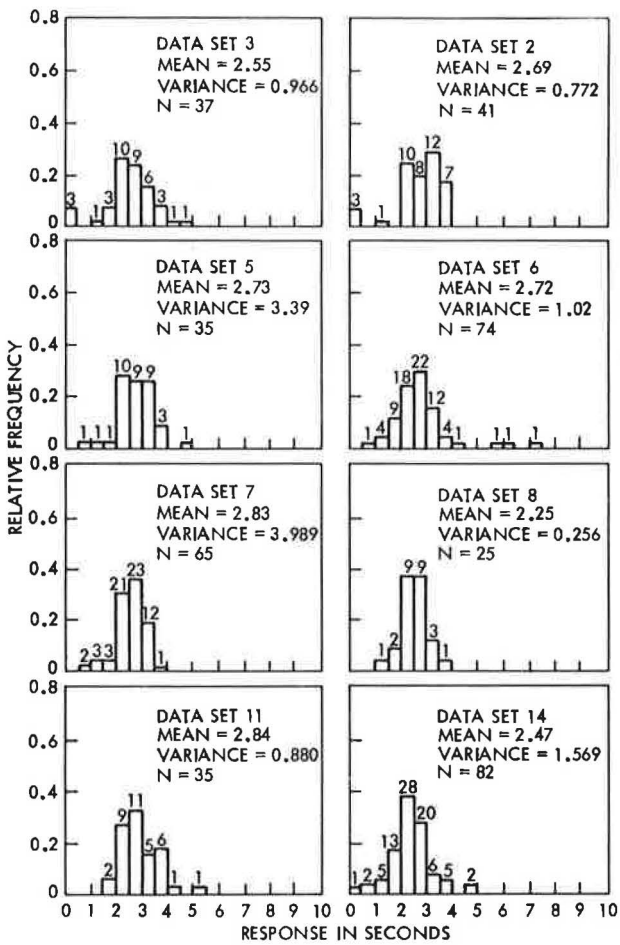

Figure 3. Driver-vehicle response at ramp signal (unobstructed vehicle).

TABLE 4

DRIVER-VEHICLE RESPONSE TO RAMP SIGNAL STIMULUS TEST FOR NORMALITY

Data Set	Number of Vehicles	Mean Time	Variance of Time	Calculated Chi-Square	Degrees of Freedom	Tabulated Chi-Square[a]
2	41	2.69	0.772	16.13	5	11.1
3	37	2.55	0.966	5.38	5	11.1
5	35	2.73	3.390	39.92	9	16.9
6	74	2.72	1.020	12.61	7	14.1
7	65	2.83	3.989	109.58	9	16.9
8	25	2.25	0.256	7.36	2	5.99
11	35	2.83	0.830	7.94	5	11.1
14	76	2.47	1.569	46.78	8	15.5

[a]Probability of greater value is 0.05.

TABLE 5

TESTS FOR EQUAL MEANS AND VARIANCES OF DRIVER-VEHICLE RESPONSE TO A RAMP SIGNAL

Data Sets Tested	Calculated F Statistic	Table F	F-Test Significant?	Calculated t Statistic	Table t	t-Test Significant?
3, 6	1.06	1.86	No	0.846	1.983	No
3, 11	1.16	1.98	No	1.272	1.994	No
6, 11	1.23	1.86	No	0.590	1.983	No

mean value can be considered to be a good measure of the driver-vehicle response to be used in a model. All the data, grouped together, have a mean of 2.62 sec and a variance of 0.705 sec.

It is obvious that if the move-up time is to be negligible, there must be some other minimum time required at the signal that tends to exceed the move-up time. The approximate lower bound on a background cycle to flash the red, green, and amber signal indications is 3.0 sec. In all cases, the majority of the data points are less than 3.0 sec, thus indicating that, on the average, the initial assumption was permissible.

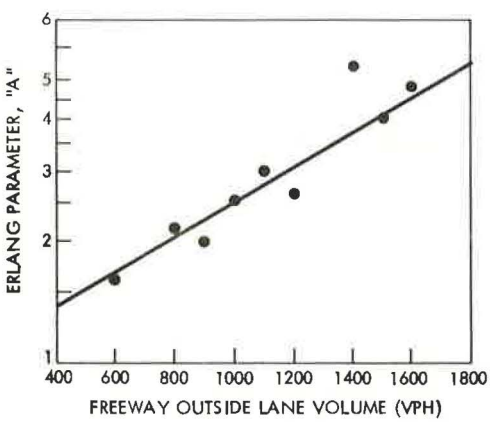

Figure 4. Empirical relation of freeway volume to Erlang "a".

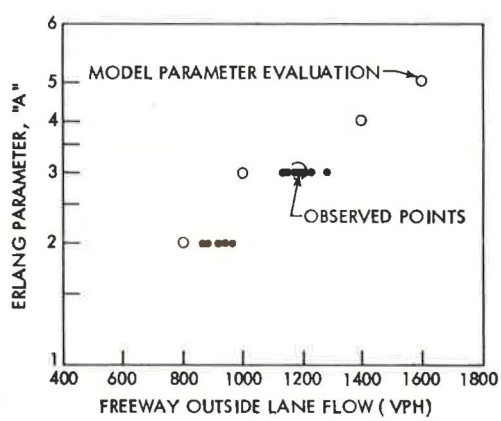

Figure 5. Observed and utilized freeway flow to Erlang "a" relation.

However, any predictions based on the model could be expected to represent only average trends.

Erlang Gap Distribution

If signal control is based on response to the availability of gaps in the freeway stream, then the assumed pattern of freeway traffic should be a reasonable model of the actual process. The Erlang headway distribution has been studied previously for applicability to traffic flow (10). The parameter of interest with respect to outside freeway lane flow is the value of the Erlang "a" parameter. Drew, Buhr, and Whitson (1) reported an empirical approximate relationship between the Erlang "a" parameter for the headway probability density and the average freeway lane flow as shown in Figure 4. A number of data sets of freeway gaps recorded at the gap detector (5-min and 1-min intervals) were evaluated to establish Erlang distribution parameters for the total study period. Table 6 gives a summary of the headway analysis for one such data set. The

TABLE 6

SUMMARY OF FREEWAY GAP-DISTRIBUTION ANALYSIS

Erlang "a"	Erlang "b"	Average Headway	Headway Variance	Average Freeway Flow[a]	Average Freeway Speed
Total period					
2	0.706	3.0	4.21	1,210	37.40
5-min intervals					
3	1.172	2.7	2.27	1,344	36.09
2	0.619	3.2	5.22	1,116	37.77
3	1.246	2.7	2.19	1,320	36.24
2	0.576	2.7	4.68	1,332	34.22
2	0.547	3.1	5.68	1,164	37.47
2	0.645	3.0	4.65	1,200	39.25
2	0.677	3.5	5.18	1,020	41.42
1-min intervals					
3	1.257	2.3	1.80	1,560	35.78
3	1.170	2.8	2.42	1,260	34.85
3	0.894	3.2	3.57	1,080	35.95
4	1.623	2.7	1.69	1,260	36.76
3	1.160	2.5	2.16	1,560	36.96
1	0.346	3.0	8.69	1,200	36.64
2	0.599	3.4	5.60	1,080	37.54
3	1.010	3.3	3.31	1,080	36.68
2	0.592	3.5	5.98	1,020	38.19
3	0.886	3.0	3.38	1,200	39.72
3	1.084	3.0	2.78	1,200	36.10
4	1.580	2.6	1.63	1,380	36.18
3	1.062	2.9	2.74	1,260	34.54
4	1.545	2.3	1.50	1,560	34.23
3	1.138	3.0	2.59	1,200	40.56
2	0.524	3.2	6.04	1,140	33.34
1	0.530	2.7	5.18	1,320	34.52
2	0.795	3.0	3.77	1,140	34.12
4	1.976	2.1	1.06	1,800	32.84
1	0.307	2.8	9.09	1,260	36.75
2	0.507	3.5	6.99	1,020	40.27
2	0.588	3.3	5.68	1,080	38.21
2	0.630	2.6	4.16	1,320	35.41
5	1.981	2.7	1.38	1,260	37.94
1	0.302	3.5	11.49	1,140	36.13
5	1.844	2.8	1.51	1,200	36.91
1	0.364	3.4	9.22	1,140	40.29
2	0.542	3.1	5.73	1,140	34.42
2	0.853	2.5	2.95	1,440	39.23
2	0.704	3.4	4.84	1,080	40.09
2	0.492	4.2	8.56	840	44.14
2	0.512	3.5	6.85	1,020	43.65
4	1.171	3.0	2.60	1,200	39.29
2	0.587	3.3	5.68	1,080	40.35
4	0.982	3.7	3.73	960	40.52

[a]Outside lane flow rate for interval.

range of variation on the Erlang "a" parameter in Table 6 is typical for a sample of stable peak-period flow.

Figure 4 is based on a 5-min interval to measure the flow rate and gap distribution. Because 1-min counts of gaps are unduly influenced by one very large or very small gap, the 5-min count was used in this research as the basis for establishing the value of the Erlang "a". Figure 5 shows the Erlang "a" values versus a 5-min freeway flow rate obtained from the gap analysis. The values used to predict the wait at signal are also shown in Figure 5; 5-min flow rate parameters are stable and reasonably well predicted.

PREDICTED TRAFFIC CHARACTERISTICS OF OPERATION

Constant Fixed-Rate Metering

When the fixed-rate metering is employed, it is presumed that the rate of release of vehicles at the signal is in fact a constant. If driver-vehicle characteristics vary in a manner that distorts the effective metering rate, they must be verified. A control schedule developed on the basis of erroneously predicted metering rates could undo all the anticipated freeway benefits.

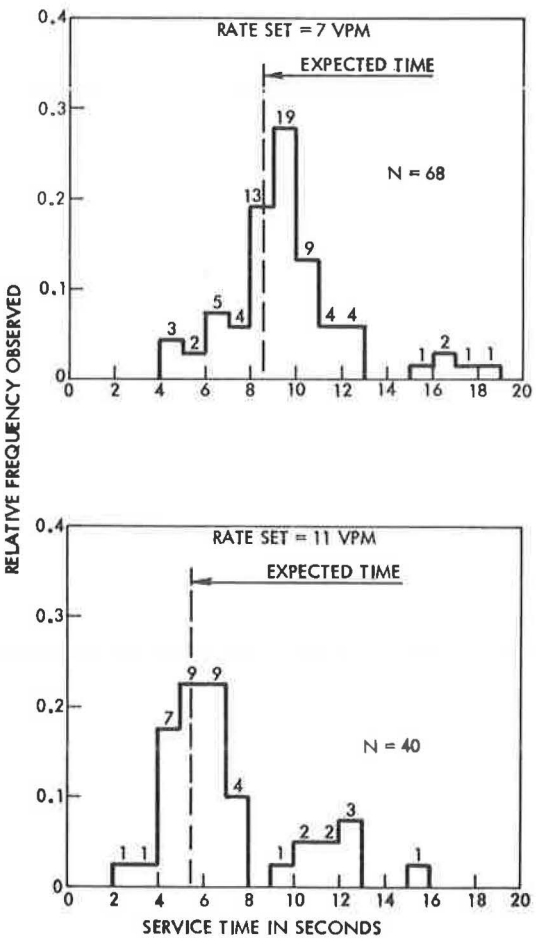

Figure 6. Observed and expected service time for fixed-rate metering.

In Figure 6 the inverse of the set metering rate, the average observed service time for unobstructed vehicles, and the individual observed service time for unobstructed vehicles are shown. The data points were obtained for two different metering rates (7 vehicles per min and 11 vehicles per min). If the service time had been a constant, the individual observed points should be scattered about either the line representing the inverse of the set or the observed average service time with variation caused by measurement errors. At a set rate of 11 vehicles per min (expected service time of 5.47 sec), the observations vary less than those at a set rate of 7 vehicles per min (expected service time of 8.57 sec), but the variation does exceed possible measurement error (on the order of 0.05 sec). The variability can possibly be caused by the driver's response to the signal that would tend to produce a service time longer than expected. The service times considerably shorter than expected are probably due to signal violators that accounted for 10.1 percent of the sample. As can be seen in Figure 6, the set rate of metering is a good central tendency rate of ramp vehicle input to the freeway.

Wait at Ramp Signal

The service time (wait) of each ramp vehicle was measured as the time expiring between the instant that the check-

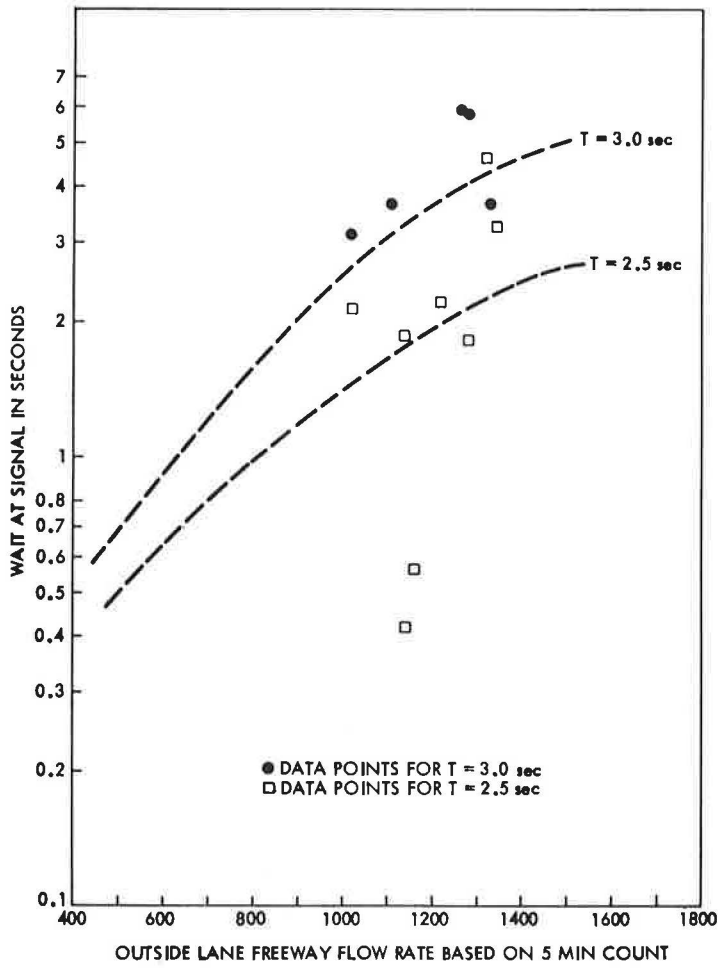

Figure 7. Theoretical and observed mean service times at ramp signal under gap-acceptance control.

in detector was first actuated until the instant that the ramp signal turned green. In order to exclude delays caused by other vehicles stopped in the merging area, service times were measured only when the merge detector was off. In addition, owing to a severe limitation on ramp queue storage, some waits at the signal had to be omitted because the vehicles were released under a fixed-rate override metering rate rather than gap-acceptance control. The mean service time was calculated for each 5-min period of gap-acceptance control during stable freeway speeds (no slowdown or shock wave). A 5-min period was used because the Erlang parameters for the predictive model are based on a relationship to 5-min freeway flow rates.

Figure 7 shows, for service gap settings of 2.5 and 3.0 sec, the observed mean service and the theoretical expected delay as predicted by an evaluation of Eq. 9. The observed values fluctuate about the predicted curve, which is to be expected because the theoretical curve is based on steady-state conditions. In general, however, the predicted service times seem to be shorter than the observed times. This is probably due to the assumption, inherent in the theoretical derivation of the delay, that a vehicle

TABLE 7

PREDICTED AND OBSERVED AVERAGE QUEUE LENGTH FOR STUDY PERIOD

Data Set	Type of Control	Average Observed Queue Length	Predicted Average Queue Length
2	Fixed-rate metering	0.71	0.48
3	Fixed-rate metering	1.29	1.27
13	Fixed-rate metering	2.71	2.55
6	Gap-acceptance	3.82	0.53
7	Gap-acceptance	7.21	1.04
8	Gap-acceptance	1.18	0.37

accepting the first available gap is not delayed and has a service time of zero. This would be true except for a minimum background cycle that fixes the minimum time between the release of two consecutive vehicles.

By taking the theoretical relationship to be a reasonable representation of the delay at the signal and measuring the headway characteristics approaching the merging area, the average wait at the signal can be projected on a minute-by-minute basis. This is useful in considering two problems associated with merging control: (a) the wait at the signal that a driver will tolerate before violating the red signal indication, and (b) the approximate number of vehicles that can be expected to be served in the next minute. If the tolerance for a driver's wait at the signal is known, the upper limit on controller settings can be established for given freeway flow conditions. If the headway characteristics approaching the merging area are known, then the inverse of the expected delay yields an average number of vehicles that may be served in the next time interval for the present merging controller setting.

Queue Lengths at Ramp Signal

Equation 4 was used to predict the average queue length based on the controller-set fixed metering rate. Both the average measured queue length and the predicted queue length are given in Table 7. Under the fixed-rate metering, Eq. 4 yielded a good measure of the queue on the three studies that had no freeway stoppages.

Equation 1 produced the predicted average queue length during gap-acceptance control. In comparing the observed and predicted values, it is obvious that Eq. 1 grossly underestimated the queue length. (Note that the mean and variance of the wait at the signal used in Eq. 1 are based on the gap-acceptance control release of every vehicle.) A considerable number of vehicles were unduly delayed because a driver stopped in the merging area, thereby terminating gap-acceptance control until the merge area of the ramp cleared. During this time the queue builds up, but allowance is made for this in the expected service time used in Eq. 1.

FINDINGS AND CONCLUSIONS

The following can be concluded with respect to predicting ramp operating characteristics under signal control by a queuing approach:

1. The assumption of Poisson arrivals during a peak period is valid for ramp arrivals.
2. The wait at the ramp signal for vehicles released under gap-acceptance control is reasonably well predicted by the renewal process development. It does, however, tend to underestimate the wait.
3. For fixed-rate metering control, the queuing model yields a good estimate of the expected queue length.

Additional findings include the following:

1. A set fixed metering rate does not represent a constant rate of release of vehicles from the ramp signal. On the average, it approximates the controller setting.
2. Driver-vehicle units do not respond to the green signal in a constant fashion. The response time appears to be normally distributed about a mean response.
3. Average queue lengths are not predicted well by the gap-acceptance queuing model over any length of time. It is not possible to sufficiently describe mathematically all the control mechanisms by which the queue can be depleted. The study site would not permit adjusting the controller to only gap-acceptance release of vehicles.

ACKNOWLEDGMENT

The author gratefully acknowledges the guidance and counsel of his graduate advisory committee including Donald R. Drew, Charles J. Keese, Charles Pinnell, A. W. Wortham, and Glen D. Self. This paper was a portion of a doctoral dissertation written at Texas A&M University under their supervision. The support of the Engineering Research Insititue of Iowa State University, Ames, is also acknowledged.

REFERENCES

1. Drew, D. R., Buhr, J. H., and Whitson, R. H. Determination of Merging Capacity and Its Applications to Freeway Design and Control. Highway Research Record 244, 1968, pp. 47-68.
2. Brewer, K. A., Buhr, J. H., Drew, D. R., and Messer, C. H. Ramp Capacity and Service Volume as Related to Freeway Control. Texas A&M Univ., College Station, TTI Rept. 504-5, 1968.
3. Buhr, J. H., Whitson, R. H., Brewer, K. A., and Drew, D. R. Traffic Characteristics for Implementation and Calibration of Freeway Control. Texas A&M Univ., College Station, TTI Rept. 504-2, 1968.
4. Weiss, G. H., and Maradudin, A. A. Some Problems in Traffic Delay. Operations Research, Vol. 10, No. 1, 1962, pp. 74-104.
5. Adams, W. F. Road Traffic Considered as a Random Series. Jour. of the Institute of Civil Engineers, Vol. 4, 1936, pp. 121-130.
6. Kendall, D. G. Some Problems in the Theory of Queues. Jour. of the Royal Statistical Society, Series B, Vol. 13, 1951, pp. 151-185.
7. Newman, L., Dunnet, A. M., and Meis, G. J. Freeway Ramp Control—What It Can and Cannot Do. Traffic Engineering, Vol. 19, No. 7, 1969, pp. 14-21.
8. Drew, D. R., McCasland, W. R., Pinnell, C., and Wattleworth, J. A. The Development of an Automatic Freeway Merging Control System. Texas A&M Univ., College Station, TTI Rept. 24-19, 1966.
9. Brewer, K. A. Description and Evaluation of Controlled Freeway Merging. Texas A&M Univ., College Station, PhD dissertation, 1968.
10. Buckley, D. J. Road Traffic Headway Distributions. Australian Road Research Board Proc., Vol. 1, Pt. 1, 1962, pp. 153-187.

Effect of Trucks on the Urban Freeway

JACK B. HUMPHREYS, Department of Civil Engineering, University of Tennessee

An investigation was made into the effect of trucks or grades or both on urban freeway level of service. The primary parameter used was acceleration noise, a well-known and widely used traffic research parameter. A traffic stream composed of both cars and trucks was examined. A short section of the roadway was considered and the entering and leaving energy of the stream equated. Assumptions concerning the resistance to both motion and acceleration were also developed. For verification of the model developed, aerial time-lapse photographs supplied the bulk of the data. Utilizing 100-ft sections marked off on the freeway shoulder, speeds and accelerations for each vehicle photographed were calculated. From these, macroscopic speed and acceleration noise profiles were determined. The results of the research indicate that acceleration noise definitely increases on a positive grade of a rolling urban freeway. The amount of change is independent of the lane studied, however. Because of a wide variance in the percentage of trucks on the different lanes, the conclusion is that trucks do not affect the overall noise values under the conditions studied. This conclusion was strengthened by microscopic noise values and by an examination of typical time-space diagrams. Finally, conclusions were made concerning the type of parameter needed to ascertain the effect of trucks on the road user.

•THE TRAFFIC ENGINEER of today is currently profiting from an unprecedented 20-year boom in highway transportation. The end of World War II and gasoline rationing, the availability of mass-produced automobiles, and the general increase in living standards initially caused tremendous increases in transportation needs. Centralization of the population into large urban areas accompanied by increased industrial growth in the suburbs, primarily along freeways, has added to the problem of transportation. By the early 1950's cities had begun the development of freeway systems that were designed to provide uninterrupted traffic flow.

The number of automobile and truck trips has increased, and the desires of the motorists have changed. Drivers have begun to press for better driving conditions more in line with their powerful and sophisticated automobiles. The quality of the driving conditions now encountered by a motorist on a particular roadway at a particular time has become important to the traffic engineer, who has termed it "level of service". As a result, means of improving traffic conditions as well as increasing volumes are currently under study.

One factor that is now frequently considered as influencing the quality of traffic flow is the number of trucks or slowly moving vehicles or both in the traffic stream. Studies have been made to determine the influence of trucks on rural highway flow, but to date little work has been devoted to this consideration on urban freeways. The effect of trucks or grades or both on the level of service of urban freeways has not been widely investigated. This paper considers this problem area, in order that future driving conditions encountered by the urban freeway motorist may be understood and predicted.

Many parameters, such as Platt's "level of service index" (1) and Herman's so-called "acceleration noise" (2), have been advanced as a means of measuring the level of service of urban facilities. It is this latter parameter that was primarily used in the analysis reported herein.

By definition, acceleration noise, σ, is the root-mean-square of the acceleration of a vehicle. It has been shown by Dudek (3) that σ may be approximated by use of the formula

Paper sponsored by Committee on Characteristics of Traffic Flow and presented at the 49th Annual Meeting.

$$\sigma = \left[\frac{(\Delta\mu)^2}{T}\sum\frac{1}{\Delta t}\right]^{1/2} \quad (1)$$

where

$\Delta\mu$ = speed change of a predetermined magnitude,
T = total trip time, and
Δt = time increment required for $\Delta\mu$.

The value of this parameter has been well established by Drew and Keese (4) and Drew and Dudek (5). Because it does measure to some degree the interactions between the driver, the road, and traffic conditions, numerous test runs have been made over various categories of roads both in the United States and abroad. Results of such tests indicate that σ may give a better measure of traffic conditions than travel and stopped times. More specifically, σ has been proven to be an excellent measure of the level of service of freeway flow.

MODEL DEVELOPMENT

Drew and Keese (4) and Drew and Dudek (5) have reported the reliability of considering the traffic stream as a one-dimensional, compressible fluid stream. If this analogy is to be true, the principle of the conservation of energy must be maintained.

The general form of the energy equation may be recalled as

$$\frac{W_1\mu_1^2}{2g} + \frac{W_1P_1}{\gamma} + W_1Z_1 + U_1 = \frac{W_2\mu_2^2}{2g} + \frac{W_2P_2}{\gamma} + W_2Z_2 + U_2 + \text{losses} \quad (2)$$

where the total head at section one equals the total head at section two plus any losses between the sections. The four terms that combine to make up the total energy at a section are the kinetic, pressure, elevation, and internal energies respectively.

In the foot-pound-second system, the units of each of these terms are foot-pounds (ft-lb). If the pressure energy, internal energy, and losses are all considered as a form of internal energy, I, then the units of I must be foot-pounds. Previous research has indicated that σ is a measure of I (5), or $I \approx \sigma$. If I is to be in foot-pounds, then

$$I = \text{foot-pounds} = \phi ML\sigma$$

where

ϕ = dimensionless constant;
M = mass, slugs;
L = length of section, feet; and
σ = acceleration noise, feet per second squared.

Dimensionally, then

$$I = \left(\frac{\text{lb sec}^2}{\text{ft}}\right)\left(\text{feet}\right)\left(\frac{\text{feet}}{\text{sec}^2}\right) = \text{foot-pounds}$$

A change I is then measured as

$$I = \Delta\phi ML\sigma = \left(\frac{W_1P_1}{\gamma} - \frac{W_2P_2}{\gamma}\right) + (U_1 - U_2) - \text{losses}$$

Combining and rearranging yields

$$\Delta\phi ML = (W_2Z_2 - W_1Z_1) + \frac{W_2\mu_2^2}{2g} - \frac{W_1\mu_1^2}{2g} \quad (3)$$

which states that a positive change in internal energy occurs when elevation or kinetic energy increases. If the section is short and traffic continuity is maintained such that $W_1 = W_2$ and $\gamma_1 = \gamma_2$, then we obtain

$$\Delta\phi ML\sigma = W(Z_2 - Z_1) + \frac{W}{2g}(\mu_2^2 - \mu_1^2)$$

or

$$\Delta\phi \frac{W}{g} L\sigma = W(Z_2 - Z_1) + \frac{W}{2g}(\mu_2^2 - \mu_1^2)$$

which yields

$$\Delta\phi\sigma = \frac{g(\Delta Z)}{L} + \frac{(\mu_2^2 - \mu_1^2)}{2L} \tag{4}$$

Because ΔZ is the change in elevation, it is approximately equal to $L\alpha$ (if α is small). By substitution we get

$$\Delta\phi\sigma = \frac{g}{L}(L\alpha) + \frac{(\mu_2^2 - \mu_1^2)}{2L}$$

and

$$\Delta\phi\sigma = g\alpha + \frac{(\mu_2^2 - \mu_1^2)}{2L}$$

If $\beta = 1/\phi$, then

$$\Delta\sigma = \beta\left[g\alpha + \frac{(\mu_2^2 - \mu_1^2)}{2L}\right] \tag{5}$$

This constant β allows flexibility in fitting a change in acceleration noise to a particular roadway and its profile.

If the speeds of the traffic stream as measured at the end points of the section are the same, the second term of Eq. 5 goes to zero and

$$\Delta\sigma = \beta g\alpha = \text{Constant } (\alpha) \tag{6}$$

This states that the change in acceleration noise is directly proportional to the grade under the conditions assumed.

The importance of this model lies in the fact that the weight of the vehicles in the traffic stream does not appear, either microscopically or macroscopically. It can be shown that the change in the velocity of a vehicle on a grade is only dependent on its capability of overcoming the component of the vehicular weight parallel to the grade. If, on short grades such as those encountered on urban freeways the capability of light and heavy vehicles to overcome this grade component is similar, the assumptions pertaining to the acceleration noise model may be met. Field studies were conducted to determine the actual conditions encountered.

CONSIDERATIONS CONCERNING STUDY DESIGN

In determining the scope of this research, various complexities regarding adequate samples were considered. Desirably, several urban freeway grades of varying magnitude and length should be studied. For each of these grades, then, the operating characteristics of trucks would need to be studied. Furthermore, any effect caused by a truck would depend on many variables, such as its weight, power, age, and mechanical condition. In addition, the position of the trucks in the traffic stream and their initial speeds would vary greatly.

All possible combinations of these parameters being possible, the number of conditions under which trucks could be observed was quite large. It was decided, however, to concentrate the study at one freeway site. The grade was to have a magnitude and length such that it would represent a typical grade on an urban freeway with a rolling profile. A number of sites in Houston and Fort Worth, Texas, were considered. In

addition, average values for each of the trucks were assumed. However, both macroscopic and microscopic speed analyses were conducted so that the variability of data resulting from the physical characteristics of the trucks could be examined.

DESCRIPTION OF THE STUDY AREA

The site selected for this study was on the Gulf Freeway in Houston, Texas. This freeway, carrying the designations of Interstate 45 and US-75, runs from the Houston central business district to the southeast, ultimately terminating at Galveston, Texas. The first freeway built in Texas, it has six 12-ft lanes with a 4-ft raised median. Basically an at-grade type, the freeway undulates over each of the major cross streets, causing a so-called "roller coaster" effect.

Because of associated research being carried out at the Telephone Road interchange, the inbound upgrade at this interchange was chosen as the specific study site. Approximately one-third of the study section was on a 1-degree horizontal curve, with the remainder on a tangent. Entry grade to the section was -0.3 percent and the maximum grade encountered within the section was +2.445 percent. A plan-profile of the study section is shown in Figure 1.

DATA COLLECTION AND REDUCTION

After selecting the upgrade to be studied, the nose of the Telephone Road on-ramp (inbound) was selected as a reference point. One hundred-foot stations were measured along the inbound shoulder in the outbound direction and marked with 6-in. pressure-sensitive striping tape. These stations were located as shown in Figure 1.

Continuous time-lapse photography was utilized to obtain data for all phases of this study. Because of the length of the study section, it was determined that these films should be made from an aircraft circling the study area.

Because it was necessary to be able to accurately classify the vehicles in the aerial films, a motion picture camera was mounted on the rooftop of a building adjacent to the inbound Telephone Road off-ramp. By synchronizing watches and using an exact filming schedule, simultaneous films were made from the ground and aerial locations

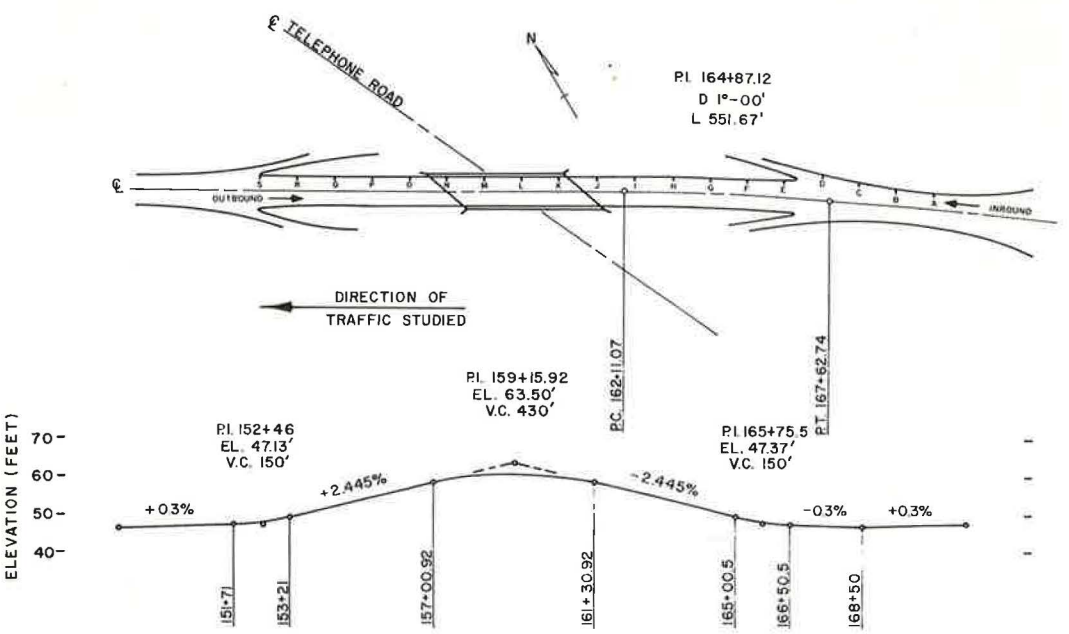

Figure 1. Plan-profile of Gulf Freeway at Telephone Road interchange.

using a 10-frame-per-second filming rate. The ground camera was directed so as to view the right-view quarter of the vehicles so that dual-tired vehicles could be easily classified as trucks.

Analysis of the 35-mm aerial films required a detailed study of every freeway vehicle. Included in each frame as it was photographed was a data board that included a film identification, date, military time clock, and frame counter. By projection of the film on an opaque screen, the location of any particular vehicle with respect to the striped ground stations could be determined. For each vehicle a record was made of the frame number when the front of the vehicle was most nearly opposite each station. As a result, the number of frames required to traverse each 100 ft could be determined. Knowing the film speed in frames per second, speeds and accelerations were computed for each vehicle as it progressed through the study area.

The data were organized and transferred onto IBM punch cards as they were obtained. An edit routine was programmed that checked the cards for errors in logic and key-punching. After editing, all data were analyzed through use of an IBM 7094 computer.

MACROSCOPIC ACCELERATION NOISE PROFILES

Through this analysis, speeds and accelerations of all vehicles passing through the study area were determined for each 100-ft section. For programming ease, particularly in subscripting variables, the letter nomenclature used for the study stations was dropped and the stations were numbered with consecutive odd numbers beginning with 1 at station A. These numbers are hereafter called section numbers.

To show grade correlation with these section numbers, Figure 2 has been included. Figure 2 merely exaggerates the profile as previously shown in Figure 1, and serves as an aid when visualizing the study section. It should be noted that the grade starts about section 9, and the crest of the vertical curve is located near section 23.

Utilizing a basic computer program, macroscopic values of accleration noise through each 100-ft study section were determined. A plot of these values by film and lane is shown in Figure 3. A discussion of the analysis of these profiles follows.

Because the acceleration noise model (Eq. 6) indicated a relationship between acceleration noise and grade, a step-down regression was performed with σ as the dependent variable and the first, second, and third powers of distance into the section as independent variables. Nonsignificant variables were eliminated until all remaining variables were significant at the 0.050 level.

Results of this analysis indicated that σ was dependent on location in at least eight of the twelve data sets. Further significance possibly could have been found by using

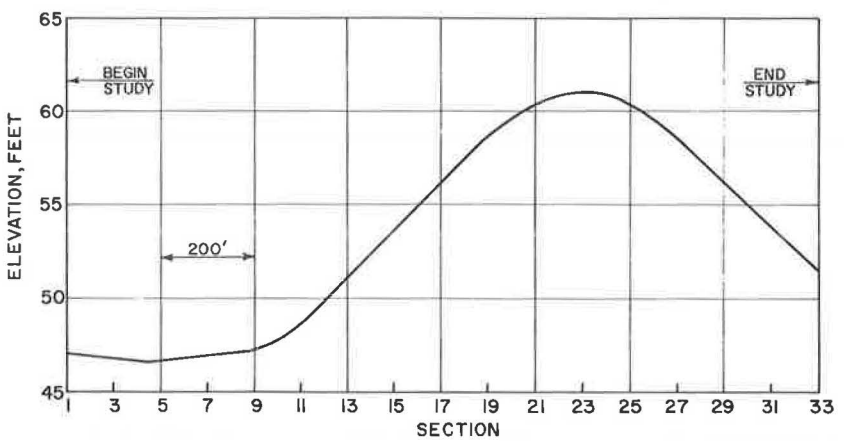

Figure 2. Profile of study area.

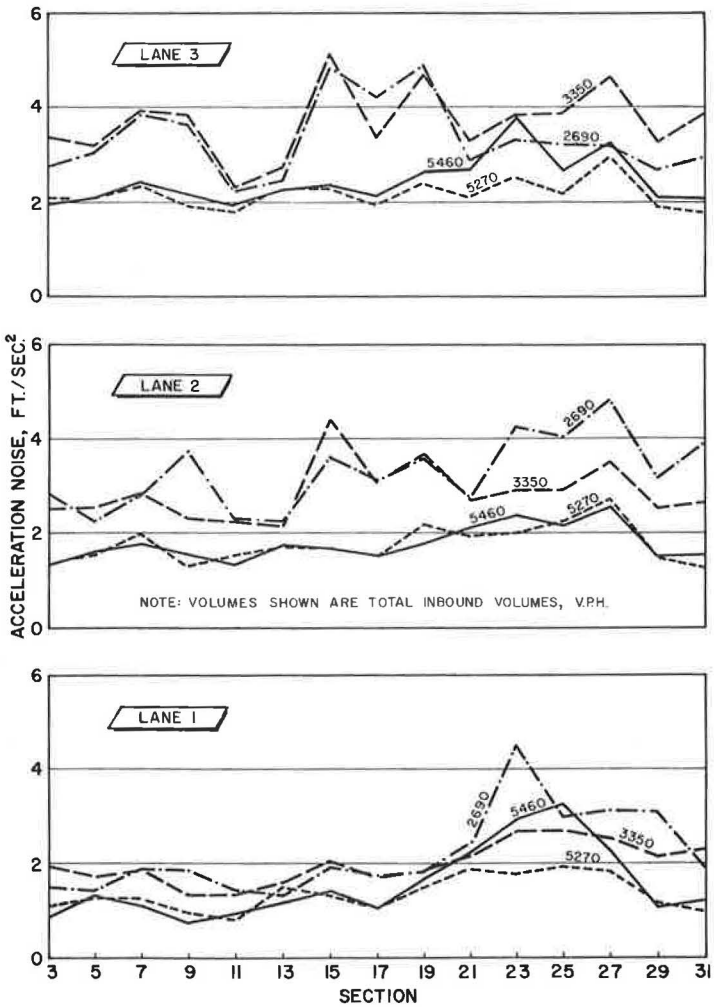

Figure 3. Acceleration noise versus section.

other transformations of the distance such as log x. It was only intended to show the significance of σ on x, however, because it was felt that samples taken on several grades of varying length and slope would be required to determine an empirical relationship of any value.

The model, or $\Delta\sigma$ = Constant (α), indicates that the slope of all of the acceleration noise profiles shown in Figure 3 should be equal. This relationship should be true regardless of the volume or lane considered. Visual examination of the profiles indicates an equality of slopes, especially during the higher flow conditions.

To test the model, a linear regression was made with σ as the dependent variable and distance into the section up to the crest (sections 3 to 23) as the independent variable. Using the F-test for the equality of regression line slopes as outlined by Ostle (6), all acceleration noise profiles were seen to have the same slopes at the 95 percent confidence level. This was true for all volumes taken together, and for the higher flow conditions only. In other words, $\Delta\sigma$ was equal in each noise profile.

MACROSCOPIC SPEED PROFILES

Having thus verified the model, an investigation was made into the assumptions inherent in the model. These assumptions were based on the premise that the speed

characteristics were similar for all vehicles—that is, that trucks had enough reserve power while cruising at normal freeway speeds to overcome the grade component of weight without a decrease in velocity.

By averaging the speeds for all vehicles for each film and lane, speed profiles were developed (Fig. 4). Because speeds were computed by section and all lane changes

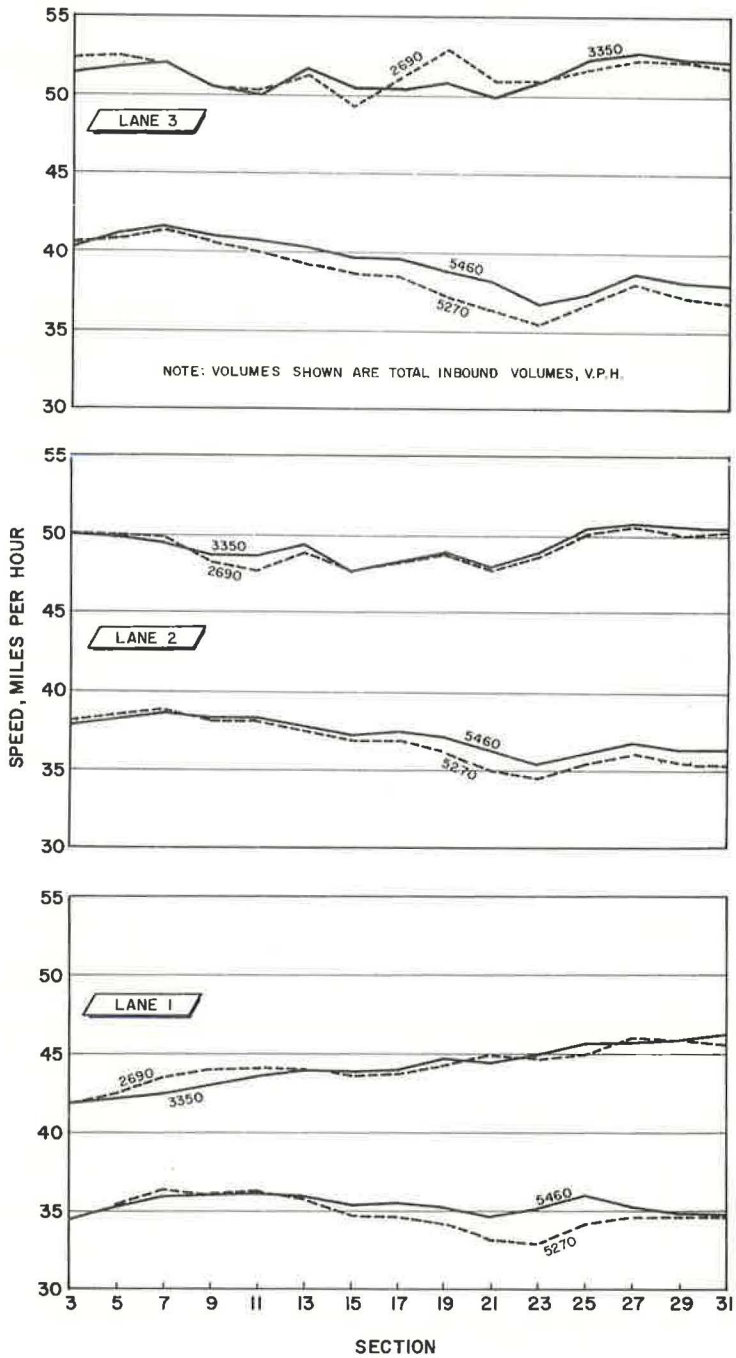

Figure 4. Average speed profile by lane.

considered, this figure reflects all vehicular speeds except those during the 100-ft section in which each lane change took place.

As shown on the speed profiles, all lane speeds tended to decrease during the peak flow periods. However, lane 1, with the higher truck percentage, shows a decrease of only some 2 mph on the grade, whereas lanes 2 and 3 decrease approximately 3 and 5 mph respectively.

Off-peak data showed little, if any, change in overall speed for vehicles on the grade for lanes 2 and 3. Lane 1, however, indicated a definite speed increase obvious through the entire study area. A leveling off of the lane 1 speeds appeared to be taking place on the downgrade, but was not pronounced enough for identification. It was concluded at this point that speed decrements on the grade, if any, were of less magnitude for the lane 1 traffic stream.

Truck volumes and percentages were also calculated for each of the data sets. As expected, truck volumes were higher in lane 1 than in lanes 2 and 3. Lane 1 truck percentages ranged from 4.5 to 10.0, whereas lane 3 ranged from 0.6 to 3.1. Thus, speed decrements were judged not to accompany the lane with the highest percentage of truck flow.

MICROSCOPIC SPEED AND ACCELERATION NOISE PROFILES

Because regression analyses indicated some increase in σ as vehicles traverse the study section up to and across the crest of the grade, a cause for this increase was sought. As an aid in examining the individual vehicular contributions to the noise parameters, two additional programs were developed.

The first of these determined the space and time headways of each vehicle as it entered the study area, as well as the 5-min flow rate in which it was operating. This program also determined σ for each vehicle over the 1,600-ft study section. By studying this output, changes in the magnitude of σ before and after tractor-trailer trucks were noted.

To determine the influence of these particular trucks on the stream, the program was modified to output speed and acceleration profiles of each truck. Examination of these profiles revealed a finding that indicated the validity of the assumptions made in model development. Virtually all tractor-trailer vehicles maintained or increased their speed as they passed through the study area, and no deceleration was found that could be attributed to the grade. This fact, examined in light of the accuracy of the data as previously discussed, was not in keeping with average results for average trucks as reported in the 1965 Highway Capacity Manual (7). The Manual indicates that an average truck on a multilane freeway grade of 2½ percent loses about 3 mph within 500 ft at an initial speed of 40 mph. However, the magnitude of this expected loss in speed is admittedly small, and could be lost very easily in the variability of the available data.

At this point, a time-space diagram of each traffic stream under study was machine-plotted. Each truck, tractor-trailer and otherwise, was identified on these plots, and the speed profile studied. At this point, it was conceded that, for the grade in question and under the traffic volumes filmed, trucks were able to maintain (or increase) their speeds so that the traffic stream should not be disrupted because of their speed characteristics.

As mentioned, however, some variation in the magnitude of σ before and after tractor-trailer trucks (and other trucks as well) was noticed. After determining from the time-space plots queues of vehicles before and after trucks, an average value of σ for each queue was determined. In order for the computed noise values to represent the effect of the trucks, not all of the trucks were analyzed in this manner. For example, if a truck was constrained by the vehicle in front of it, the average noise for the queue following the truck would not be a true reflection of the truck effect, but the effect of some other vehicle. Two such computation are given in Table 1. The results of some additional comparisons are given in Table 2. Note that, in each instant, σ was relatively high for the queue preceding the truck and low for the queue following. In most instances σ was lowest for the truck, indicating a smooth speed profile throughout the study area.

TABLE 1

TABULATION OF ACCELERATION NOISE BEFORE AND AFTER TYPICAL TRACTOR-TRAILER TRUCKS

Lane Data	Lane Rate of Flow	σ for Queued Vehicles	Average σ for Queue
Tractor-trailer truck			
Film 1, lane 1	1,740	2.35	
		2.23	
		2.93	
		2.33	2.46 before truck,
		1.03	
		1.64	
		0.16	1.69 after truck
		0.50	
		2.65	
		1.93	
		2.10	
		1.66	
Film 1, lane 2	2,364	7.44	
		6.18	
		3.73	5.78 before truck,
		2.04	
		3.66	
		2.09	2.38 after truck
		1.98	
		2.83	
		1.63	
		2.10	

TABLE 2

ADDITIONAL AVERAGE VALUES OF σ FOR QUEUED VEHICLES BEFORE AND AFTER TRUCKS

Film	Lane	σ, Queue Before Truck	σ, Queue After Truck
1	1	3.01	0.89
1	1	2.82	2.39
1	1	2.94	2.22
2	2	2.12	1.62
2	2	3.38	2.35
3	1	4.10	2.13
3	2	4.52	2.91
4	2	5.48	2.91

TIME-SPACE DIAGRAMS

After completing the microscopic analyses, time-space diagrams for all data were studied in detail. Sections were then isolated that illustrated some facet of the operational characteristics or problems encountered in the research. No attempt was made to weight one type of situation more than another. Four diagrams illustrating points of interest are included herein.

An explanation of these diagrams is in order. Vehicles in the particular lane being illustrated are plotted by a solid line. If a vehicle changed lanes, the plot is dashed when it is in the adjacent lane. Disappearance of a vehicle indicates that a vehicle moved two lanes over from the lane being plotted. For example, a vehicle starting out in lane 1, then changing to lanes 2 and 3 is, on a lane 1 plot, plotted as a solid line, dashed, then blank. No attempt was made to separate lane changes on lane 2 plots, with dashed lines indicating changes to or from lanes 1 and 3.

Figure 5 shows perhaps the most common idea of the behavior of trucks on grades. Each of the tractor-trailer units shown was traveling at a speed less than that desired by most of the cars in the stream. As a result, large gaps appeared before these vehicles at the crest of the grade. Behind the trucks, vehicle headways tended to decrease, with some changing of lanes evident.

Note that the speed of each truck was virtually constant. In fact, slight increases in speed (as measured by the slope of the line) were evident. An additional point of interest is that the second truck driver actually had no opportunity to increase his speed because of the preceding car. Therefore, while the queued vehicles behind the truck

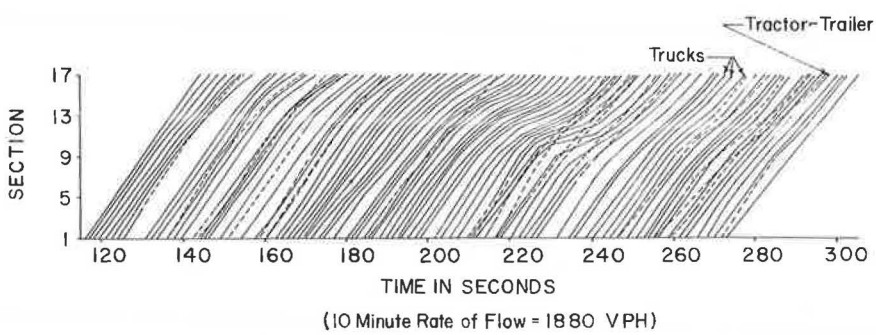

Figure 5. Time-space diagram from film 2, lane 2.

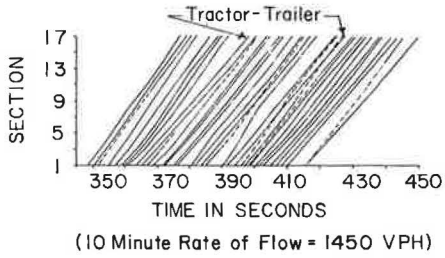

Figure 6. Time-space diagram, lane 1 (350-450 sec).

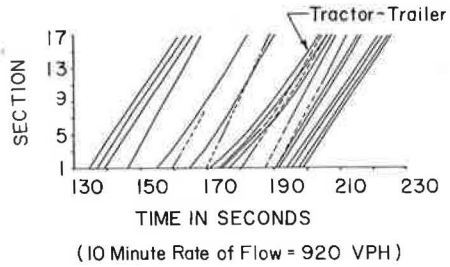

Figure 7. Time-space diagram, lane 1 (130-230 sec).

were being hampered by "that truck", the actual problem vehicle was a slower moving car.

Several shock waves were evidenced as the data were being analyzed. One of the more serious ones is shown in Figure 6. The origin of this shock wave is not known, but it is seen to begin or back into the study area at the upper left of the plot. Prolonged by a heavy flow rate, the wave eventually caused rapid decelerations near the crest of the hill. A 5-sec gap decreased the intensity of the shock wave, which was dampened even more by three trucks moving through the system. The passage of a tractor-trailer unit, however, removed virtually all traces of the disturbance. It is not evident in the plot as shown, but flow after this remained smooth and stable.

The time-space diagram for the tractor-trailer unit shown in Figure 7 is familiar to those personnel engaged in ramp control research on the Gulf Freeway. Ramp and acceleration lane designs on this facility are such that many vehicles are forced to enter the freeway at greatly reduced speeds. Furthermore, for this roller-coaster-type design, on-ramps are in many instances located just prior to upgrades and vehicles are forced to accelerate up to freeway speeds while on the grade. The acceleration capabilities of many loaded trucks thus cause profiles as shown in Figure 7.

Even though this vehicle had the capability of accelerating from 22 mph up to 42 mph through the section, severe conditions might have resulted if this had occurred during the peak flow period. A car obviously would have been able to accelerate more rapidly, causing less disturbance. In this case, lane changes and large headways caused this particular truck to present no operational problems.

Consideration of the problems caused by slow-moving vehicles of any type suggested that Figure 8 should be included. Vehicle A was a car that maintained a speed less than

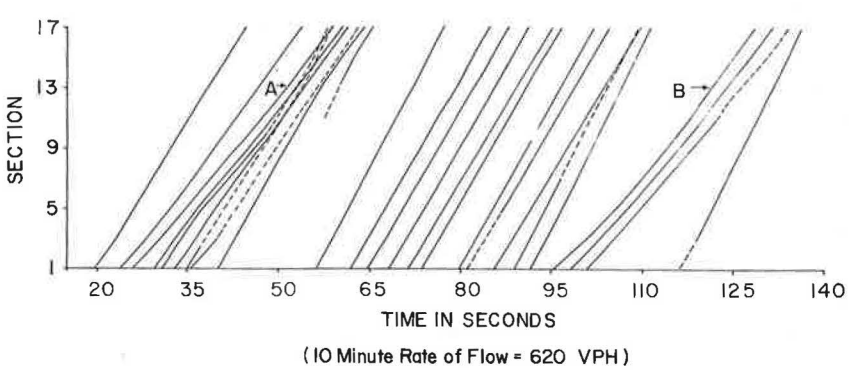

Figure 8. Time-space diagram from film 4, lane 1.

the prevailing lane speed. As can be seen, three lane changes resulted as well as a slowing down of at least four other cars. No indication is evident that the vehicle was forced to this speed. Vehicle B was a tractor-trailer unit that was also traveling slower than the prevailing lane speed. In this instance, B caused no problems, but had it been in the position of A, quite similar conditions to those described above would probably have occurred.

DISCUSSION OF RESULTS

As motorists drive over a given section or roadway, their vehicular speeds are subject to considerable variation. Not only will the speeds between vehicles vary, but each driver will vary his speed as he progresses. Although all the reasons for these speed differences are not known, it has been recognized that they may be physical or psychological, tangible or intangible (8).

When driving at a speed suited to the driver's mood and the surrounding traffic conditions, particularly on a level freeway, the instinctive feeling of many motorists when approaching a grade may be to press down on the accelerator. Although no research was conducted in specially equipped vehicles capable of detecting this movement, many persons have stated to the author that this typifies their actions.

The results of this type of driving action were observed repeatedly while studying in detail the time-space profiles of well over 3,000 vehicles. As observed from the time-space plots, many trucks appeared to be decelerating while moving up the grade, but in reality the vehicles immediately around the trucks were slightly accelerating. In most instances the speed of the trucks was quite steady as they passed through the section.

It will be recalled that in the derivation of Eq. 6 an assumption was made concerning the speed of vehicles. Certain terms were eliminated by the assumption that the speed of the traffic stream was relatively constant up the grade. This finding relating to the truck speeds indicates that this simplifying assumption is a reasonable one. The reason for this maintenance of speed appears obvious. Trucks operating on an urban freeway under average stable flow conditions are not operating at maximum power. The excess power available to each driver is therefore available to overcome the increased gradient resistance, thus resulting in no appreciable speed changes.

This finding was further substantiated by a study of the macroscopic speed profiles shown in Figure 4. The overall speed changes were not great, but they were slightly positive under off-peak conditions. Where motorists drive in peak periods with more attention given to the traffic around them and, in general, disregarding the roadway profile and its relationship to the flat, surrounding terrain, speeds were seen to decrease slightly. From these speed profiles it is seen that, if the automobile driver has sufficient headway as he sees a grade approaching, he tends to compensate for an expected speed loss, thus at least maintaining his speed. To fully verify this occurrence, additional data collected from other grades would be necessary.

Many, if not most, freeway drivers presuppose that trucks cause undesirable disturbances in the traffic stream. Because acceleration noise measures speed disturbances, any such action by trucks should result in an increase in this parameter. Furthermore, because the outer lane carries the highest percentage of trucks, this influence should be noted most in that lane. In analyzing the acceleration noise profiles shown in Figure 3, however, the most obvious feature is the stability of lane 1 flow compared to lanes 2 and 3. Noise values in lane 1 under widely varying volumes are relatively the same, with a general increasing trend as the crest of the grade (section 23) is reached. Volume levels do not separate these profiles into high and low volume groups, and large fluctuations in the profiles are noticeably absent.

Lanes 2 and 3, however, do not follow this trend in that the lower volume profiles are higher in magnitude. Large fluctuations in σ are also apparent at the lower volumes, reflecting again the desires of the driver to compensate for grade by accelerating, rather than by maintaining a constant speed over the grade.

Volume segregations on the lane 2 and 3 profiles are to be expected. For the inbound volumes of 5,460 and 5,270 vph (vehicles per hour), the speed profiles

in Figure 4 range between 35 and 40 mph. On the other hand, speeds from 48 to 52 mph are noted for volumes of 3,350 and 2,690. As derived and confirmed by Drew and Dudek (5), minimum acceleration noise occurs at about 40 mph; thus, further proof of the validity of these data is offered.

It has been shown by regression analysis that σ was dependent on distance into the section. As can be seen from Figure 3, this dependence is quite apparent for peak period flow. From values of approximately 1.0 for lane 1, 1.4 for lane 2, and 2.0 for lane 3, σ increased smoothly up to average values of 2.5, 2.7, and 3.0 ft/sec^2 respectively.

Truck percentages were determined to be quite small for lane 3 during the peak flow period. In fact, during the two filming periods in the peak, no tractor-trailer units were observed in this lane, and a total of only three vehicles classified as trucks were observed. The increase in acceleration noise, particularly on this lane, is therefore seen to reflect the characteristic noise of a stream of cars passing over a grade.

A study of the change in acceleration noise for each of the three lanes indicated that the change in σ was equivalent for the three lanes. Because the truck percentages over the lanes varied widely, the validity of Eq. 6 is proved, and, thus, the change in acceleration noise is a function of the grade and not of the percentage of trucks operating in the lane.

One word of caution must be included at this point to prevent incorrect conclusions concerning the effect of trucks. Although it is true that the vehicles directly behind the trucks tended to have low values of σ, those in front had high values of σ. Macroscopically, the change in σ, or $\Delta\sigma$, was shown to be the same in all lanes. Thus, although trucks did not improve the flow, they did not cause an increase in the average value of $\Delta\sigma$.

Again referring to Figure 3, the acceleration noise appears to be higher in lanes that had the lower truck percentages. This can be attributed to the fact that the left-hand lanes are conventionally used as passing lanes, and the passing maneuver will involve accelerations and decelerations, thus increasing σ. Therefore, the author concludes that the effect of the trucks should be given by the change in σ, and not its magnitude.

Trucks and Automobile Drivers

The author has been offered several suggestions by his colleagues as a result of the findings presented herein. Perhaps the most striking is one offered in jest. This proposal was that a large fleet of trucks might someday be stationed at the outskirts of a city near the freeway. If no heavy vehicles were observed during the morning peak flow period, trucks would be arbitrarily injected into the traffic stream in order to improve the level of service. Obviously this is a major extrapolation of the data presented herein. However, if conditions of flow are much better behind trucks, and if trucks do maintain a more constant speed, the question of "What's the problem?" is surely in order. After studying all the time-space diagrams in this research, several hypotheses are offered that might answer this question in part.

In those diagrams vehicles were seen to pass trucks on the grade even though the trucks were maintaining the average speed of the lane. Other vehicles tended to queue up behind trucks, awaiting their chance to pass and move to a position where they evidently felt more free to "jockey" for speed and position. In other words, automobile drivers were not content to drive behind a truck, which probably would have ensured them of a smoother journey.

Perhaps one reason for this driver feeling is the fume problem experienced when behind certain diesel-powered vehicles. An even better reason put forth by many drivers is that the restricted sight distance is annoying and dangerous. Much of the answer, however, possibly relates to the vagaries of man, who has always tended to be capricious when placed in a man-made environment such as the automobile and the traffic stream. Uncertainties surrounding the "monstrous" truck—"Will he swerve?" "Will he tip over?" and the like—all cause the average motorist to avoid it as if it were the plague.

This type of psychological thinking was also observed by Podesta (9). He stated that, from his observations, large trucks seemed to be a "rather important cause of disturbance for automobile drivers". Although he had no data to verify his comments, he surmised that this disturbing effect was due to noise and fumes, restriction of sight distance, and sensitivity of trucks to grade changes. Because the data presented herein do not support this latter supposition under conditions of short, low grades, his comments relative to the motorist's irritations have become even more important.

Of course, instances do occur where slow-moving trucks enter the freeway just prior to grades and cause a problem. At times of operational breakdowns when flow becomes unstable, the accelerating capability of some trucks is also a problem. As pointed out, however, slow-moving cars also present the "moving bottleneck" problem. Evidently drivers remember the problem trucks much longer than the problem cars, and drive accordingly.

CONCLUSIONS

Before drawing any conclusions from this research, the author would again like to emphasize the limitations of the study. The data were all collected at a single freeway site, and thus no variations due to location of the facility or varying geometric features were obtained. It is felt, however, that the grade at this site represents the average magnitude and length of grade encountered on a rolling freeway. Because of this, results are considered applicable to many similar grades on various roller-coaster-type freeways.

With these limitations in mind, the following findings may be listed:

1. During conditions of light flow, i.e., excluding peak periods, automobiles tend to accelerate up moderate urban freeway grades. Trucks tend to maintain a constant speed on these grades so long as they are not constrained by other vehicles.
2. Conventional acceleration noise increases on a grade. Furthermore, the increase in acceleration noise is independent of the percentage of trucks in the traffic stream. Because this parameter has been related to the jerkiness of flow in a traffic stream, an increase in σ is undesirable. It is concluded, then, that urban freeway grades are undesirable from a level of service standpoint.
3. The acceleration noise of a truck and vehicles immediately following the truck are appreciably less than corresponding values for other vehicles. Furthermore, trucks tend to stabilize flow and suppress shock waves because of the driving characteristics of truck operators.
4. Poorly designed ramps and acceleration lanes, particularly those located just prior to an upgrade, present special geometric problems. Slowly accelerating vehicles often cause undesirable operations, possibly resulting in a breakdown of stream flow.
5. The parameter called acceleration noise, although useful in grade computations as shown in the third finding, is not adequate to measure the effect of trucks on level of service. Some quantified value reflecting the many vagaries of human nature would be required, necessitating a human factors research study.

The following recommendations are offered as a logical follow-up to these findings:

1. Research efforts should be continued in studies relating to stable flow operating conditions. Because trucks in general do not cause serious problems as long as stable flow conditions are maintained, this recomendation appears to be an obvious requirement.
2. The design and location of freeway entry points must be considered not only from the level of service encountered at the merge area, but also from the level of service to be expected downstream. For example, inadequate acceleration lanes should never be built and marginal ones never located just upstream of a positive grade.
3. Research should be considered that would allow a quantification of the dependency of $\Delta\sigma$ on grade. This would necessarily entail research involving several grades of varying magnitude and length on different freeways.
4. Indications are that the physical effects of trucks under stable flow conditions, as measured by acceleration noise, are not disruptive to the flow conditions. It is recognized, however, that this is not the belief of the general driving public. Thus,

future research studies attempting to quantify the effect of trucks on the traffic stream should consider including a human factor analysis of automobile drivers.

5. Consideration should be given to depressed (or elevated) freeways from a level of service point of view. We should consider not only certain aesthetic principles such as noise and view, but also the operational problems on the proposed freeway itself. In addition to operational advantages already claimed for depressed profiles, this study indicates that the overall level of service would be improved by removing the "roller coaster" effect of present designs.

REFERENCES

1. Platt, F. N. A Proposed Index for the Level of Traffic Service. Traffic Engineering, Vol. 34, No. 2, Nov. 1963, pp. 21-25.
2. Herman, R., Montroll, E.W., Potts, R.B., and Rothery, R.W. Traffic Dynamics: Analysis of Stability in Car Following. Operations Research, Vol. 7, 1959, pp. 86-106.
3. Dudek, C. L. A Study of Acceleration Noise as a Measurement of the Quality of Freeway Operation. Texas A&M Univ., College Station, Master's thesis, May 1965.
4. Drew, D. R., and Keese, C.J. Freeway Level of Service as Influenced by Volume and Capacity Characteristics. Highway Research Record 99, 1965, pp. 1-47.
5. Drew, D. R., and Dudek, C. L. Investigation of an Internal Energy Model for Evaluating Freeway Level of Service. Texas Transportation Institute, TTI Res. Rept. No. 24-11, June 1965.
6. Ostle, Bernard. Statistics in Research. Iowa State Univ. Press, Ames, 1964, pp. 201-205.
7. Highway Capacity Manual, 1965. HRB Spec. Rept. 87, 1965, p. 30.
8. Rowan, N. J., and Keese, C. J. A Study of Factors Influencing Traffic Speeds. HRB Bull. 341, 1962, pp. 30-76.
9. Podesta, Claudio. The Effect of Trucks on Distance Spacing and Headways on an Urban Freeway. Northwestern Univ., Evanston, Ill., Master's thesis, July 1961.

Discussion

JOHN J. HAYNES, University of Texas at Arlington—The author has carried out an interesting research study involving an approach that is unique. The study actually centers around the attempt to utilize acceleration noise as a possible means of identifying the effect of trucks on freeway traffic flow. Acceleration noise has been used in studies to identify the level of service of freeway flow. However, it is doubtful that this paramater is an "excellent one" in this respect. As outlined in the 1965 Highway Capacity Manual, the level of service is identified by freedom to maneuver, by speeds that can be attained, and, most graphically, by the density of the traffic stream itself.

The mathematical relationship that was to be utilized in this research states that the change in acceleration noise is directly proportional to the highway grade, and is derived utilizing several simplifications including the assumption that the density of the traffic stream will not change and that the speeds of the traffic stream at the end points of a section are equal. Thus, the model indicated that for some specific roadway grade, σ, the change in acceleration noise, $\Delta\sigma$, would be directly proportional to that particular grade and independent of such things as traffic volumes and percentage of trucks.

The study site involved in this research was a single-crest vertical curve on the Gulf Freeway with a plus $2\frac{1}{2}$ percent grade of about $\frac{1}{8}$ mile followed by a minus $2\frac{1}{2}$ percent grade of equal length. This research did not include a study of several urban

freeway grades of varying magnitude and length, and thus the validity of the model, $\Delta\sigma = K\alpha$, was not evaluated.

It was not stated just how many individual vehicles were traced for the purposes of this study nor was an error analysis discussed concerning the study methods involving both recorded actuations from pressure-sensitive striping tape and continuous time-lapse photography from a circling aircraft. Because this was a study of the change in acceleration, any small errors in the estimation of the successive positions of the vehicles would magnify the periodic estimates of acceleration and, even to a greater extent, the sucessive changes in acceleration.

The author analyzed the data and found, in a majority of the cases, that there was a rather significant relationship between acceleration noise and the distance into this particular test section. This was true for the combined data for all volumes as well as for higher flow conditions only. In other words, the change in acceleration noise was comparable in each noise profile regardless of the flow quantity. It would be constructive to determine just how much of the variability in acceleration noise was accounted for by the distance and how much was accounted for by the slope.

The author gave considerable attention to the operating characteristics of trucks on this singular test section. This section involved a plus grade of approximately 2½ percent for a distance of approximately 650 ft. According to data published in "A Policy on Geometric Design of Rural Highways" a heavily loaded truck with a very poor weight to horsepower ratio of 400 lb per horsepower would be expected to lose only 4 mph in negotiating this particular test section. Most of the trucks observed in this study doubtless were not heavily loaded. One should expect a speed reduction of only 1 mph when averaging all the trucks observed regardless of size or load.

When studying the microscopic speed profiles, the author has determined that there was a speed reduction of 2 or 3 mph on the grade during peak flow periods in lanes 1 and 2 and a slightly greater speed reduction in lane 3. He makes the point that lane 1 contains a higher percentage of trucks than lanes 2 or 3. During the off-peak periods, the speed in lane 1, with the higher truck percentages, seemed to have increased slightly through the section while the speeds in lanes 2 and 3 either decreased slightly or remained virtually constant. The differences in these speed profiles were very slight and the percentage of trucks ranged from 5 percent to 10 percent in lane 1 and ranged down to less than 1 percent in lane 3. The author has stated that "speed decrements were judged not to accompany the lane with the highest percentage of truck flow". It might also be stated that the average speeds in lane 1 were always lower than in lane 2 or lane 3.

In a microscopic speed and acceleration noise study, the author pointed out that the acceleration noise of the vehicles following tractor-trailer trucks was noted and compared to the acceleration noise for the vehicles in advance of such trucks. As has been determined previously, the acceleration noise for a queued vehicle was less than for a free-moving vehicle. This paper did not, however, explain the criteria used in identifying the vehicles "following" a tractor-trailer truck and how the differentiation was made between those following one truck and those leading a subsequent truck. By whatever definition the author used, he did find that the acceleration noise was relatively high for the vehicles preceding trucks and low for the queue following trucks.

Analysis of time-space traces of successive vehicles through the study sections led to several conclusions, one of which concerned the hypothesis that the passage of a tractor-trailer unit removed the traces of a disturbance, or shock wave, in the flow pattern. From a careful study of these data, it may be observed that this disturbance had disappeared two or three vehicles prior to the passage of this tractor-trailer. It is difficult to conclude that the passage of the tractor-trailer unit was responsible for this observed dampening or smoothing effect. In another example, it was pointed out that the trace of a tractor-trailer unit moving in the traffic stream showed that it was actually not holding up traffic, but was, in fact, being held up by a slow-moving vehicle in front of it. It can be noticed, however, that a car did weave from an adjacent lane into the gap between this truck and the vehicle leading it.

In connection with the conclusions drawn in Humphreys' paper, the following observations are offered:

1. The author did admit that the study represented only one study site. It is his contention, however, that the study site is representative, or average, of most "roller-coaster-type freeways".
2. This discussant will concede that the study did indicate that automobiles do tend to accelerate slightly up a moderate urban freeway grade of a few hundred feet and that trucks tend to maintain a slightly more constant speed up such a grade, although the difference observed was very slight.
3. The fact that acceleration noise in general increases on a grade does indicate that urban freeway grades are undesirable from a level of service standpoint. This conclusion is supported by other considerations indicating that grades are undesirable.
4. The conclusion that trucks tend to stabilize flow and suppress shock waves because of the driving characteristics of truck operators is subject to question and further study. It is likely that the gaps existing in front of trucks may tend to help dampen possible shock waves.
5. Certainly, the conclusion that "poorly designed ramps and acceleration lanes present special geometric problems" because some "slowly accelerating vehicles often cause undesirable operations" must be correct but is not properly substantiated in this paper.
6. The final conclusion, indicating that acceleration noise is not adequate to measure the effects of trucks on the level of service of freeway flow, is perhaps a valid one.

In many instances, scholarly research brings to light methods that do not work, rather than those that do. The author is to be commended for attempting to evaluate the effect of trucks by the use of acceleration noise as the parameters and should be encouraged to pursue this topic in accordance with his recommendations for future study.

PATRICK J. ATHOL, Expressway Surveillance Project, Oak Park, Illinois—Humphreys addresses the problem of establishing the influence of truck operations on urban freeways. He presents his ideas in two parts, the first attempting to establish acceleration noise in the traffic stream as the measure of truck influence, the second discussing the operation of trucks in terms of individual travel trajectories. The analytical approach is emphasized in the use of acceleration noise in his first part, whereas he handles the effect of slower vehicles in a much more conversational manner.

In terms of general interest, I think the initial analysis falls short of its potential, whereas the second part gets into an area of widespread public interest. In the conclusions, the shortcomings of acceleration noise in identifying the impact of truck performance are presented. The latter part of his work could, I suggest, be considered as one facet of the more general topic of the influence of slower moving vehicles on the traffic stream.

Acceleration noise is chosen as the level of service of operations (2). It reflects the changes in acceleration of the vehicle along its route weighted by the square of the changes. Describing measures as noise is derived from the wide use of this expression in control and communications and relates actual performance with nominal or desired performance. Noise precludes the achievement of the ideal effect.

Helly (9) looked at acceleration noise along city streets, particularly with respect to the influence of traffic signals and congestion. Acceleration noise did reflect, by definition, changes in the acceleration; however, in the case of arterial streets, he found noise alone nondiscriminatory between operations at 3 a.m. and a congested peak period. Both noise values were approximately 2 to 3 ft/sec^2.

On the same section of the Gulf Freeway, Drew presented results of acceleration noise measurements. He concluded that noise at free-flow conditions was highest, diminishing toward maximum flow level, then increasing again in congested traffic.

These changes were proportionately very large, from 0.1 to 1.6 ft/sec^2. Again, acceleration noise by itself tended to be nondiscriminatory between free flow and congestion and needs further specification in speed or similar measurement to establish performance.

From the rudimentary measure of acceleration noise, the attempt was made to relate it to the total internal energy of freeway traffic. The extension of this energy analogy had a confusing result; Drew came to the conclusion that acceleration noise is directly proportional to slope of the grade. Humphreys, from the same concepts, concludes that the change of acceleration noise is proportional to the slope of the grade. The slope of acceleration noise along the grade was tested for difference between lanes, and was found constant. What is not made clear is whether or not these slopes are significantly different from zero. If it is zero, then both ideas agree. Drew's own results infer zero noise on level sections; this of course, as Drew states, must be disagreed with. From the data used in both studies, it appears that neither case is proved; thus, one is alerted to potential contradiction in using the underlying energy analogy.

The energy analogy, as Humphreys used it, assumed no change in kinetic energy, and hence no speed change in the area. In some of his data, speed changes at least of the order of 2 mph within a lane and 8 mph between lanes were presented. The presented speed profile data showed speed changes of 3 ft/sec at speeds of 60 ft/ sec on a 500-ft section.

Following Eq. 5,

$$\Delta\sigma = \beta\,(0.64 + 0.35)\ \text{ft/sec}^2$$

where 0.35β is the component resulting from the change in kinetic energy. For 3 ft/sec changes in speed at 60 ft/sec, the rate of change of acceleration noise is changed by 50 percent, showing the keen sensitivity of the model. There are, therefore, grounds for concern that the assumptions were not completely substantiated by the data.

In the second discussion, Humphreys is looking at the trajectory of vehicles through a section of highways as illustrated by the time-distance charts. In his charts he really gets to the fundamental point of showing the performance of slower vehicles. Paraphrasing his conclusion, the report says that slower vehicles do influence performance, but not all slower vehicles are trucks. This point, I suspect, would have wide acceptance among operating engineers. Under certain geometrics the majority of slow vehicles will be trucks traveling slowly, i.e., up the long, steep grades, but this is not so on the Houston "roller coaster". In the data presented, it can be seen how slow-moving vehicles encourage lane-changing. Faster moving lanes have to accept lane changes caused by slower vehicles and they are constantly required to adjust, thus creating more acceleration noise. Slower moving traffic behaves in a sense similar to the 35-mph freeway condition in which minimum acceleration noise occurs; all vehicles are constrained to the lower speeds.

The presence of slower moving vehicles does introduce longer headways, which are in a detailed sense low volumes that can help absorb the impact of shock waves. In routine traffic operations, the police in Los Angeles and some other highway departments utilize a system of introducing vehicles into the traffic stream in advance of a problem area. These vehicles slow the stream down to a uniform speed until past the problem. By this action they introduce a large headway and temporarily delay input to diminish the shock wave impact. This action can be used for severe weather conditions where visibility is impaired, such as by fog.

The Gulf Freeway section under study would be difficult to match in other existing areas and, one would hope, never in the future, so the results are limited in future applications. There remains the continuing need to establish the impact of slower vehicles and trucks along urban freeways. The measures must go beyond acceleration noise alone. Other measures that can be included are desired speed (nominal performance), the demands on the driver to gain information, as shown by the work done by Gordon (10), and the control actions taken by the driver in response to his environment.

Other aspects of the influence of trucks is shown by the work of Michaels and Cozan (11) of Northwestern University, and the work of Moskowitz (12) in California. All of these studies present important factors. Humphreys' conjecture into operational areas is certainly stimulating. The slow driver, be he the truck driver or self-assured automibile driver who is convinced that his slow speed is the safest, is a problem, and it is his influence we are trying to establish. Humphreys has reiterated the question, "What is their impact?" and shows us that we are not likely to get a simple answer.

References

9. Helly, W. Efficiency in Road Traffic Flow. Second Internat. Symposium on the Theory of Traffic Flow, London, 1963.
10. Gordon, D. A. Experimental Isolation of the Driver's Visual Input. Highway Research Record 122, 1966, pp. 19-34.
11. Michaels, R. M., and Cozan, L. W. Perceptual and Field Factors Causing Lateral Displacement. Public Roads, Vol. 32, No. 11, Dec. 1963, pp. 233-240.
12. Newman, L., and Moskowitz, K. Effect of Grades on Service Volume. Highway Research Record 99, 1965, pp. 224-243.

Pedestrian Gap-Acceptance

CHARLES M. DiPIETRO, Southwestern Pennsylvania Regional Planning Commission;
and
L. ELLIS KING, Department of Civil Engineering, West Virginia University

The object of this research project was to investigate the gap acceptance of pedestrians at an unmarked midblock crossing. Data were collected by means of time-lapse photography and analyzed with the aid of a photo-optical data analyzer. Statistical tests, such as the Kolmogorov-Smirnov test, the chi-square test, and analysis of variance, were utilized to investigate the relationship between size of gap accepted and various factors such as time waited at curbside, volume of traffic, number of persons waiting at curbside, speed of approaching vehicle, and walking speed of the pedestrian. Some conclusions drawn from the results of the tests are that female pedestrians were willing to wait longer at curbside for a suitable gap than were male pedestrians; male pedestrians accepted shorter gaps than did female pedestrians; the minimum acceptable gap in a single stream of traffic was 3 sec or 75 ft; shorter gaps were accepted by groups of pedestrians rather than by individuals; and individual pedestrians crossed the roadway at greater walking speeds than did groups of pedestrians.

•CONSIDER a pedestrian standing at curbside waiting to cross a road on which traffic is flowing. At some instant he decides that an acceptable gap in the traffic stream has presented itself and that it is safe to cross. His decision is usually correct, but occasionally a pedestrian errs in his judgment with the possible result of an injury. The objective of this study was to determine what factors influence the choice a pedestrian makes to accept or reject a given gap in the traffic stream. Throughout this report a gap is defined as the space interval between successive vehicles, expressed either in time or distance. For two-directional traffic flow, a total gap is defined as the sum of the near-stream traffic gap and the far-stream traffic gap.

Although almost 20 percent of the traffic accident fatalities in the United States are those involving pedestrians, research directed at pedestrians has been slight (1, 2, 3). A library search reveals that the amount of available literature relating to the vehicle-vehicle conflict is extensive, but material concerning pedestrian-vehicle conflict is limited, in all but a few cases, to the theoretical study of mathematical models assumed to adequately simulate the problem. However, such agencies as the British Road Research Laboratory have conducted detailed research (4, 5, 6, 7, 8) in England concerning the pedestrian-vehicle conflict. Investigated were such factors as pedestrian risk taken in crossing a street, the willingness of pedestrians to use footbridges or tunnels, and the relative risks of crossing streets at various places and under various conditions.

STUDY DESIGN

Time-lapse photography was used for data collection. This allowed a continuous recording of the exact positions occupied by all vehicles and pedestrians within the camera range at ¾-sec intervals. Color film was used in order to aid in identifying vehicles and pedestrians from frame to frame.

Paper sponsored by Committee on Characteristics of Traffic Flow and presented at the 49th Annual Meeting.

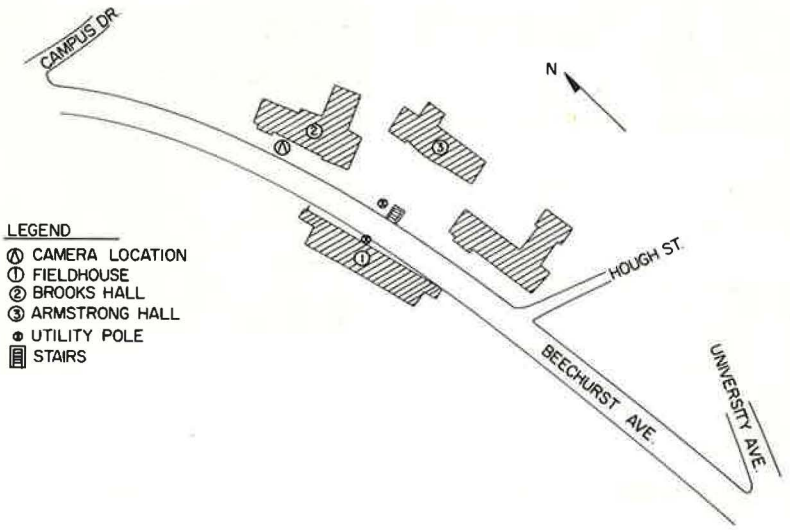

Figure 1. Study site.

An unmarked crossing located in front of the West Virginia University Fieldhouse on Beechurst Avenue was chosen as the study location. In Figure 1, a detailed sketch of the study site is shown. The characteristics of the site that lent themselves to this study are as follows:

1. An uncontrolled midblock crossing (thus reducing the unwanted elements of turning vehicles and traffic signal);
2. Frequent pedestrian crossings at a well-defined point;
3. Free-flowing traffic (frequent gaps of various sizes); and
4. A clear, unobstructed observation point.

In order to ensure a large number of pedestrians, filming was timed to include the changing of physical education classes, and only those periods in which pedestrian-vehicle conflicts appeared were recorded. During periods of no pedestrian activity, the camera was shut off. The camera remained off until a pedestrian approached the crossing area, at which time it was again turned on. This procedure was followed in order to better utilize the available film footage. An attempt was made to film only under similar weather conditions.

Markings were placed at 25-ft intervals at the curbside on both approaches to the crossing in order to define a grid to be used later in film reduction. Using a film segment on which a subject appears as an aid in locating the grid points, a coordinate system was drawn on the projection screen. This grid appeared as a network extending 150 ft on both sides of the crossing point with lines at 25-ft intervals. A sample film segment and the camera setup are shown in Figures 2 and 3.

DATA REDUCTION

A model 224 L&W Photo-Optical Data Analyzer was used to project the film onto the calibrated screen grid and the following information was extracted for each pedestrian observed:

1. Direction of crossing;
2. Pedestrian observation number and sex;
3. Film frame number in which pedestrian first appeared;
4. Group size;
5. Near-side gap accepted in frames;
6. Near-side gap accepted to the nearest 25-ft increment;

7. Far-side gap accepted in frames;
8. Far-side gap accepted to the nearest 25-ft increment;
9. Time waited at curbside in frames;
10. Selected near-side gaps rejected in frames;
11. Selected near-side gaps rejected to the nearest 25-ft increment;
12. Selected far-side gaps rejected in frames;
13. Selected far-side gaps rejected to the nearest 25-ft increment; and
14. Number of frames required for the pedestrian to cross from the near-side curb to the quarter point, centerline, three-quarter point, and far-side curb of the roadway respectively.

Figure 2. Sample film segment.

In addition to the pedestrian data, traffic volumes for each observation period were taken from the film.

DATA ANALYSIS AND RESULTS

Male Versus Female Pedestrians

Of the 740 pedestrians observed during the study, 602 were male and 138 female. An analysis was conducted, using the Kolmogorov-Smirnov two-sample test, to determine if there was a difference between male and female pedestrian crossing characteristics. It was hypothesized that a female would be more cautious, wait for a longer gap, and cross the roadway at a slower speed than would a male pedestrian. The Kolmogorov-Smirnov two-sample test may be used for this comparison because it allows the determination of whether or not two independent samples have been drawn from the same distribution (9). All tests were made at a 5 percent level of significance. From the tests it was concluded that female pedestrians tend to be more cautious and patient than male pedestrians. Females will wait longer at curbside for an adequate gap to occur, and in the process of this waiting, females tend to reject more gaps of equal duration than would males.

Figure 3. Camera setup.

As to the gap finally accepted by a male or female pedestrian, there appears to be some question as to whether or not there is a difference. By the Kolmogorov-Smirnov two-sample test it was determined that no difference exists for the total near-side plus far-side gap accepted (either in seconds or feet) by males and females. The confusion arises when either the near-side or far-side gap is studied alone. From the tests it was concluded that (a) females accept longer near-side gaps in seconds than males, but there is no significant difference for near-side gaps accepted in feet, and (b) females accept longer far-side gaps in feet than males, but there is no significant difference for far-side gaps accepted in seconds.

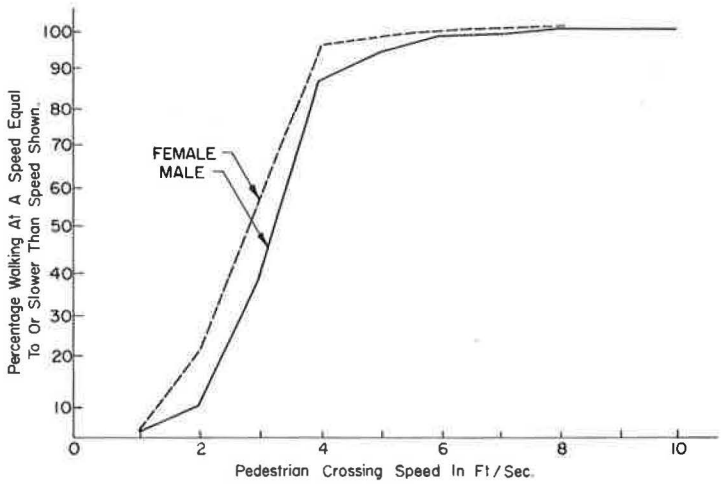

Figure 4. Cumulative overall pedestian crossing speed for males and females.

Finally, the Kolmogorov-Smirnov two-sample test concluded that females cross the roadway at a slower walking speed than do males. This is shown in Figure 4, which graphically compares the walking speed of male and female pedestrians. Table 1 gives the summary of male and female pedestrian crossing characteristics.

Effect of Time Waited at Curbside on Gap Accepted

Figures 5, 6, and 7 show the effect of time waited at curbside on the near-side gap, far-side gap, and total gap finally accepted by the pedestrian. The 1-, 5-, 14-, and 17-sec time-waited curves shown in the graphs were selected for plotting because a large number of observations had been recorded for these increments. The graphs may be interpreted as follows (Fig. 5): (a) 50 percent of the pedestrians who waited 17 sec accepted a gap of 11 sec or less, and (b) 50 percent of the pedestrians who waited 1 sec accepted a gap of 12 sec or less.

TABLE 1

SUMMARY OF MALE VERSUS FEMALE PEDESTRIAN CROSSING CHARACTERISTICS

Hypothesis H_O	Alternative H_O	Test Statistic[a]	Conclusion
Males and females wait the same time at curbside before accepting a gap.	Females wait longer at curbside than do males before accepting a gap.	6.242	Reject H_O
Males and females accept the same near-side gaps in seconds.	Females accept longer near-side gaps in seconds than do males.	7.589	Reject H_O
Males and females accept the same near-side gaps in feet.	Females accept longer near-side gaps in feet than do males.	5.69	Accept H_O
Males and females accept the same far-side gaps in seconds.	Females accept longer far-side gaps in seconds than do males.	2.15	Accept H_O
Males and females accept the same far-side gaps in feet.	Females accept longer far-side gaps in feet than do males.	8.90	Reject H_O
Males and females accept the same total near-side and far-side gaps in seconds.	Females accept longer total near-side and far-side gaps in seconds than do males.	5.633	Accept H_O
Males and females accept the same total near-side and far-side gaps in feet.	Females accept longer total near-side and far-side gaps in feet than do males.	1.408	Accept H_O
Males and females will reject similar near-side gaps in seconds.	Females will reject larger near-side gaps in seconds than will males.	28.949	Reject H_O
Males and females will reject similar near-side gaps in feet.	Females will reject larger near-side gaps in feet than will males.	30.731	Reject H_O
Males and females have the same overall crossing speed.	Males have a greater overall crossing speed than do females.	17.339	Reject H_O

[a]The acceptance region for the test statistic is $-\infty \leq X^2 \leq 5.991$.

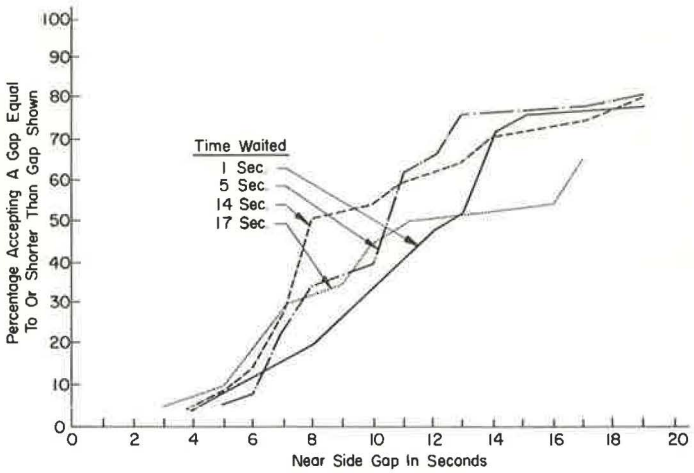

Figure 5. Effect of time waited at curbside on the near-side gap accepted.

From Figures 5, 6, and 7, no consistent conclusion could be drawn as to the effect of time waited on the gap accepted by a pedestrian. Next, these data were subjected to a one-way, fixed-effects analysis of variance test to determine if time waited had a statistically significant effect on the gap chosen (10). In addition, an attempt was made to isolate differences in levels of time waited, such as 1 sec versus 17 sec. The analysis was one-way because only one factor, time waited, was tested as to its effect on the gap chosen. In addition, the model was considered to have fixed effects because the conclusions drawn from this analysis apply only to the 39 intervals of time waited in seconds that were observed at the test site. For the analysis, a level of significance of 5 percent was chosen and the following conclusions were drawn from the test: (a) time waited at curbside has a significant effect on the near-side gap finally accepted in seconds, and (b) time waited at curbside has a significant effect on the total near-side plus far-side gap accepted in seconds.

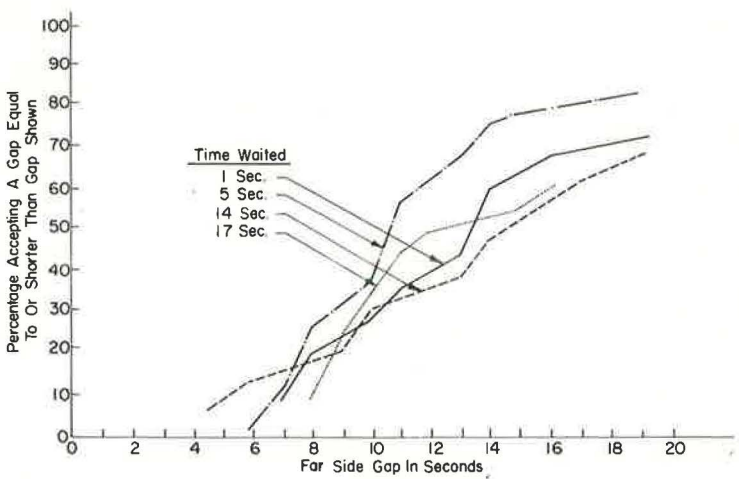

Figure 6. Effect of time waited at curbside on the far-side gap accepted.

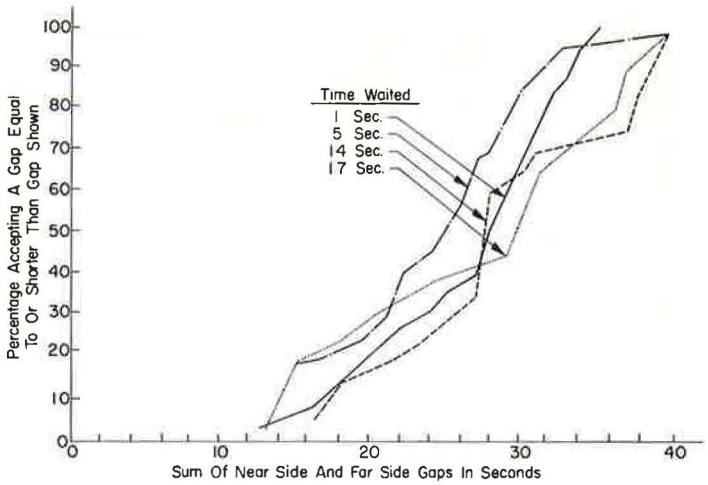

Figure 7. Effect of time waited at curbside on the total gap accepted.

With a significant difference known, an attempt was made to determine the effect of specific changes in the time-waited values. This attempt was unsuccessful because the critical difference in all cases was too large to ascertain statistically.

Thus, it has been shown that, on an overall basis as the time waited increases, the gaps accepted by pedestrians tend to become longer. Individual cases occurred in which pedestrians who waited a long period at curbside actually accepted shorter gaps, but a time-waited value at which this occurred could not be established.

Effect of Group Size on Gap Chosen

To determine statistically if group size had a significant effect on the final gap chosen by the pedestrian, a one-way, fixed-effects analysis of variance test was performed on the data plotted in Figures 8 and 9. In visually comparing the different curves of group size as seen in either Figure 8 or 9, no discernible pattern could be distinguished and

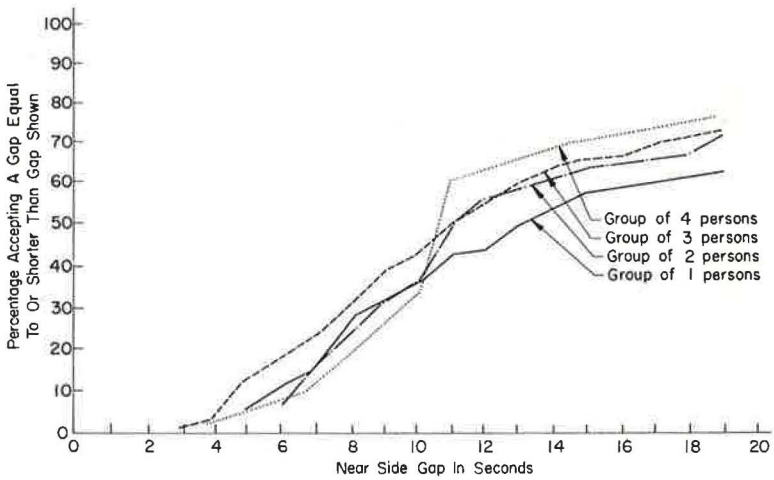

Figure 8. Effect of group size on the near-side gap accepted.

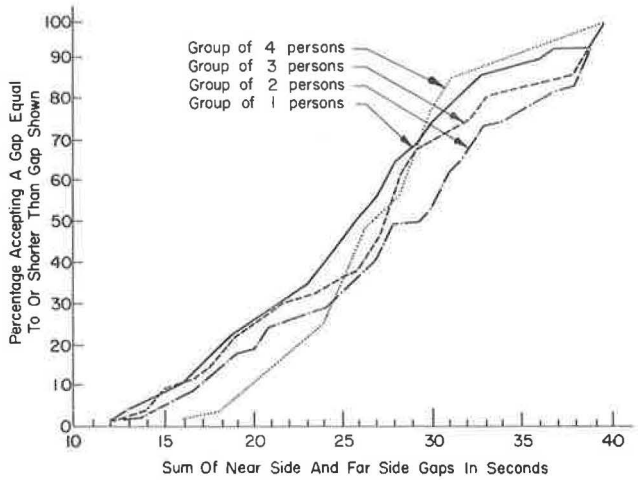

Figure 9. Effect of group size on the total gap accepted.

the only conclusion drawn was that it appeared that group size helps to determine the gap accepted by the pedestrian. Again, as in studying the effect of time waited on the gap eventually chosen by a pedestrian, a level of significance of 5 percent was chosen. The following conclusions were reached: (a) the number of pedestrians waiting at curbside has a significant effect on the near-side gap accepted in seconds by an individual pedestrian within the group, and (b) the number of pedestrians waiting at curbside has a significant effect on the total near-side plus far-side gap accepted in seconds by an individual pedestrian within the group. An attempt was also made to detect where a difference existed between specific group sizes, but this could not be determined from the analysis of variance calculations.

Finally, an attempt was made to pinpoint a difference between specific group sizes by use of the chi-square test and the Kolmogorov-Smirnov two-sample test (previously

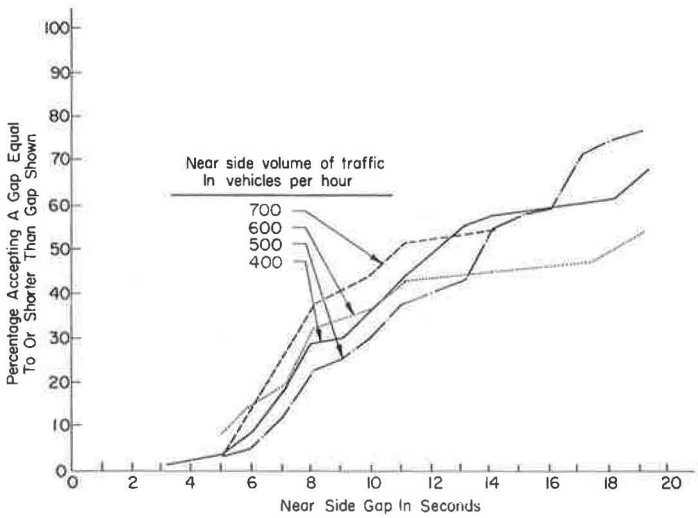

Figure 10. Effect of volume of traffic on the near-side gap accepted.

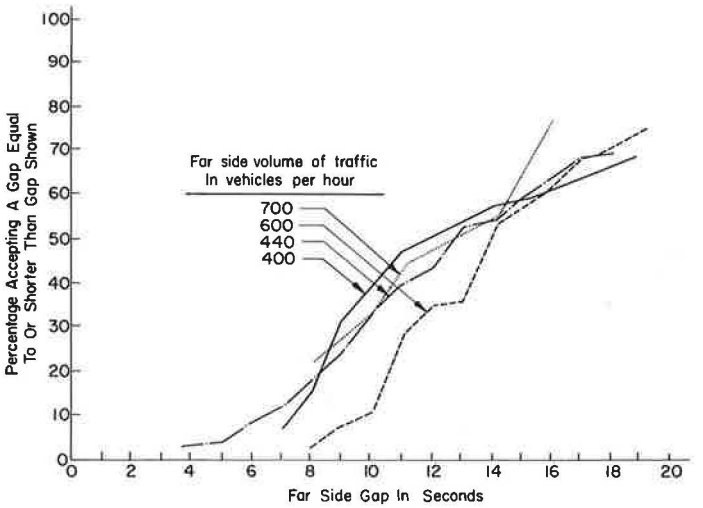

Figure 11. Effect of volume of traffic on the far-side gap accepted.

used in comparing male versus female characteristics). The chi-square test may be used to test whether two samples of data differ in any manner and the Kolmogorov-Smirnov two-sample test determines whether or not two independent samples have been drawn from the same distribution. The chi-square and the Kolmogorov-Smirnov two-sample tests resulted in the following conclusions in comparing a group size of one person first with a group size of three persons and then with a group size of four persons: (a) a group size of three persons tends to accept shorter gaps than a group size of one person, and (b) a group size of four persons tends to accept shorter gaps than a group size of one person.

Effect of Volume of Traffic on Gap Chosen

The effect of traffic volume on the near-side gap accepted and the far-side gap accepted is shown graphically in Figures 10 and 11 respectively. The indicated volumes of traffic plotted were chosen because (a) these values represented a wide range of traffic conditions, and (b) a large amount of film footage was taken during these periods. Several one-way, fixed-effects analysis of variance tests were run on these data. Again, all tests were run at a 5 percent level of significance.

The tests were unable to determine whether or not pedestrians accept shorter gaps as traffic volume increases, as one might hypothesize. Statistically, it was found only that traffic volume does enter into the pedestrian crossing decision. Further research work may tie volume of traffic to the critical gap in the traffic stream discussed later in this paper. When this occurs, volume of traffic can then serve as a warrant for a traffic engineering measure.

Pedestrian Crossing Speed

It appears that the shorter the gap accepted by the pedestrian, the greater is his crossing speed. This conclusion was drawn from the data shown in Figure 12. From the graph it can be observed that 50 percent of the pedestrians who crossed the roadway at 6 ft/sec accepted a near-side gap of 8 sec or less, whereas 50 percent of those crossing the roadway at 3 ft/sec accepted a near-side gap of 13 sec or less. Thus, the pedestrians who crossed the roadway at 6 ft/sec accepted shorter gaps than the pedestrians who crossed the roadway at 3 ft/sec. This relationship of increased pedestrian crossing speed with decreased size of gap accepted is shown in Figure 12. It holds true for a near-side gap of approximately 7 sec or less. At this point the 5

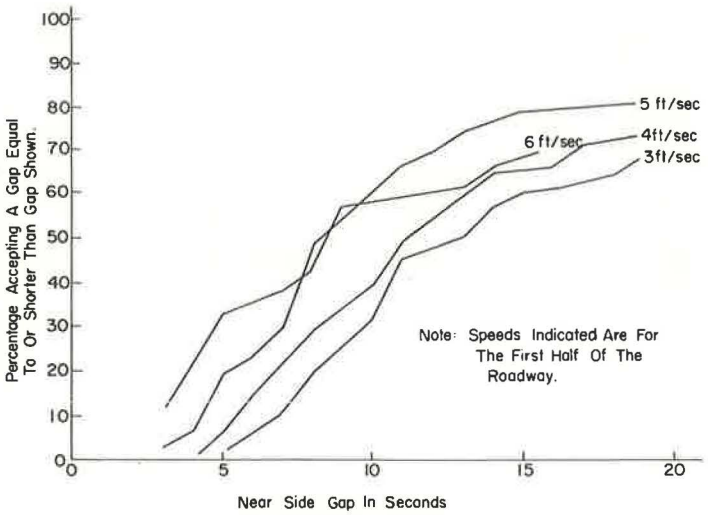

Figure 12. Effect of pedestrian crossing speed on the near-side gap accepted in seconds.

ft/sec and the 6 ft/sec curves cross. An explanation for this may be as follows: If gaps are greater than a certain duration, the gap may be acceptable at a wide variety of crossing speeds. The pedestrian may be in a hurry and run across the street utilizing only a part of the available gap. For example, if a pedestrian selected a 7-sec near-side gap and crossed at 3 ft/sec, he could reach the centerline of the 29-ft roadway in 5 sec, thus leaving a full 2 sec of unused time.

A one-way, fixed-effects analysis of variance test was run to determine whether or not crossing speed had a significant effect on the gap accepted. Using a level of significance of 5 percent, the following conclusions were drawn:

1. Pedestrian crossing speed for the first half of the roadway has a significant effect on the near-side gap in seconds accepted by a pedestrian. In general, as the size of gap accepted decreases, the pedestrian crossing speed for the first half of the roadway increases. However, the change in pedestrian crossing speed required to affect the gap accepted could not be determined.
2. Overall pedestrian crossing speed for the entire roadway width has a significant effect on the total near-side plus far-side gap in seconds accepted by a pedestrian. In general, as the total gap accepted decreases, the overall pedestrian crossing speed increases. However, the change in overall crossing speed required to affect the total gap accepted could not be determined.

Effect of Group Size

The effect of group size on walking speed is shown in Figure 13. Group sizes of one, two, three, and four persons were plotted against pedestrian crossing speed. The curve for a group size of one person is seen to be displaced from the curves of group sizes of two, three, and four persons, but little difference in crossing speed exists between groups of two, three, or four persons. This may be explained by considering that for the individual, the decision to cross is made without judging the movements of other adjacent group members. The individual tends to cross at his own speed and not be influenced by a group "bunching effect" that may tend to slow the individual pedestrian's crossing speed to that of the group.

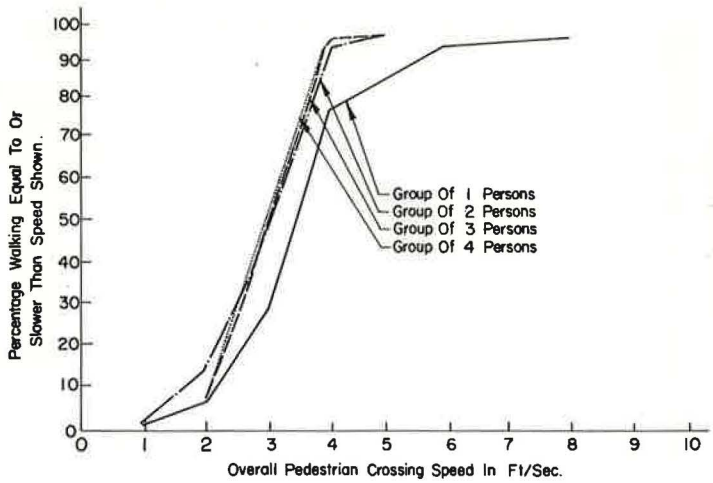

Figure 13. Effect of group size on overall pedestrian crossing speed for the entire roadway width.

Determination of the Limits of a Critical Gap

A minimum acceptable gap may vary from pedestrian to pedestrian, but it is possible to determine a minimum gap acceptable to all pedestrians observed during the study. The following limiting values were determined from the data plotted in Figures 14, 15, and 16:

1. No pedestrian accepted a near-side gap shorter than 3 sec;
2. No pedestrian accepted a near-side gap shorter than 75 ft;
3. No pedestrian accepted a far-side gap shorter than 4 sec;
4. No pedestrian accepted a far-side gap shorter than 75 ft;

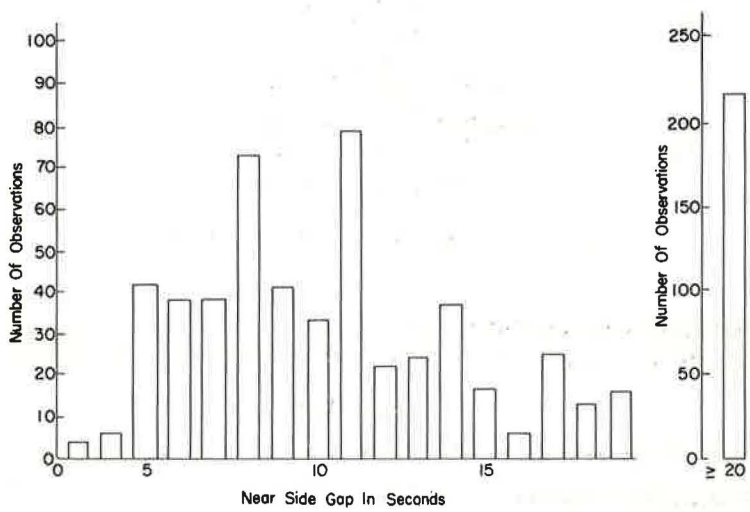

Figure 14. Frequency distribution of near-side gaps accepted.

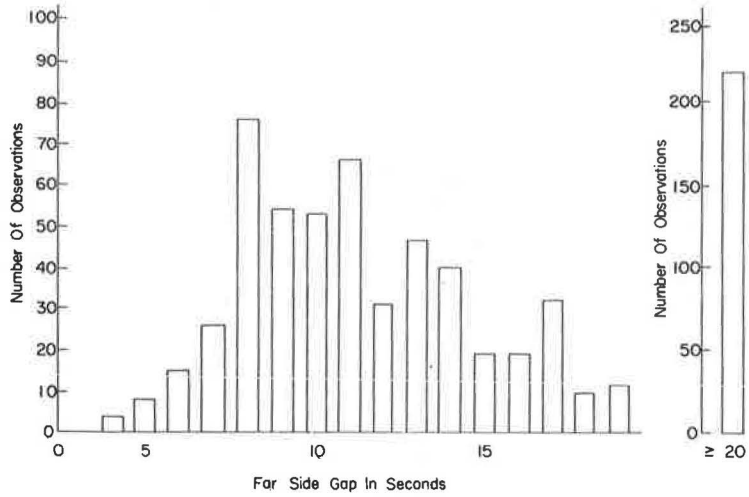

Figure 15. Frequency distribution of far-side gaps accepted.

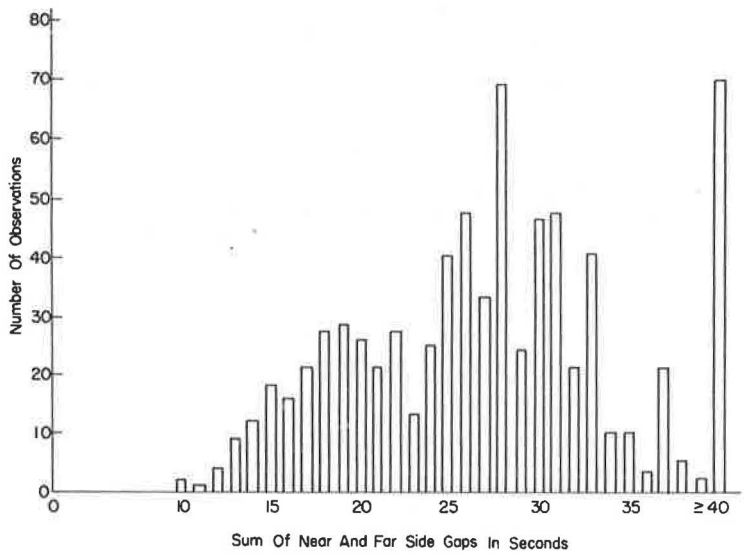

Figure 16. Frequency distribution of total gaps accepted.

5. No pedestrian accepted a total near-side plus far-side gap shorter than 10 sec; and
6. No pedestrian accepted a total near-side plus far-side gap shorter than 200 ft.

SUMMARY

The results of this research may be briefly summarized as follows:

1. Female pedestrians were willing to wait longer at curbside for an adequate gap to occur in the traffic stream.
2. There was no difference in the size of the total gap (near-side plus far-side gap) accepted by male or female pedestrians. However, males accepted shorter near-side

gaps, measured in seconds, than did females, and shorter far-side gaps, measured in feet, than did females. There was no significant difference for near-side gaps measured in feet, nor far-side gaps measured in seconds.

3. Time waited at curbside had a statistically significant effect on both the near-side gap and total gap accepted. In general, the gap size increased as the time waited at curbside increased. However, there were many exceptions.

4. Groups of pedestrians accepted shorter gaps than did individual pedestrians.

5. The effect of traffic volume on gap acceptance could not be statistically verified from the study data. Statistically it was found only that volume of traffic does enter into the pedestrian crossing decision.

6. Pedestrians crossing the roadway at higher walking speeds accepted shorter gaps than those crossing at normal walking speeds.

7. The individual pedestrian crossed the roadway at a greater walking speed than did groups of pedestrians.

8. No pedestrian accepted a near-side gap of less than 3 sec or 75 ft nor a far-side gap of less than 4 sec or 75 ft. No pedestrian accepted a total gap of less than 10 sec or 200 ft.

REFERENCES

1. The State of the Art of Traffic Safety—A Critical Review and Analysis of the Technical Information on Factors Affecting Traffic Safety. Arthur D. Little, Inc., Cambridge, Mass., June 1966.
2. Traffic Engineering Handbook. Institute of Traffic Engineers, Washington, D. C., 1965.
3. Herman, R., and Weiss, G. H. Comments on the Highway Crossing Problem. Operations Research, Nov.-Dec., 1961.
4. Adams, W. F. Road Traffic Considered as a Random Series. The Institute of Civil Engineers Journal, Nov. 1956.
5. Mayne, A. J. Some Further Results in the Theory of Pedestrians and Road Traffic. Biometrika, Vol. 41, 1954.
6. Cohen, John, Dearnaley, E. J., and Hansel, C. E. The Risk Taken in Crossing a Road. Operations Research Quarterly, Sept. 1955.
7. Research on Road Traffic. Road Research Laboratory, London, England, 1963.
8. Research on Road Safety. Road Research Laboratory, London, England, 1963.
9. Siegel, Sidney. Nonparametric Statistics. McGraw-Hill Co., New York, 1956.
10. Bowker, A. H., and Lieberman, G. J. Engineering Statistics. Englewood Cliffs, N. J., 1959.

A Pulsed Doppler Radar Experiment for Highway Traffic Research

RICHARD F. SCHNEEBERGER and ROBERT A. HAYMAN,
Electronics Research Department, Cornell Aeronautical Laboratory, Inc.

Traffic flow is a continuous process wherein space and time measurements are important and variables (e.g., numbers of vehicles, vehicular speeds, headways, and the like) form the basis for development. The use of a precision pulsed Doppler radar to estimate continuously the variations in parameter values is described. The radar was positioned to survey a length of high-speed highway. Using range-gating techniques, the radar responses could be limited to only those vehicles on a specific length of the highway, the length and position of the length being determined by the range-gating system. The instantaneous speeds of each vehicle in the range gate (to a resolution of 0.15 mph) were measured by the Doppler radar to provide a time history of the distribution of speeds along a length of highway. Other important measurements in traffic flow theory are also suggested by the results obtained.

•THIS PAPER describes a brief experimental program to investigate the applicability of a pulsed Doppler radar to the measurement of traffic flow parameters. Particular emphasis was placed on that phase of traffic flow in which high densities and flow rates are encountered, a condition presently instrumented only with arrays of instruments requiring considerable data processing.

In the development of traffic flow theory, several approaches are used, each approach placing emphasis on a particular aspect of the traffic problem. In the microscopic approach, relationships between individual vehicles are examined in car-following studies (1). One macroscopic approach uses fluid flow analogies to examine traffic density, volume, flow rate, headway, and similar variables (2). A second macroscopic approach treats traffic flow as a problem in statistical theory to develop descriptors such as distribution of instantaneous vehicle speed, distribution of overall vehicle speeds, space mean speed, time mean speed, and other moments of these and other distributions (3).

The experimental verification of the analytical treatments is generally carried out with instrumentation specific to each approach. Measurement of distance between two test vehicles by a number of means (e.g., adjustable length of wire) is used in support of the car-following studies. Pneumatic tubes, induction loops, acoustic detectors, and photography from hovering or orbiting aircraft or stationary points are used in experiments related to the fluid-flow analog studies. This sensor class is also used in support of the statistical methods. However, some statistical descriptors have proven exceedingly difficult to estimate. In most cases, for example, the instantaneous speed of a single noncooperative vehicle in a traffic stream cannot readily be obtained.

One instrumentation approach offering significant promise in the measurement of vehicle speeds in various levels of traffic density is a range-gated radar employing the Doppler principle. The familiar continuous-wave Doppler speed meter used in traffic control is limited because it does not provide range information; the standard pulse

Paper sponsored by Committee on Characteristics of Traffic Flow.

radar is limited by the large number of stationary objects present in a typical traffic situation. A combination of the two types, a pulsed Doppler radar having the advantages of both range and Doppler discrimination, offers a new and flexible approach to the traffic flow problem. In this system, vehicles falling within selected range and speed intervals are observed, while vehicles at other ranges and fixed reflecting objects in the same range interval will be eliminated.

To test the conclusions developed in an analysis of the Doppler radar-traffic flow problem, a radar experiment was recommended. Because a pulsed Doppler radar of broad flexibility has been developed at Cornell Aeronautical Laboratory (CAL) and is maintained as a research tool, a direct determination of its applicability to traffic flow problems was proposed. Subsequently, under CAL internal research sponsorship and in cooperation with the police department of the town of Cheektowaga, New York, and the New York State Police, a demonstration program utilizing a section of the New York State Thruway was performed.

DESCRIPTION OF THE RADAR

The CAL pulsed Doppler radar (Fig. 1) uses both the pulsed and Doppler principles, thus permitting the simultaneous measurement of range and vehicle velocity. A brief description of the radar's operating principles follows.

An ultrastable CW oscillator supplies a low-level signal at the radiated microwave frequency to the pulsed microwave amplifier. The amplifier is gated-on for a period of time established by the pulse-former network and at a recurrence rate established by the PRF (pulse repetition frequency) generator. A sequence of microwave pulses (Fig. 2) are sent through the transmit-receive switch to the antenna for radiation. The pulse modulating the microwave amplifier also triggers a time base generator. By

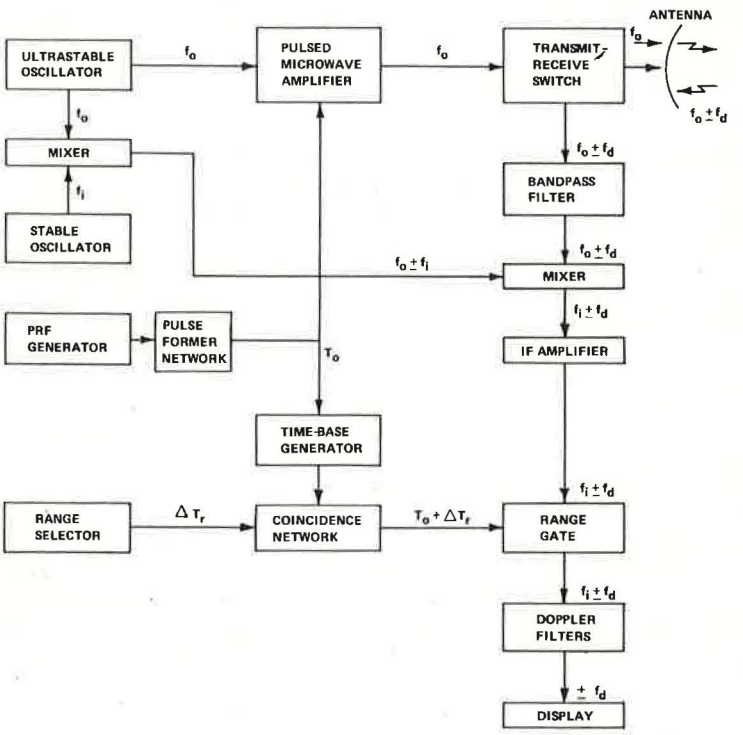

Figure 1. Simplified block diagram of radar.

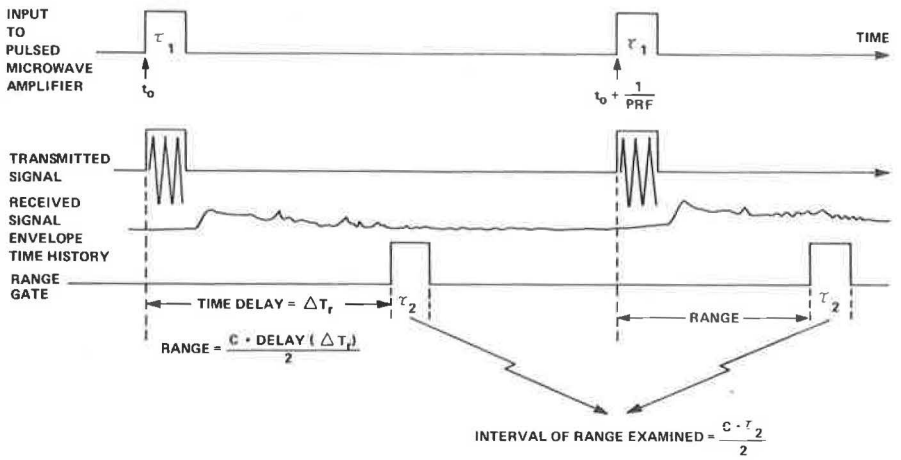

Figure 2. Timing.

setting the range selector to the desired position, a signal is developed that is compared in the coincidence network with that of the time base. When coincidence occurs, the range gate is opened to allow passage of the received signal through the processing networks. The time base coincidence circuitry forms a delay network such that the signal received at a selected time following transmission can be processed and all other signals removed.

The ultrastable oscillator output is also mixed with that of a second stable frequency source to provide a local oscillator signal whose frequency differs from that of the transmitted signal by the center frequency of the intermediate frequency (IF) amplifier. The received signal is mixed with this local oscillator signal, translating the received signal to the IF. Following amplification, a short burst of the signal is allowed to pass through the range gate for processing.

Reflection of the transmitted microwave pulse from the moving target causes the frequency of the reflected wave to be shifted from that of the transmitted wave by an amount f_d proportional to the velocity of the target. Thus, $f_d = 2V_r f_o/c$, where V_r is the target velocity, f_o the transmitted frequency, and c the velocity of light. For a fixed position of the range gate, each target in the range gate will add a component to the overall received signal during that gate interval. This component will have an RF frequency of $f_o \pm f_d$, depending on the velocity of the target. If targets traveling at several different speeds are simultaneously present, the RF signal will be a composite in which the strength of each component will be a function of the radar cross section of the target giving rise to that component.

The effect of frequency translation from RF to IF is to preserve the Doppler frequency (and phase) shifts that originally occurred on the RF carrier such that spectral analyses of the range-gated IF signal are fully equivalent to similar analyses at RF. The subsequent discussion will deal with the IF signal unless otherwise specified.

Following gating, the signal is applied to the Doppler filter bank, which consists of a set of narrow bandwidth, bandpass filters, each having a different center frequency and the center frequencies being separated by the bandwidth of the filters. Thus, the various components of the IF signal applied to all filters are passed through only those filters having the appropriate center frequency. A vehicle traveling at 60 mph would provide frequency content different from that of a vehicle traveling at 30 mph and the differences would be denoted by the outputs of the narrow-band filters. The speed difference that is detectable is a function of the bandwidth of each filter. The range of speeds that can be examined is a function of the filter bandwidth and the number of filters contained in the filter bank.

In summary, when a vehicle enters the range gate of the radar and is illuminated by the transmitted beam, the frequency of the backscattered radiation is changed by the velocity of the vehicle. The backscattered signal is received by the radar, filtered, amplified, and passed to the Doppler filter bank, where the signal is detected in the appropriate filter.

This simplified description will provide a basic understanding of the radar used in this experiment. Detailed presentations of pulsed Doppler systems may be found elsewhere (4, 5). A detailed description of the radar used is given by Tripp and Rogers (6).

A brief discussion of some of the important radar parameters follows. A complete listing is given in Table 1. The antenna consisted of an 8-ft paraboloidal reflector with feed. Because the beam width of this antenna was 0.9 degree, the roadway right-of-way included within the beam at its half-power points at a range of 10,000 ft was approximately 175 ft.

The pulse repetition frequency (PRF) was 5,000 pulses per second. It can be shown that the width of the Doppler frequency range that can be observed and measured is also 5,000 Hz. To allow for two-way traffic, 2,500 Hz are assigned to each direction of travel. From the Doppler frequency formula given, the maximum speed is found to be

$$V_{max} = \frac{f_d \times \lambda}{2} = \frac{2{,}500 \times 3.2}{2} = 4{,}000 \text{ cm/sec} = 90 \text{ mph}$$

because $\lambda = 3.2$ cm is the radiated wavelength.

The radiated pulse width was 0.5 μsec; therefore, the minimum length of highway that could be examined was approximately 250 ft. The pulse width of the range gate, τ_2, was adjustable from a minimum of 0.5 μsec (≈250 ft) to 5 μsec (≈2,500 ft).

The Doppler filter bank used with the CAL pulsed Doppler radar consisted of 250 bandpass filters, each 4 Hz wide. The velocity band accepted by each filter is therefore 0.144 mph. Thus, resolution of velocity differences as small as 0.144 mph was available without further refinement of the data. The total range of the filter bank was, therefore, 36 mph. This bank could be positioned anywhere in the -90 to +90 mph unambiguous velocity acceptance band by setting the spectrum analyzer local oscillator to the appropriate frequency. Examples of the output of the spectrum analyzer will be shown later in Figure 8.

TABLE 1

PULSED DOPPLER RADAR PARAMETERS

Item	Measurement
Transmitter frequency	9,310 MHz
Peak power	6 kW nominal
Pulse width	0.5 μsec, fixed
Pulse repetition frequency	2 or 5 kHz, selectable
Receiver range gate	Position continuously variable; width adjustable from 0.5 to 10 μsec
Overall receiver noise figure	≈12 dB
Receiver dynamic range	≈50 dB
Coherent oscillator frequency	9,250 MHz
Coherent oscillator stability	1 part in 10^6, averaged over 1 sec
Antenna	8-ft parabolic dish; 0.9 deg beam width (one way); gain 43 dB; first sidelobes ≈-20 dB
Displays	PPI; gated and ungated A-scopes; Doppler spectrum analyzer
Doppler spectrum analyzer	4- and 100-Hz resolution bands; post-detection integration time constants 0.3, 1, 3, or 10 sec
Ancillary instrumentation	
Calibrated AGC	
Mean Doppler frequency tracker	
R-meter	
Strip chart and magnetic tape recorder	

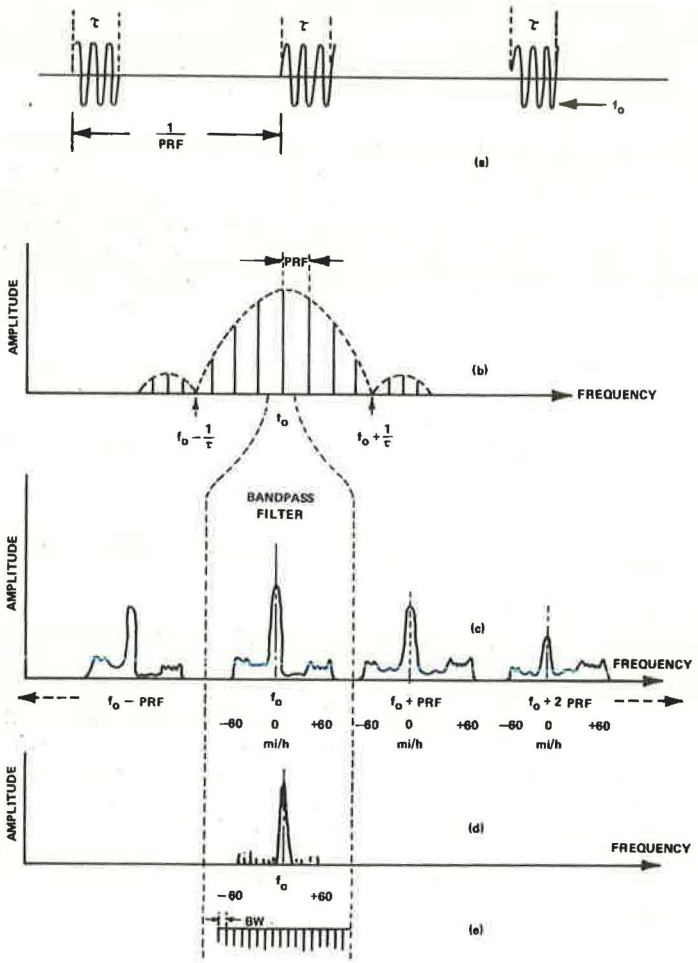

Figure 3. Doppler spectrum.

As backup instrumentation for this experiment, the received and range-gated signal applied to the Doppler filter bank was also recorded on magnetic tape. Because additional heterodyning was required to translate the signal to a frequency band within the recorder capability, it was found convenient to display the signal being recorded on a swept frequency audio spectrum analyzer. Typical results are shown later in Figure 10.

The velocity measured by the Doppler technique is the radial velocity of the vehicle with respect to the radar (i.e., the vector component directed toward or away from the radar). For the situation shown later in Figure 6, most vehicles (exceptions are those vehicles on crossroads) were traveling radially to the radar. For other radar-roadway sites, it may be necessary to compute the true velocity from the relation $V_T = V_m/\cos\theta$, where V_T is true velocity, V_m the measured velocity, and θ the angle between the radar pointing direction and vehicle velocity vector.

PULSED DOPPLER RADAR-TRAFFIC FLOW RELATIONS

In the development of the statistical methods of traffic-flow analysis, emphasis is placed on the speed and position of all vehicles passing through a given length of high-

way. Starting from a description of the density function $\phi_V(v)$ for the instantaneous speed (v) of a single vehicle over the length of road of interest, the space mean speed for a single vehicle and the variance of that distribution can be developed. Following the analysis given by Mori, Takata, and Kisi (3), it can be seen that

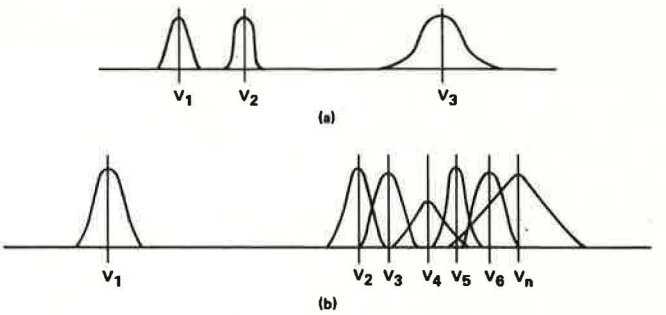

Figure 4. Distributions of instantaneous speeds.

$$V = \int_0^\infty v\phi_V(v)dv$$

and

$$\varphi^2(V) = \int_0^\infty (v - V)^2\phi_V(v)dv$$

where V is the vehicle space mean speed and $\varphi^2(V)$ the variance of speed fluctuations about the space mean speed.

Consider the radar system directed at a roadway with its range gate of width τ_2 positioned so that its leading edge is located at some range R. When a single vehicle passes through this gate, it will be observed by the radar on each pulse (i.e., 5,000 times per second). To develop the Doppler spectrum (Fig. 3) and thus measure velocity, integration of many pulse responses is required. Additional data smoothing is used to minimize the graininess caused by pulse sampling. In the present case, a smoothing time constant of 0.3 sec was used. The time history of the vehicle speed as observed through this 0.3-sec time-constant filter can be determined. The density function for "instantaneous" speed, $\phi_V(v)$, and other derived parameters will therefore also be weighted by this time constant.

When two or more vehicles are within the range gate, a similar analysis will apply and the time histories of the speeds of the two or more vehicles will be described. To distinguish speeds from one another, they must be separated by at least the width of one of the Doppler bandpass filters (i.e., by at least 0.144 mph). In effect, this requirement demands that vehicle speed distributions follow the general outline shown in Figure 4a. The distributions of the instantaneous speed of three vehicles are shown as distinct, nonoverlapping distribution functions.

A number of traffic flow characteristics may be examined at this point. For a single vehicle, the mean and variance as a function of time of day, weather conditions, vehicle type, related road conditions, and roadway design can be determined. For multiple vehicles, relative speeds (instantaneous and on-the-average) may be studied, as well as the changes in $\phi_V(v)$ with changes in traffic density. For high-density conditions, the characteristics of a single vehicle moving relative to the average (much higher or lower speed than the average, as shown in Figure 4b) can be studied.

If, in addition to $\phi_V(v)$, the density function for the space distribution of overall speed [i.e., $G_S(V)$] can be determined, then the density function for the space distribution of instantaneous speed is found to be

$$g_S(v) = \int_0^\infty G_S(V)\phi_V(v)dv$$

In the radar approach considered, $g_S(v)$ can be developed directly from the instantaneous Doppler measurements, provided that vehicle speeds differ instantaneously by the 0.144-mph minimum resolution of the Doppler filter bank. For example, $g_S(v)$ may be

determined for the situation shown in Figure 4b. Then the space mean speed of the instantaneous speed, $\bar{v}_S$, and the space mean speed for the overall speed, $\overline{V}_S$, can be determined from

$$\bar{v}_S = \int_0^\infty v g_S(v)dv = \int_0^\infty G_S(V) \int_0^\infty v\phi_V(v)dvdV = \int_0^\infty VG_S(V)dV = \overline{V}_S$$

that is, directly from the radar data.

The radar approach thus offers a direct method of providing the information from which the density functions are developed. In addition, these measurements can be made over a period of time when a variety of traffic conditions (e.g., densities, volumes, and flow rates) are encountered. Thus, broader descriptors, such as joint distribution functions (i.e., functions of more than one variable, one of which may be time), can be developed. In addition, the change of these descriptors with time can also be developed so that effects of traffic perturbations (e.g., a very slow or very fast vehicle) can be analyzed.

Time distributions for spot speed and mean speed can be related to the space distribution measurements. Time distribution measurements consider the speeds of vehicles passing a point in the highway. Such a point may be the location of the start of the range gate or, if the range gate can be made sufficiently narrow, the speed in the range gate. By observing the speed of each vehicle on entry into the range gate and thus into the data system, the corresponding time distribution descriptions can be developed.

It is also possible to consider the measurement of traffic volume and density, but it is important to note an instrumental limitation. If two vehicles travel at approximately the same velocities (within 0.144 mph), they may be indistinguishable insofar as this test radar is concerned. As traffic density increases, the probability that such masking occurs increases. Radar design changes, such as reducing the duration of the transmitted pulse, can be introduced to reduce this problem. Such changes, however, were beyond the scope of the existing effort.

TEST SITE

The preliminary determination of the feasibility of using the radar in its intended role was made with slow-speed, low- to moderate-density traffic in the field of view. For more representative test purposes, a site with a wide range of traffic conditions (including high density) was sought. Therefore, emphasis was placed on limited-access-type highways. Other restrictions were imposed by the radar itself. Because of its size (Fig. 5) and transportability, consideration of locations of easy access and minimal impedance to normal traffic flow was necessary. Finally, because it was planned to examine traffic at a number of ranges from the radar, a straight and level stretch of roadway was required, preferably one that would include entrances and exits.

Figure 5. The CAL pulsed Doppler radar.

Following a brief examination of potential sites within close proximity to CAL's main Buffalo Laboratory, the site shown on the map of Figure 6 was selected. The radar was positioned on a bridge over the New York State Thruway at the Cleveland Drive overpass so that Thruway traffic south of Cleveland Drive and almost as far away as Walden Avenue could be viewed.

Traffic in both directions could be observed over most of that range. Several entrances and exits are included in this test section. Included are a number of bridges as shown and a number of signs and other obstructions that are not shown.

On this stretch of road, traffic density varies widely. Maximum density measured southbound during the 2-day interval was 120 vehicles per minute. The density varies with the time of day, and this time variation is different for the northbound and southbound lanes. The types of vehicles constituting the traffic flow also vary with time of day.

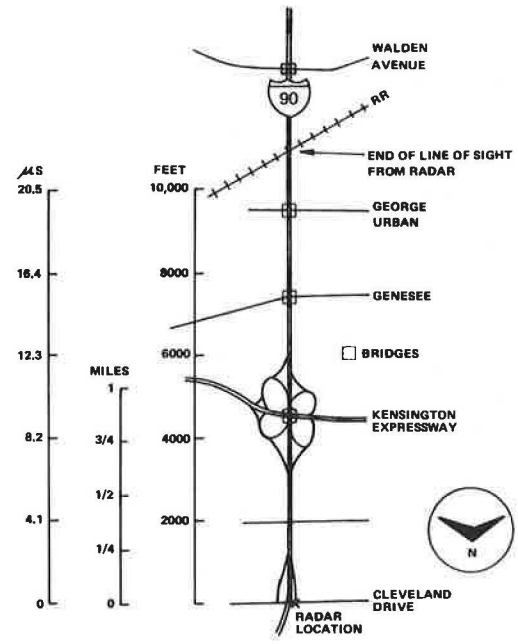

Figure 6. Test road.

RESULTS OF TESTS

Doppler Resolution in High-Clutter Background

One of the principal sources of concern was that signal returns from fixed obstacles in the radar beam might be so large that receiver saturation masking of small signals would be encountered. It was found, however, that Doppler signals could be resolved when vehicles were present in the range gate at most ranges within the radar field of view and within line of sight, i.e., out to the maximum range of approximately 11,000 ft, with a time delay of approximately 22 μsec, as indicated in Figure 6.

Photographs were taken of the raw video signal before Doppler processing. Shown in Figure 7 is the expanded A-scope presentation (received signal amplitude versus range) that was typically observed. Each of the vertical deflections represents the amplitude of return from a target, some of the targets being vehicles and others being fixed obstacles. Figure 7b was taken approximately 1 minute after Figure 7a. The change in signal distribution with range caused by moving targets (vehicles) is clearly evident. These photographs were taken at 3:30 a.m., a period of very low vehicle density.

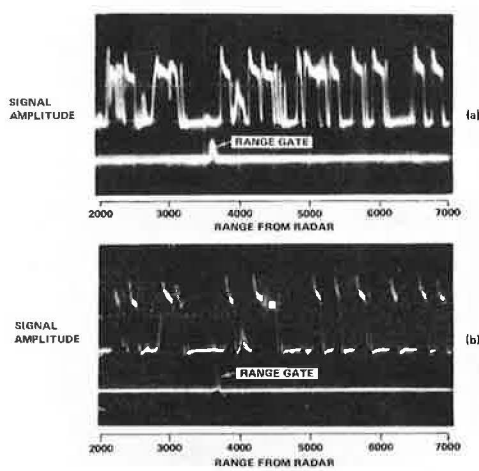

Figure 7. Raw video signal versus range.

Velocity measurements could not be carried out at every range gate setting over the 300- to 11,000-ft range. If a large fixed target (e.g., a bridge) was contained in the range gate, its signal would mask those from vehicles also contained in that gate. In the length of highway selected for this test, only four positions were so observed: three locations containing bridges, and one large sign. The bridges, however, did not seriously obscure targets at greater ranges.

Radar Peak Power Required

The peak power output of the radar was adjustable from the maximum value of 50

kilowatts down to the minimum level required to actuate the transmit-receive switch of Figure 1. Peak powers used ranged from 10 to 100 watts. A series of different levels was used to determine the relationship among Doppler resolution, maximum range capability, and peak power. It was found that a peak power of 10 watts was optimum for the range increment (300 to 11,000 ft) available. For larger ranges, the peak power must necessarily be increased. Peak power is, of course, one of the critical design parameters required in the design of specific radar equipment.

High-Resolution Doppler Velocity Measurements

The high-resolution filter bank system consists of 250 bandpass filters, each having a bandwidth of 4 Hz or 0.144 mph. The total Doppler range that can be examined at any time is therefore 1,000 Hz or 36 mph. The position of the 36-mph, 250-channel window can be positioned anywhere in the -90 to +90 mph range by appropriate adjustment of a reference oscillator. A typical set of results is shown in Figure 8, the radar parameters of which are given in the table below. The pictures were taken with a shutter opening of 1-sec duration.

Frame	Range to Start of Gate	Gate Width	Time of Day
A	3,190 ft (6.5 μsec)	250 ft (0.5 μsec)	1:26 p.m.
B	3,190 ft (6.5 μsec)	250 ft (0.5 μsec)	1:18 p.m.
C	3,190 ft (6.5 μsec)	250 ft (0.5 μsec)	1:32 p.m.
D	3,190 ft (6.5 μsec)	500 ft (1 μsec)	1:36 p.m.
E	2,940 ft (6 μsec)	250 ft (0.5 μsec)	3:40 p.m.
F	2,940 ft (6 μsec)	250 ft (0.5 μsec)	3:45 p.m.

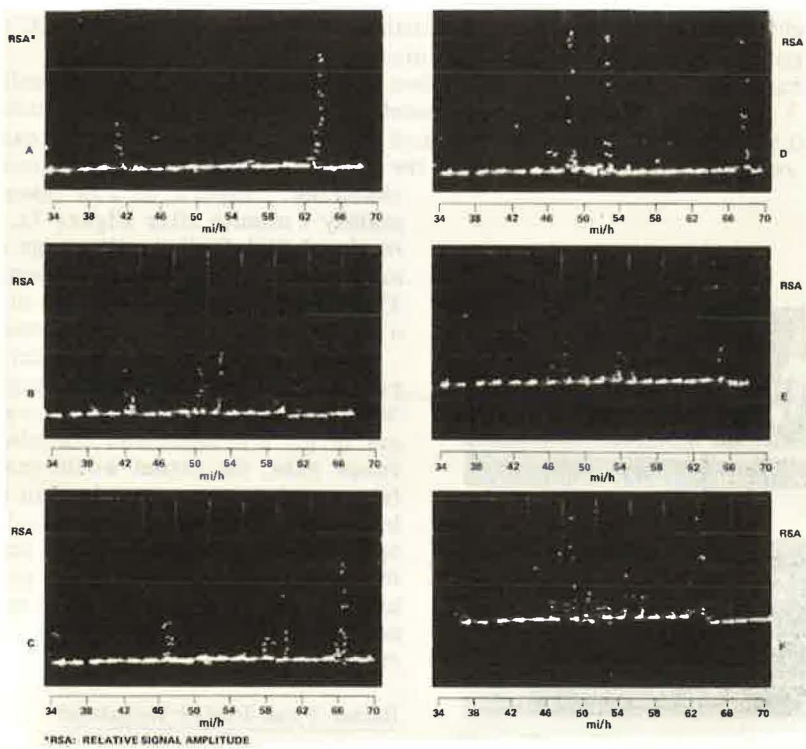

Figure 8. High-resolution Doppler velocity data.

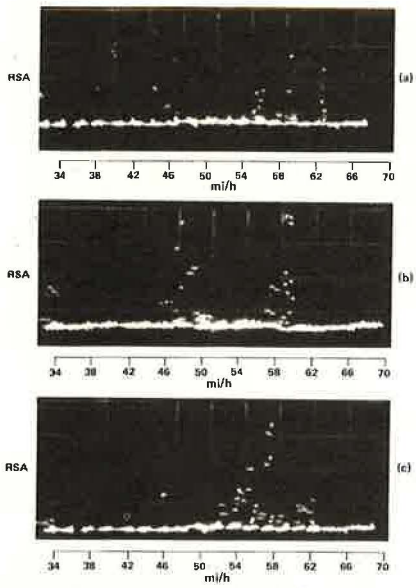

Figure 9. High-resolution Doppler velocity data (250-ft range gate set 11,000 ft from radar).

The following interpretation is applied to each frame. There may exist, within the gate width and at the range setting of the radar, a number of vehicles traveling at a corresponding number of velocities. The 250 filter outputs are scanned sequentially, with zero filter output amplitude (representing absence of vehicle at that speed) displayed as the horizontal base line. Thus, the abscissa becomes the velocity axis and can be calibrated as shown in each frame. When a filter output differs from zero (a vehicle of the matching speed is contained in the range gate), a vertical deflection occurs. Detailed interpretation of amplitude differences is not within the scope of the present study. The number of individual vertical deflections defines the least number of vehicles that may be in the gate during the frame interval. Consider frame D as an example. There are at least six vehicles in the range gate and they have measured velocities of 43, 47, 50, 53, 58, and 68 mph.

Similar information was obtained at other times and for other ranges. Shown in Figure 9 are three frames of data collected at the maximum range available, approximately 11,000 ft (22 μsec), in this experiment. (At this point, the New York

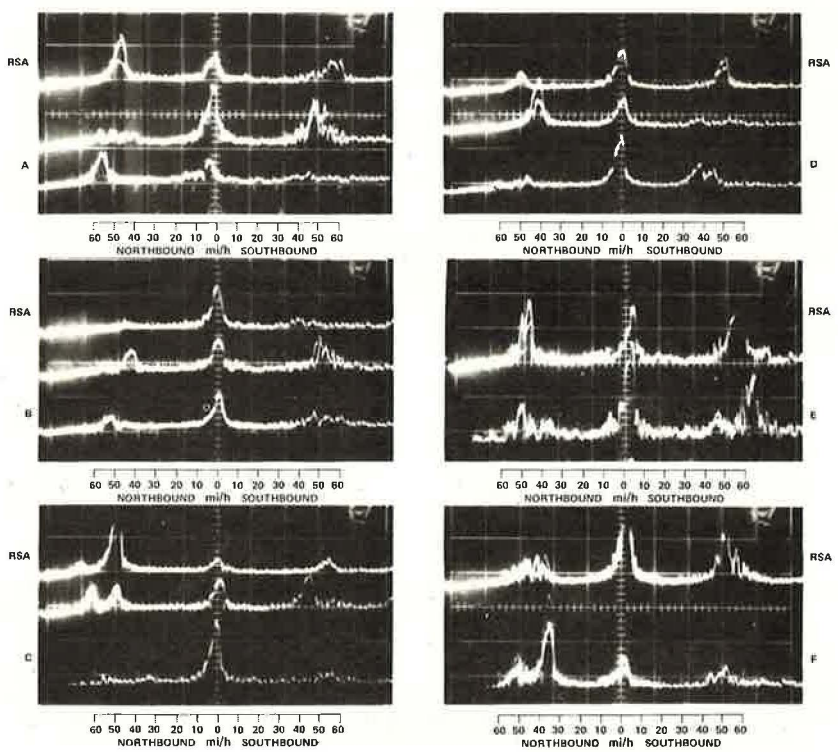

Figure 10. Swept-frequency Doppler velocity display.

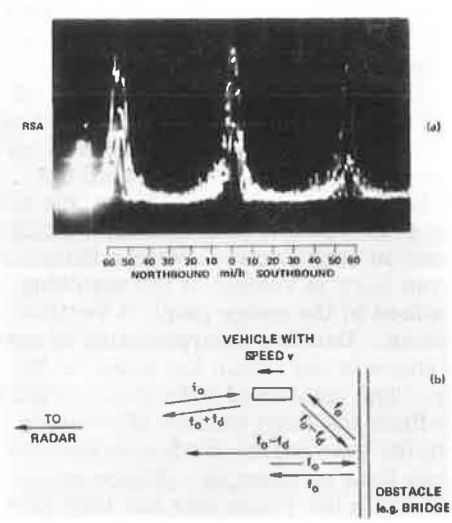

Figure 11. Multipath problem.

State Thruway passes over a railroad and greater ranges lie below the line of sight.) The gate width for each frame was 250 ft.

An uncertainty exists as to the number of vehicles respresented by a line of many dot elements. However, when observations are made in real time, the rise and fall of vertical signals can easily be followed. Cine photography synchronized with the frame rate of the display would provide a much clearer and more detailed analysis of these parameters and would be a desirable adjunct to the present system.

Swept-Frequency Doppler Display

A second type of spectrum analyzer, which permitted the display of the full Doppler spectrum of the signal, was used. In this instrument, a sweep voltage synchronized with the horizontal sweep of the display drives a tunable narrow-band filter through a selectable frequency band. The received, range-gated signal is applied to the input of the filter so that when the signal frequency matches that to which the filter is tuned, a vertical deflection voltage proportional to the signal amplitude is developed. The response time of the filter is an inverse function of the filter bandwidth, and the time to complete a sweep is also a function of that response time. Therefore, the resolution attainable for practical sweep rates is much poorer than that of the multiple filter bank.

Several examples of the type of data obtainable with this display are shown in Figure 10. In each of the six frames, the speed range is given on the abscissa. Vertical deflections again indicate the presence of a vehicle at that speed in the range gate. However, because of the limited resolution, the response caused by a single vehicle now covers a range of velocities. In each frame, several sweeps are shown; each sweep was taken in time sequence, the first being the lowest trace in each frame. The other traces were taken at approximately 15-sec intervals, the time required to reposition the camera with respect to the display.

The following radar data apply to each of the frames:

Frame	Range to Start of Gate	Gate Width	Time of Day
A	2,000 ft (4 μsec)	250 ft (0.5 μsec)	6:50 p.m.
B	2,500 ft (5 μsec)	250 ft (0.5 μsec)	6:55 p.m.
C	6,400 ft (13 μsec)	250 ft (0.5 μsec)	7:12 p.m.
D	11,000 ft (22 μsec)	250 ft (0.5 μsec)	7:18 p.m.
E	6,400 ft (13 μsec)	250 ft (0.5 μsec)	8:11 p.m.
F	11,000 ft (22 μsec)	250 ft (0.5 μsec)	8:15 p.m.

The major peaks in these spectra lie in the range of 50 to 60 mph. In some cases, multiple vehicles can be seen in a single trace, as, for example, in the middle sweep of frame C. Much greater speed differences must be present to provide for vehicle separation than was the case in the high-resolution system. This instrumentation approach provides for some rough estimation of traffic characteristics, but is of much less value than the high-resolution system in the measurement of speed distributions, both instantaneous and averaged.

Multipath Considerations

In addition to vehicle-masking by the large stationary targets discussed previously (which places a restriction on some lengths of highway that can be observed), there is the effect of multipath, which is described briefly in the following.

It can be seen in Figure 11 that in the four superimposed sequential Doppler sweeps, two Doppler speed peaks are present, one at approximately 60 mph (southbound) and one at 60 mph (northbound). However, visual observation of the traffic scene showed that only a single vehicle was present at the time. The range gate was set at 4,000 ft from the radar, with a gate width of 250 ft. The misrepresentation, which indicates two vehicles where only one is present, is serious and must be suppressed or properly interpreted in an operational system.

The cause of this problem is found in a process called multipath, a process by which the transmitted energy follows several paths, each including the target vehicle, before reception in the receiver. To visualize the problem, consider an approaching vehicle with a fixed obstruction slightly behind it (from the point of view of the radar). Some of the transmitted power falls directly on the vehicle and, on reflection, returns with a higher frequency than that transmitted. During the same range gate interval, transmitted power is also incident on the fixed obstacle. The reflected power is scattered in all directions in the quarter sphere facing the radar. Some of that power will be received directly by the radar at the same frequency as that transmitted. Some will be incident on the vehicle; a portion will be reflected back to the fixed object and then back to the radar. But in this geometrical situation, the vehicle appears to be moving away from the radar and the frequency of the return signal will be less than that of the transmitter. An outline of the process is shown in Figure 11b.

There are many ways in which unwanted reflections (multipath) can occur from moving as well as fixed objects. This is particularly so in the traffic problem because of the enormous range of radar cross sections that the full spectrum of vehicles can provide and because of the relatively large fixed obstacles that may be present. In most cases in this program, multipath problems were not encountered. But for general application, a more detailed examination will be required.

CONCLUSIONS

1. Pulsed Doppler radar may provide a unique instrumentation technique that would allow the acquisition of new forms of traffic flow data that not only would be most applicable to the statistical methods of traffic flow theory, but also would allow examination of traffic dynamics not presently possible.
2. The present radar system has some limitations, when operated in the traffic environment, that require further exploration. Some of these limitations may be minimized through radar design (e.g., narrower beam width, allowing only a single direction of traffic to be viewed at one time, or shorter range gates to restrict the number of vehicles and fixed obstacles contained within the measurement gate). A wide range of design and application area trade-offs is available, the proper choices likely leading to a minimization of this type of problem.
3. Further development of display and data-recording methods is desirable to realize the full utility of this instrumentation system.
4. The radar may be structured to contain range and Doppler frequency tracking systems, the inclusion of which would provide for examination of additional classes of highway problems. By tracking a single vehicle, its instantaneous speed can be described as a function of time, and, in addition, the speeds of other vehicles in the tracking range gate (that is, those in close proximity to the tracked vehicle) can be measured relative to the tracked vehicle.
5. The radar offers an all-weather remote sensing capability. Although weather conditions ranged from clear and dry to heavy thunderstorm, Doppler speed data were collected throughout the test period.

REFERENCES

1. Montroll, E. W., and Potts, R. B. Car Following and Acceleration Noise. HRB Spec. Rept. 79, 1964, pp. 37-48.
2. Lighthill, M. J., and Whitman, G. B. On Kinematic Waves: II. A Theory of Traffic Flow on Long Crowded Roads. HRB Spec. Rept. 79, 1964, pp. 6-35.
3. Mori, M., Takata, H., and Kisi, T. Fundamental Considerations on the Speed Distributions on Road Traffic Flow. Transportation Research, Vol. 2, Pergamon Press, 1968, pp. 31-39.
4. Skolnik, M. I. Introduction to Radar Systems. McGraw-Hill Book Co., 1962.
5. Burdic, W. S. Radar Signal Analyses. Prentice Hall, Inc., Englewood Cliffs, N. J., 1968.
6. Tripp, B. R., and Rogers, R. An Experimental X-Band Coherent Pulse Doppler Radar; Design, Capabilities, and Applications. Presented at 11th Annual Radar Symposium, Fort Monmouth, N. J., June 8-10, 1965; Michigan Univ. Rept. 6400-45-X, pp. 161-173.